OXIDATIVE ADDITION AND CO INSERTION OF RHODIUM CUPFERRATE COMPLEXES CONTAINING ARSINE LIGANDS

Fessahaye Tekeste Kahsai

OXIDATIVE ADDITION AND CO INSERTION OF RHODIUM CUPFERRATE COMPLEXES CONTAINING ARSINE LIGANDS

A thesis submitted to meet the requirements for the degree of

Magister Scientiae

in the

Department of Chemistry
Faculty of Natural and Agricultural Sciences

at the

University of the Free State

by

Fessahaye Tekeste Kahsai

Supervisor

Dr. J.A. Venter

Co-supervisor

Prof. W. Purcell

November 2008

CONTENTS

ABBREVIATIONS

COD	*cis*,*cis*-1,5-cyclooctadiene
Cy	cyclohexyl
D_n	solvent donocity
DMF	N,N-dimethylformamide
DMSO	dimethylsulphoxide
Et	ethyl
Hacac	2,4-pentanedione, acetylacetone
Hanmetha	4-methoxy-N-methylbenzothiohydroxamate
Hba	1-phenyl-1,3-butanedione, benzoylacetone
Hbpha	N-benzoyl-N-phenylhydroxylamine
Hbzaa	3-benzyl-2,4-pentanedione, di-acetylbenzylmethane
Hcacsm	methyl(2-cyclohexylamino-1-cyclopentene-1-dithiocarboxylate)
Hcupf	N-phenyl-N-nitrosohydroxylamine, cupferron
Hdbbtu	N,N-dibenzyl-N'-benzoylthiourea
Hdbm	1,3-diphenyl-1,3-propanedione, dibenzoylmethane
Hdmavk	dimethylaminovinylketone
Hdppe	$Ph_2PCH_2CH_2PPh_2$
HEt_2dtc	N,N-diethyldithiocarbamate
HEtmt	1-(ethylthio)-maleonitrile-2-thiolate
Hfctfa	1-ferrocenyl-4,4,4-trifluorobutane-1,3-dione, ferrocenoyltrifluoroacetone
Hhacsm	methyl(2-amino-1-cyclopentene-1-dithiocarboxylate)
Hhfaa	1,1,1,5,5,5-hexafluoro-2,4-pentane, hexafluoroacetylacetone
Hhpt	1-hydroxy-2-pyridinethione
Hmacsm	methyl(2-methylamino-1-cyclopentene-1-dithiocarboxylate)
Hmnt	maleonitriledithiolate
Hneocupf	N-naphthyl-N-nitrosohydroxylamine, neocupferron
Hox	8-hydroxyquinoline, oxine
Hpbtu	N-benzoyl-N-phenylthiourea
Hpic	2-picolinic acid
Hquin	2-carboxyquinoline
Hsacac	thioacetylacetone

Hsalnr	N-*o*-tolylsalicylaldimine
$HSpymMe_2$	4,6-dimethylpyrimidine-2-thiol
Hstsc	salicylaldehydethiosemicarbazose
Htfaa	1,1,1-trifluoro-2,4-pentanedione, trifluoroacetylacetone
Htfba	1,1,1-trifluoro-4-phenyl-2,4-butanedione, trifluorobenzoylacetone
Htfdma	1,1,1-trifluoro-5-methyl-2,4-hexanedione
Htfhd	1,1,1-trifluoro-2,4-hexanedione
Htftma	1,1,1-trifluoro-5,5-dimethyl-2,4-hexanedione
Htrop	tropolone
Htta	2-thenoyltrifluoroacetone
IR	infrared spectroscopy
L,L′-Bid	mono anionic bidentate ligand
L	one of the two donor atoms of the bidentate ligand L,L′-Bid
L′	the second donor atom of the bidentate ligand L,L′-Bid
Me	methyl
MeO	methoxy
MTBK	methyl tertiary butyl ketone
NMR	nuclear magnetic resonance spectrometry
PGM	platinum group metals
Ph	phenyl
Phen	1,10-phenanthroline
$P(OPh)_3$	triphenylphosphite
PPh_3	triphenylphosphine
PX_3	tertiary phosphine with substituents X
S	solvent
T	temperature
TBP	trigonal bipyramidal
THF	tetrahydrofuran
Tol	tolyl
UV	ultraviolet spectroscopy
ε	dielectric constant
θ	Tolman cone angle of tertiary phosphine
υ_{CO}	infrared stretching frequency of carbonyl

CHAPTER 1

INTRODUCTION AND AIM OF THE STUDY

1.1 HISTORICAL BACKGROUND OF ORGANOTRANSITION METAL COMPLEXES

Life has a beginning and an end, but chemistry as a science is dynamic, it is changing and developing continuously. Organotransition metal chemistry, being part of this dynamic science, is one of the fastest growing disciplines in chemistry and has played an important role in the modern renaissance of inorganic chemistry that has begun in the early 1950's. Today this subject is one of the most heavily investigated areas of chemistry in both academic and industrial laboratories. As a result, organotransition metal chemistry has led to the development and production of a number of very useful and important products such as insecticides and drugs which are needed in our everyday life. It is appropriate to start the discussion by first defining the chemistry of these complexes which will then be followed by the historical background of these vital complexes.

Organotransition metal chemistry is concerned with compounds that have an organic group bound to a transition metal through at least one metal-carbon bond, which can either be σ or π bound (Collman, Hegedus, Norton & Finke, 1987:1). According to this

definition, coordination compounds having donor bonds from elements other than carbon, such as bonds with metal amines, halide ions and the like, are excluded by this strict definition. Organotransition metal complexes tend to be more covalent in character and the metal is often in a lower oxidation state compared to the classical coordination compounds that contain metal-oxygen bonds such as the aqua ions of $[M(H_2O)_6]^{+2}$, where M = V, Cr, Mn, Fe, Co, or Ni (Crabtree, 1988:1).

Most inorganic chemists agree that the first organometallic complexes that were synthesised were very stable and easily prepared, such as Zeise's salt and a few nickel-carbonyl complexes. A Danish pharmacist, W.C. Zeise prepared the first organometallic complex by reacting KCl and $PtCl_2$ in ethanol in the early 19^{th} century (Collman *et al*., 1987:8). The original formulation of this complex suggested that it is a double salt with the chemical formula of $KCl.PtCl_2.EtOH$, but was later crystallographically characterised as the potassium salt of an anionic ethene-complex, and thus its formula changed to $K[(C_2H_4)PtCl_3].H_2O$. About 115 years ago, a chemist by the name of Mond prepared the first binary metal carbonyl, $Ni(CO)_4$, using elemental nickel and CO gas (Collman *et al*., 1987:8; Lukehart, 1985:3). This discovery had great significance since it led to a commercial process for refining nickel metal. This process, also called the Mond process, uses the facile formation of $Ni(CO)_4$ to extract nickel from a crude mixture of metals. Gaseous $Ni(CO)_4$ is removed from the reaction chamber and decomposed thermally to afford very pure nickel metal and CO gas. The process is also environmentally friendly since the liberated CO gas is recycled and used again.

In the early 1900's, the organometallic chemistry was dominated by non-transition metal compounds such as alkyl and aryl compounds of magnesium and lithium and transition metal compounds of zinc and lead, which were synthesised by Edward Frankland, Victor Grignard and others (Crabtree, 1988:38). Examples of these type of compounds are

diethylzinc (ZnC_2H_4) and organomagnesium halides with a general chemical formula of RMgX, (R = alkyl, X = halide). The synthesis of such a large number of organometallic compounds stimulated the research for analogous transition metal compounds. As a result, compounds such as $CrEt_3$, $CoEt_3$, *etc*. were prepared (Lukehart, 1985:4). Although these compounds were thermally unstable and air sensitive, which made it difficult to identify their structures, it was the first small step towards the development of this highly important discipline in inorganic chemistry.

The rebirth of organotransition metal chemistry from 1951 into the 1970's was initiated by the preparation of ferrocene, $Fe(C_5H_5)_2$, by two independent groups led by Kealy (Collman *et al*., 1987:13) and Miller (1952:632). Ferrocene, with unusually high stability, was later identified as metallocenes with a sandwich structure (Crabtree, 1988:108). This stability is due to the fact that in ferrocene, unlike cobaltocene, all the bonding and nonbonding orbitals are filled (Crabtree, 1988:108). Nowadays, chemists suggest that the cyclopentadienyl group can be used as stabilizing ligand for at least all the group 8 atoms such as iron, ruthenium and osmium (Crabtree, 1988:104). The successful synthesis of this compound, as well as the invention, improvement and availability of different apparatus such as for X-ray crystallography, IR and NMR spectroscopy for molecular elucidation of the complexes played a vital role in the rebirth of this chemistry.

The role of organotransition metal complexes as catalysts was demonstrated by the preparation of different organic compounds such as alcohols, organic acids and aldehydes which were performed during the 1930's by researchers such as O. Roelen (Collman *et al*., 1987:9) and W. Reppe (Collman *et al*., 1987:9). Research by scientists like G. Wilkinson (1965:131), Ziegler and Natta (Collman *et al*., 1987:10), Monsanto (Haynes, Mann, Morris & Maitlis, 1993:4093) and others also drove the research in organotransition metal chemistry towards new dimensions and in the process

demonstrated the wider application of organotransition metal complexes. Today, organotransition metal complexes are widely applied in industry in fields such as homogeneous catalysis (Halpern, 1981:11), for example in the production of large-scale commercial chemical products such as aldehydes, organic acids, and alcohols as well as the production of polymers such as polyethylene and polypropylene.

The discovery that some rhodium complexes have the ability to catalyse asymmetric hydrogenation of prochiral olefins stimulated a new field of application, namely that of drug design. This led to the important application of a rhodium complex containing a chiral phosphine ligand called DiPAMP (see Figure 1.1) to synthesise the well-known drug called L-Dopa (Collman *et al*., 1987:537; Lukehart, 1985:410). This drug is a chiral amino acid which is extensively used for the treatment of Parkinson's disease. Rhodium complexes are also used as pesticides, for example the $[RhCl(O_2)(PPh_3)_3]$ complex as well as antitumour agents like [Rh(acac)(COD)] (Dickson, 1985).

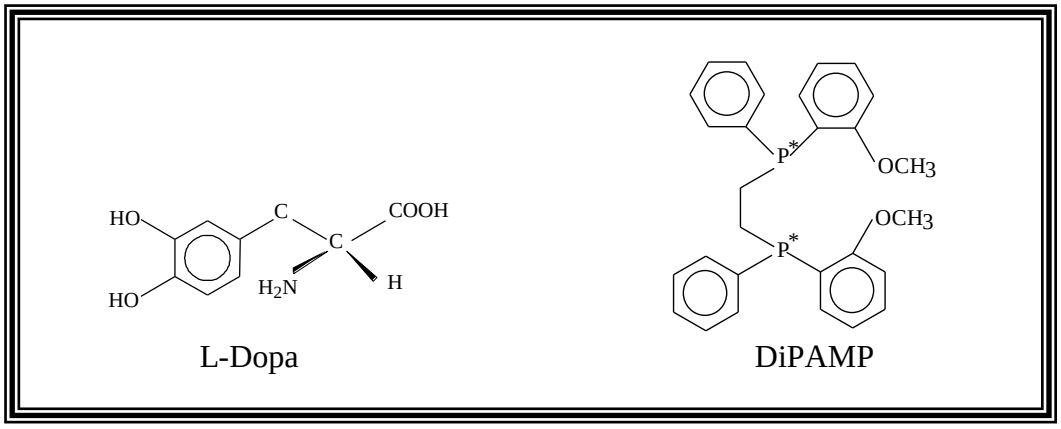

Figure 1.1 Chemical structures of L-Dopa and DiPAMP.

In short, the renaissance in organometallic chemistry in the last 50 years was mainly due to the application of many organotransition metal complexes in a number of important chemical processes that include industrial catalysis (Collman *et al*., 1987: 523-570;

Halpern, 1981:11 and Lukehart, 1985:388-410) the pharmaceutical industry (Sava *et al*., 1987:69; Sherman *et al*., 1987:1153) and in organic synthesis (Lukehart, 1985:347-381 and Collman *et al*., 1987:670-920). Rhodium complexes, due to their functional and remarkable chemistry played a vital role in these applications and will be discussed in the following paragraphs.

1.2 THE REMARKABLE CHEMISTRY OF RHODIUM COMPLEXES

Rhodium, one of the least abundant elements in the earth's crust (~10^{-7} % abundance), plays a vital role as homogeneous catalysts in many industrial processes and pharmaceutical preparations. The metal forms organometallic compounds with its oxidation state ranging from (-1) to (+4), with (+1) and (+3) being the most common oxidation states. The majority of the Rh(I) d^8 complexes have either square planar or trigonal bipyramidal geometries (Basson *et al*., 1987). Most of these compounds also contain π-bonding ligands such as CO, PR_3, RNC, alkenes, cyclopentadienyl and arenes.

It has already been mentioned that organotransition metal complexes play a significant role in important industrial processes that are of great economic and chemical importance. One of the main reasons for the importance of these complexes is the vital role they play as homogeneous catalysts in these processes. Although some transition metals such as Os, Ru, Co, Pt, Pd, Ni are all employed as homogeneous catalysts, it turns out that Rh and Ir are superior in their performance over the others in a variety of homogeneous catalytic reactions (Dickson, 1985; Lukehart, 1985:388-410). Comparative results for Rh and Co used in the same process are given in Table 1.1. These results clearly show that the rhodium catalyst is a far superior catalyst compared to cobalt in the same process. The rhodium process needs a lower catalyst concentration, has milder

reaction conditions, fewer by-products and produces higher yields than the cobalt process.

Table 1.1 Comparison of cobalt and rhodium catalysts for the carbonylation of methanol to acetic acid, Monsanto process (Lukehart, 1985:408).

Conditions	**Cobalt catalyst**	**Rhodium catalyst**
Metal concentration, M	ca. 10^{-1}	ca. 10^{-3}
Temperature, ^{o}C	ca. 230	ca. 180
Pressure, atm	500-700	30-40
Selectivity, on MeOH	90%	> 99%
Hydrogen effect	CH_4, CH_3CHO, EtOH	No effect

As shown in the table, the rhodium complex plays a vital role in the Monsanto acetic acid process. The complex that was initially used in this process is *cis*-$[RhI_2(CO)_2]^-$ but it has already been replaced by its Ir analogue and the process is now named the Cativa process (Forster, 1976:846; Maitlis, Hayes, Sunley & Howard, 1996:2187). However, the former process (Monsanto process) is still one of the major commercial methods for the production of acetic acid.

Like many other catalytic processes, the Monsanto process is also based on the repetition of a limited set of elementary reaction types (Forster, 1976:846; Haynes *el al*., 1996:2187). These reaction types include coordinative addition, oxidative addition and its reverse reaction (reductive elimination) as well as CO-insertion or alkyl migration. The homogeneous catalytic cycle is demonstrated in Scheme 1.1 and the process will be discussed in more detail in Chapter 2.

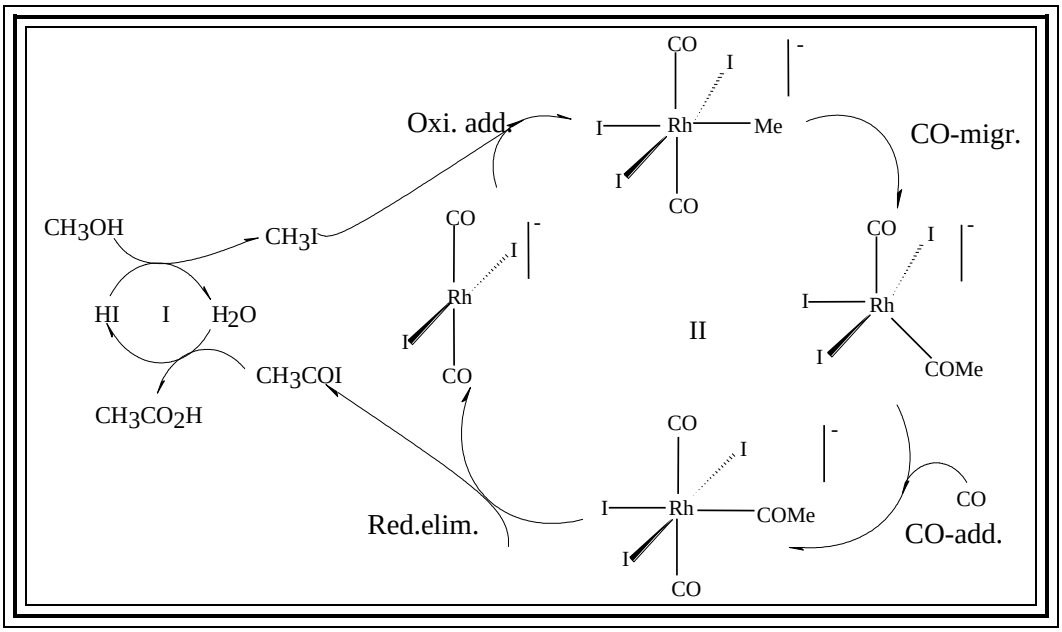

Scheme 1.1 Homogeneous catalytic cycle for methanol carbonylation (Monsanto process, where Oxi. Add. = oxidative addition, CO-migr. = carbonyl migration, CO-add. = carbon monoxide addition and Red. elim. = reductive elimination).

Another important application of rhodium as catalyst is the use of $[RhCl(PPh_3)_3]$, commonly known as Wilkinson's catalyst, which is used as a catalyst for the hydrogenation of olefins (Collman *et al*., 1987:530). Organic chemists routinely use this complex because of its selectivity, efficiency and reliability as catalyst. The carbon-carbon double bond in nitro-olefins can selectively be hydrogenated in the presence of this catalyst (Reaction 1.1), whereas heterogeneous catalysts usually react with the nitro group giving different products (Collman *et al*., 1987:542).

$$PhCH{=}CH{-}NO_2 \xrightarrow[H_2]{[RhClPPh_3]} PhCH_2CH_2NO_2 \qquad \textbf{(1.1)}$$

Another example is the use of the $[RhCl(CO)(PR_3)_2]$ catalysts in the homogeneous hydrogenation of ketones to secondary alcohols (Collman *et al*., 1987:556). In short, the

above mentioned applications of rhodium complexes as catalysts are summarised in Table 1.2, emphasizing the important chemistry and the wider application of rhodium complexes. According to a survey that was done in the early 1990's, ~60% of the world production of acetic acid was produced by using the Monsanto process. Furthermore, a survey in 1992 indicates that ~70% of all hydroformylation processes (the largest homogeneous catalytic process) were based on rhodium catalysts. Although the table is incomplete, these statistics indicate the great role that rhodium plays in the economic sector as catalyst in industrial-scale organic synthesis. It should also be noted that these products can be used as starting materials for the synthesis of many other organic compounds such as ketones, alcohols, esters, *etc*.

Table 1.2 Some of the applications of rhodium catalysts and their products.

Catalyst	**Process**	**Product**	**Amount/year**
cis-$[RhI_2(CO)_2]^-$	Monsanto process	Acetic acid	5.5 million tonnes*
$[RhH(CO)_4]$	Oxo process	Aldehyde	above 6.0 billion pounds #
$[Rh(DiPAMP)_2]$	Asymmeric hydrogenation of prochiral alkenes	Chiral alkane	------
$[RhCl(PPh_3)_3]$	Olefine hydrogenation	Alkane	-------

* 60% worldwide production (Howard *et al.,* 1993 cited in Haynes *el al*., 1996:2187).
\# Six billion pounds of butanal and 2 to 5 billion of other aldehydes worldwide production (Lukehart, 1985:388-410).

1.3 AIM OF THE STUDY

Organotransition metal complexes, their reactions, the factors that influence their properties to enable them to act as catalysts, as well as the type of intermediates that are formed during these reactions, are all at the centre of a variety of research programs. This inorganic research group, likewise, has extensively been studying the factors that

influence the rate of oxidative addition reactions of iodomethane to different rhodium(I) complexes in various solvents. The aim of these studies was to try and elucidate the mechanistic pathways of these reactions in an effort to understand the chemistry of their complexes and the effectiveness of these catalysts. Many studies have also been performed on Ir(I) complexes and the kinetic data collected by this laboratory on the analogue Rh(I) complexes can be used to compare with the iridium results. The information gained from the combination of these studies is of great importance to understand the ability of these complexes to act as catalysts as well as to understand the differences which are observed. Oxidative addition reactions received much more attention than the rest of the reactions involved in the catalytic process (see Scheme 1.1 and 1.2). This may be due to the fact that it is the rate-determining reaction step (or as IUPAC recommends, rate-controlling step (Espenson, 1981:9)) in the homogeneously catalysed carbonylation process for converting methanol to acetic acid.

Results obtained in this laboratory include the oxidative addition of CH_3I to various Rh(I) complexes such as [Rh(L-L')(CO)(PX_3)], where L-L' = different monocharged bidentate ligands containing five (Basson, Leipoldt, Roodt & Venter, 1987:31; Van Aswegen, Leipoldt, Potgieter, Roodt. & Van Zyl, 1991:369) and six-membered rings (Basson, Leipoldt & Nel, 1984:167; Roodt & Steyn, 2000:1) with various donor atoms (see Table 1.4). The different combinations of donor atoms employed include oxygen-oxygen, oxygen-nitrogen, oxygen-sulfur and sulfur-nitrogen atoms. The PX_3 entity in the general formulation of the rhodium complex represents different phosphine and phosphite ligands which are given in Table 1.3 (X = Ph, *p*-$OCH_3C_6H_4$, *p*-ClC_6H_4, Cy, *etc*.). The oxidative addition reaction is given in Scheme 1.2.

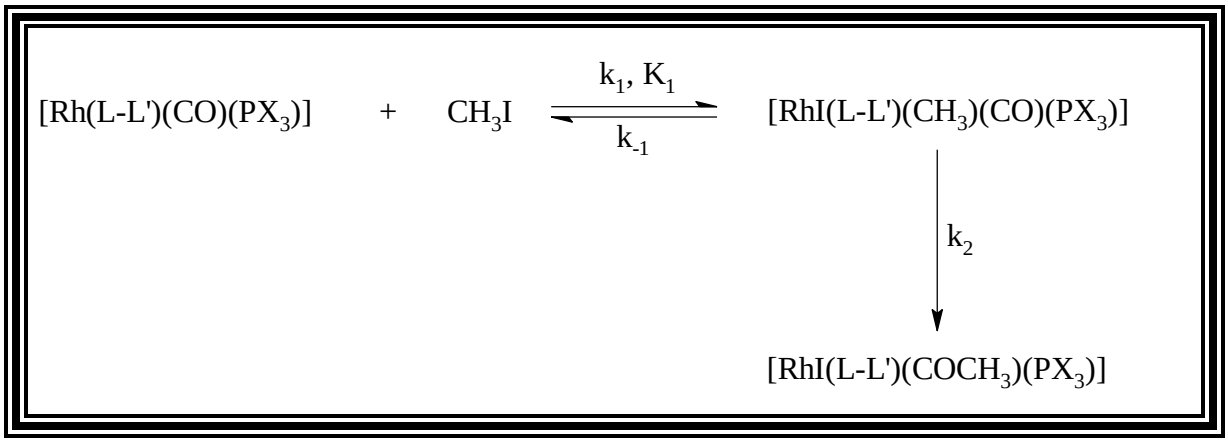

Scheme 1.2 The reaction steps in oxidative addition reactions.

The kinetic data obtained from these studies indicate that the rate of oxidative addition of these complexes is influenced by the nucleophilicity of the metal centre and hence the electronic (electron donation or withdrawing property) and steric demand of the ligands in the metal coordination sphere. The effect of the ligands on the metal centre will be discussed in detail in Chapter 2. It was found that phosphines with the less steric influence (bulkiness) and strongest electron donating ability such as P(*p*-$MeOC_6H_4)_3$ (see Table 1.3 for parameters) increase the electron density of the metal centre and enhance the rate of the reaction. Steric effects of phosphines are commonly measured by the Tolman cone angle and the electronic effect is measured in terms of pK_a. A detailed discussion on the steric effects of ligands will also be given in Chapter 2. According to the technique of measurement, steric hindrance is directly proportional to the cone angle, *i.e.* the larger the cone angle, the larger the steric hindrance. Some of the results obtained are shown in Tables 1.3 and 1.4.

Kinetic results are reported in Table 1.3 for the oxidative addition reactions of a number of different [Rh(cupf)(CO)(PX_3)] complexes with CH_3I. It is clear from these results that the different PX_3 ligands have a large influence on the rate of the oxidative addition. These differences can be attributed to either steric and/or electronic effects. The cone

angle for the three different phosphine ligands, P(*p*-$MeOC_6H_4)_3$, PPh_3, P(*p*-$ClC_6H_4)_3$ is 145º. The rate of oxidative addition however, is in the order P(*p*-$MeOC_6H_4)_3$ > PPh_3 > P(*p*-$ClC_6H_4)_3$. The difference in the rate of oxidative addition is clearly not due to steric effects (have same cone angle) but can only be attributed to the electronic effects which increases in the same order, i.e. P(*p*-$MeOC_6H_4)_3$ > PPh_3 > P(*p*-$ClC_6H_4)_3$.

Table 1.3 Oxidative addition reactions of different [Rh(cupf)(CO)(PX_3)] complexes with CH_3I in acetone at 25 ºC (Basson *et al*., 1987:31).

PX_3	**pK_a**	**Cone angle(θ)**	**$10^3k_1(M^{-1}s^{-1})$**
P(*p*-$MeOC_6H_4)_3$	4.57	145	4.2(0)
PCy_3	9.65	170	1.94(3)
PPh_3	2.73	145	1.22(2)
P(*o*-Tol)$_3$	3.08	194	0.21(2)
P(*p*-$ClC_6H_4)_3$	1.03	145	0.193(8)
$PPh_2C_6F_5$	--	158	0.091(0)

Another interesting factor that emerges from this set of results is that PPh_3 and P(*o*-Tol)$_3$ have comparative electronic effects (pK_a 2.73 and 3.08 respectively) but the rate of oxidative addition differs by a factor of almost 6. The difference in the rate of oxidative addition is attributed to steric effect which is clearly demonstrated by the large difference in cone angle between these two complexes. A number of different [Rh(β-diketone)(P(OPh)$_3)_2$] complexes were also studied in an effort to control the different parameters that may influence the rate of oxidative addition (Van Zyl, Lamprecht, Leipoldt & Swaddle, 1988:223).

The influence of different bidentate ligands on the rate of the reaction was also studied. These results are given in Table 1.4. The two most prominent factors from these results were the use of different sets of donor atoms as well as bidentate ligands having either five or six membered rings.

Table 1.4 Oxidative addition between different [Rh(L-L')(CO)(PX_3)] type of complexes and CH_3I in $CHCl_3$ at 25 °C.

L-L'[a]	L-L'	Ring size	$10^3 k_1^C / M^{-1}s^{-1}$	Ref.
Hfaa	O,O	6	0.13(1)	(Basson *et al.*, 1984:167)
Cupf	O,O	5	1.2(1)	(Leipoldt *et al.*, 1986:35)
Acac	O,O	6	24(4)	(Basson *et al.*, 1984:167)
Ox[b]	O,N	5	30(1)	(Van Aswegen, 1990)
Dmavk	O,N	6	114(2)	(Roodt & Steyn, 2000:1)
Sacac	O,S	6	40(9)	(Leipoldt *et al.*, 1990:215)
Anmeth	O,S	5	24(3)	(Preston, 1993)
Macsm	N,S	6	34(1)	(Roodt *et al.*, 1992:3477)
Cacsm	N,S	6	56(1)	(Roodt & Steyn, 2000:1)
Macsh	N,S	6	380(10)	(Leipoldt *et al.*, 1993:25)

a) See list of abbreviations. b) In acetone.
c) k_1 see Scheme 1.2

The large electronic influence of the electron rich sulfur-nitrogen donor is evident when it is compared to the electron poor O,O combination of donor atoms, clearly illustrating the isolated effect of ligands which influence the electron density on the metal centre.

A number of generalisations could be made from the results obtained in a number of studies, namely:

1. Strong electron donating phosphines increase the electron density of the metal centre and enhance the rate of oxidative addition reaction. However, bulky/steric ligands, even with a strong electron donating power such as the PCy_3 ligand with pK_a = 9.65 and cone angle of 170, decrease the rate of the reaction by shielding the metal centre from being attacked by substrates such as CH_3I (see Table 1.3). Similar kinetic results are also obtained for other phosphine ligands.

2. Bidentate ligands with the N,S donor atoms combination were observed to favour the rate of oxidative addition reaction relative to complexes containing

oxygen-oxygen, oxygen-nitrogen, and oxygen-sulfur atom combinations. However, bulky substituents on the binding atoms inhibit the rate of the reaction (compare k for cacsm and macsh in Table 1.4). It was found that the cyclohexyl group bound to the nitrogen atom in the cacsm bidentate ligand is bulkier than the methyl group on the same binding site in the macsh system. Moreover, electronegative substituents on the bidentate ligands or on the P-atom withdraw electron density from the metal centre and decrease the rate of oxidative addition reactions. For example, a significant decrease in reaction rate was observed when the two methyl groups on the acac bidentate ligand (see Table 1.4) were replaced by the two CF_3 groups (electron withdrawing groups) in the hfaa bidentate ligand.

3. The combination of all these results confirmed that both the electronic and steric properties of a ligand are operative during the oxidative addition reactions.

4. Another general observation is that the bite-angle (chelate size) of the bidentate ligand, i.e. the stereochemical demand of L-L', has a significant influence on the rate of the reaction. Generally, the equilibrium constant of complexes containing five-membered rings is much larger than those which contain a six-membered ring. This shows the relative thermodynamic stability of the alkyl intermediate of the former complexes.

5. Oxidative addition reactions are also found to be influenced by solvent variations (Basson *et al*., 1987:31; Scott, Shriver & Lehman, 1970:73; Ugo, Pasini, Fusi & Cemini, 1972:7364). In general, highly polar solvents are observed to accelerate the rate of the reaction and hence in a few cases solvent pathways were detected (Basson *et al*., 1987:31). However, in some other cases no

significant effect was exhibited even in highly polar solvents such as acetonitrile and nitromethane (Roodt & Steyn, 2000:1; Venter, Leipoldt & Eldik, 1991:2207).

It can be seen from the summary of results in Table 1.3 and Table 1.4 that a large variety of phosphines and phosphites, particularly the former, combined with different bidentate ligands have been studied in this laboratory. Clearly missing from these tables is the research done on the corresponding arsine and stibine ligands. This study is the beginning of the process to address some of the shortcomings in the research of oxidative addition reactions of Rh(I) complexes and to find answers to all factors that govern the oxidative addition reactions, particularly complexes containing arsine ligands. Some research has been done on the mechanism of carbonyl group substitution in square planar Rh(I) β-diketonato dicarbonyl complexes using arsine and stibine ligands as incoming groups.

It can also be seen from Table 1.4 that this study is not the first to use the cupferrate bidentate ligand in a Rh complex. The use of cupferrate instead of β-diketones as a bidentate ligand offered a substantial narrower bite angle in the [Rh(cupf)(CO)(PPh_3)] complex which could favour an asymmetric concerted addition step during the oxidative addition of an alkyl halide. A large number of the Rh(III) oxidative addition products were isolated and crystallographically characterised. All of these results clearly indicated a *trans* CH_3, I configuration (see Figure 1.2, 1). The crystal structure of [RhI(cupf)(CO)(CH_3)(PPh_3)] surprisingly yielded an unusual *cis* isomer (Basson *et al*., 1987:31) (see Figure 1.2, 2).

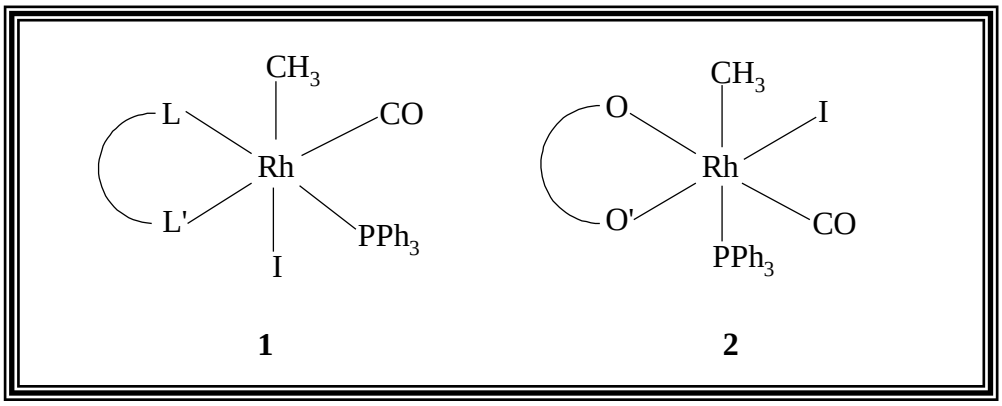

Figure 1.2 *Trans* and *cis* configuration of iodomethane after oxidative addition to a Rh(I) complex respectively where L-L' = bonded atoms of a bidentate ligand N-S, N-O, O-S and O-O' = cupferrate oxygens.

As an extension of the ongoing research, it was decided to explore the kinetic effects of triphenylarsine ligands on Rh(I) cupferrate complexes. The effect of the cupferrate bidentate ligand on the rate of oxidative addition is not well studied. The introduction of arsine ligands could help to investigate this effect as well as the electronic effects of $AsPh_3$ on the rate of oxidative addition.

With this background the objectives can be summarised as follows:

1. To synthesise a number of Rh(I) complexes containing arsine as a ligand, for example [Rh(cupf)(CO)($AsPh_3$)], [Rh(cupf)(CO)($AsMePh_2$)] as well as a new cupferrate ligand, [Rh(cupf.CH_3)(CO)($AsPh_3$)] where cupf = cupferrate (N-nitrosophenyl hydroxylamine) and cupf.CH_3 = methyl substituted cupferrate (2-methyl cupferrate) and to characterise these complexes by means of IR, UV/VIS spectroscopy and possibly X-ray crystallography.

2. To perform a kinetic study of the oxidative addition of iodomethane to [Rh(cupf)(CO)(AsX_3)] type of complexes in a range of different solvents. The

results will be compared with the oxidative addition reactions of iodomethane to [Rh(cupf)(CO)(PX_3)] from a previous study.

3. To determine a general reaction mechanism for the oxidative addition of iodomethane to [Rh(cupf)(CO)(AsX_3)] type of complexes by means of detailed kinetic studies utilising UV/VIS, IR and ^{1}H NMR techniques.

4. To study the electronic and steric effects of the $AsPh_3$, $AsMePh_2$ and the new bidentate ligand, 2-methyl cupf, on the reaction rate of the corresponding Rh(I) complexes with iodomethane.

5. To investigate the effect of organic halide substrates such as iodoethane and bromomethane on the rate of oxidative addition of these substrates with [Rh(cupf)(CO)($AsPh_3$)] and to compare the results with that obtained for iodomethane.

6. To probe the possibility of solvent effects on CO-insertion reactions by employing a range of solvents having different solvent properties. For this determination, the starting material would be the oxidative addition product, [RhI(cupf)(CO)(CH_3)($AsPh_3$)].

References

Basson, S.S., Leipoldt, J.G., and Nel, J.T., *Inorg. Chim. Acta*, (1984), **84**, 167.

Basson, S.S., Leipoldt, J.G., Roodt, A., Venter, J.A. and Van der Walt, T.J., *Inorg.Chim. Acta*, (1986), **119**, 35.

Basson, S.S., Leipoldt, J.G., Roodt, A., Venter, J.A., *Inorg. Chim. Acta*, (1987), **128**, 31.

Collman, J.P., Hegedus, L.S., Norton, J.R., Finke, R.G., *Principles And Application Of Organo Transition Metal Chemistry*, 1987, University Science Books, CA., part I.

Collman, J.P., Hegedus, L.S., Norton, J.R., Finke, R.G., *Principles And Application Of Organo Transition Metal Chemistry*, 1987, University Science Books, CA, part III Application to organic synthesis, 670-920.

Collman, J.P., Hegedus, L.S., Norton, J.R., Finke, R.G., *Principles And Application Of Organo Transition Metal Chemistry*, 1987, University Science Books, CA, part II Catalytic processes, 523-570.

Crabtree, R.H., *The Organometallic Chemistry of the Transition Metals*, 1988, Wiley Interscience pub., USA, 1.

Dickson, R.S., *Homogenous Catalysis With Compounds Of Rhodium And Iridium*, (1985), Reidel, D. pub.Co., The Netherlands, Chapter 1.

Espenson, J.H., *Chemical Kinetics and Reaction Mechanism*, 1981, 2nd edition, McGraw-Hill, Inc. USA, 9.

Forster, D., *J. Am. Chem. Soc.* (1976), **98**, 846.

Halpern, J., *Inorg. Chim. Acta*, (1981), **50**, 11.

Haynes, A., Mann, B.E., Morris, G.E., Maitlis, P.M., *J. Am. Chem. Soc.*, (1993), **115**, 4093.

Kjaer, J. H., Jorgensen, J.C., *J. Chem. Soc., Perkin Trans*. (1978), **2**, 763.

Leipoldt, J.G., Basson, S.S., and Botha, L.J., *Inorg. Chim. Acta*, (1990), **168**, 215.

Lukehart, C.M., *Fundamental Transition Metal Organometallic Chemistry*, 1985, Brooks Cole Pub. Co., CA., Chapter 12, Application to organic synthesis, 347-381.

Lukehart, C.M., *Fundamental Transition Metal Organometallic Chemistry*, 1985, Brooks Cole Pub. Co., CA., Chapter 13, Industrial catalysis, 388-410.

Maitlis, P.M., Haynes, A., Sunley, G.J. and Howard, M.J., *J. Chem. Soc. Dalton Trans*. (1996), 2187-2196.

Miller, S.A, Tebboth, J.A., Tremaine, J.F., *J. Chem. Soc*. (1952), 632.

Preston, H., (1993), *Ph.D. Thesis*, Free State University, Bloemfontein, South Africa.

Roodt, A. and Steyn, G.J.J., *Rec. Res. Inorg. Chem*. (2000), **2**, 1-23.

Sava, G., Zorzet, S., Perissin, L., Mestroni, G., Zassinovich G. and Bontempi, A., *Inorg. Chim. Acta,* (1987), **137**, 69.

Scott, R.N., Shriver, D.F., and Lehman, D.D., *Inorg. Chim. Acta*, (1970), **4**, 73.

Sherman, S.E. and Lippard, S.J., *Chem. Rev*. (1987), **87**, 1153.

Steyn, G.J.J., Roodt, A., and Leipoldt, J.G., *Inorg. Chem*. (1992), **31**, 3477.

Steyn, G.J.J., Roodt, A., and Leipoldt, J.G., *Rhodium Express,* (1993), 1, 25.

Ugo, R., Pasini, A., Fusi A., Cemini, S., *J. Am. Chem. Soc*. (1972), **94**, 7364.

Van Aswegen, K.G., (1990), *M.Sc. Thesis*, Free State University, Bloemfontein, South Africa.

Van Aswegen, K.G., Leipoldt, J.G., Potgieter, I.M., Roodt, A. and Van Zyl, G.J., *Trans. Met. Chem*. (1991), **16**, 369.

Van Zyl, G.J., Lamprecht, G.J., Leipoldt, J.G., and Swaddle T.S., *Inorg. Chim. Acta*, (1988), **143**, 223-227.

Venter, J.A., Leipoldt, J.G., and Van Eldik, R., *Inorg. Chem*. (1991), **30**, 2207-2209.

Young, J.F., Osborn, J.A., Jardine, F.H., Wilkinson, G., *Chem. Commun*. (1965), 131.

CHAPTER 2

OXIDATIVE ADDITION AND CO-INSERTION REACTIONS

2.1 CATALYSIS

2.1.1 Introduction

The existence of substances that speed up reactions was realised in the early years of the 19th century. In 1817 Sir Humphrey Davy found that he could prevent explosions in coal mines if he surrounded the candles used to illuminate the mines with a platinum shield. Seventeen years later Michael Faraday, the well-known chemist of his era, examined this observation and proposed that the platinum was catalysing the termination reaction in the flame by holding the reactants in close proximity so that they could react. The question remained about the exact nature of these substances called catalysts.

Ostwald (Masel, 2001:689) defined a catalyst as a substance that changes the rate of a reaction without being consumed in the process. Catalysts are widely used in nature, in industry, as well as in laboratories and the top 20 synthetic chemicals such as sulphuric acid, ammonia, benzene and methanol are all produced directly or indirectly using catalytic processes (Shriver *et al*., 1994:709).

Generally, catalysts increase the rate of reactions that would otherwise not proceed in a reasonable time (Shriver *et al*., 1994:715). Furthermore, Shriver *et al*. noted that catalysts have the ability to select one specific reaction pathway from several possibilities for a given substrate. By doing this, they improved the utilisation of raw materials and energy and avoid the formation of by-products and hence the amount of waste. In this way catalysis made an important contribution to the development of sustainable technologies and environmentally friendly processes.

2.1.2 Transition metals as homogeneous catalysts

Among the most significant development in inorganic and organometallic chemistry during the past several decades are those associated with the application of transition metal complexes as homogeneous catalysis in a variety of reactions (Halpern, 1981:11). The most important property of transition metals is their ability to be stabilized in a large number of different oxidation states. This allows the metal to undergo a variety of successive catalytic reactions such as oxidative addition and methyl migration, which are important steps in commercial homogeneous catalytic processes and in organometallic chemistry in general (Halpern, 1981:11 and Parshall & Putscher, 1986:188). This property helps the metal to acquire electrons from or supply electrons to its neighbour atom or group of atoms or molecules reversibly and under relatively mild conditions.

Transition metals are effective as catalysts due to the following properties:

- Ability to accommodate a large variety of ligands at the metal centre.
- Various oxidation states, which can readily be interconverted.
- Undergo versatile binding modes (e.g. in alkene binding).
- Various geometries can be predicted and tuned.

- ❖ Well defined stereochemistry of transformations.
- ❖ Coordination sphere can be tuned.

Transition metal catalysts demonstrate high selectivity in their reactions and have a long lifetime in the reaction mixture to survive through a large number of cycles, hence increasing its industrial preference. Of course, selective catalysts yield high proportions of the desired product with minimum amounts of side products. In a comparison of the selectivity of the BASF catalyst and the Monsanto catalyst for methanol carbonylation, the results indicate values of 90% and 99% respectively. The relative lack of selectivity of the cobalt catalyst in the BASF process increases the consumption of the starting materials, making the Monsanto process superior (Table1.1 Chapter 1).

Transition metals play an enormous role in many chemical production processes (Halpern, 1981:11). There are many examples of reactions that are catalysed by transition metal complexes, but only a few are listed in Table 2.1.

Table 2.1 Examples of reactions catalysed by homogeneous transition metal complexes.

Process (product)	**Catalyst**	**Ref.**
Alkene polymerisation	$[TiCl_2(C_5H_5)_2]^{+2}$ or $[TiCl_2/Al(C_2H_5)_3]$, Ziegler-Natta catalyst	a
Alkene hydrogenation	$[RhCl((PPh_3)_3]$, Wilkinson catalyst	b
Wacker process (acetaldehyde)	$[PdCl_2(OH)_2]$	c
Oxo process (aldehyde)	$[CoH(CO)_4]$	d
Monsanto process (acetic acid)	*cis*-$[RhI_2(CO)_2]^-$	e
Olefine hydrocyanation	$[Ni(P(OR)_3)_4]$	f

a) Crabtree, 1988:267 and Collman *et al*., 1987:584. b) Halpern & Wong, 1973:629 and Hussey & Yakeuchi, 1970:643. c) Shriver *et al*., 1994:727. and Halpern *et al*., 1981:11. d) Lukehart, 1985:400. e) Foster, 1976:846 and Haynes *et al*., 1993:4093. f) Tolman, 1968:199.

2.1.3 Monsanto acetic acid process

The Monsanto process concerns the production of large volumes of acetic acid from methanol, using a rhodium complex as catalyst (Lukehart, 1985:409: Shriver *et al*., 1994:726 and Haynes *et al*., 1996:2187). The overall reaction is in essence the insertion of a CO-group into a methanol molecule (Scheme 1.1, Chapter1).

(2.1)

Reaction Scheme 1.1 clearly indicates that this process is not a simple one, but one which involve numerous reactions around the very important *cis*-$[RhI_2(CO)_2]^-$ catalyst. From the reaction scheme it can be seen that the conversion of methanol to acetic acid involve an oxidative addition step followed by the CO-insertion step and finally a reductive elimination step with the formation of CH_3COI. The CH_3COI is finally converted to CH_3COOH by the introduction of water into the reaction mixture. The whole catalytic process is initiated by the reaction between methanol and iodic acid (HI).

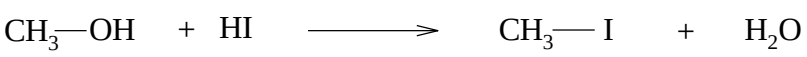

(2.2)

The formation of iodomethane is the essential species that react with the rhodium catalyst. Once methyl iodide has been generated, the catalytic cycle begins with the oxidative addition of methyl iodide to *cis*-$[RhI_2(CO)_2]^-$. In this step the rhodium metal centre is oxidised from the +1 oxidation state to the +3 oxidation state. Coordination and insertion of carbon monoxide leads to an 18-electron acyl intermediate complex which then undergoes reductive elimination to yield acetyl iodide and regenerates the catalyst. In this step the Rh(III) is reduced back to the Rh(I) metal. Spectroscopic investigations with IR and NMR confirmed the existence of the various Rh-species while GC (gas

chromatography) analysis of the reaction solution showed the presence of acetic acid and methyl acetate in solution (Forster, 1976:846).

There are clearly two reaction cycles involved in this catalytic process. Cycle (I) involves the methanol/HI reaction while cycle (II) involves the metal complex. The acetyl iodide produced in cycle (II) is then hydrolysed in part (I) to give acetic acid. In other words, the catalytic cycle begins and ends at the iodide sub-cycle. The hydrolysis step shown in Reaction 2.3 produces the desired product and the HI which is formed as a product can react with methanol to regenerate iodomethane which starts the whole catalytic process again.

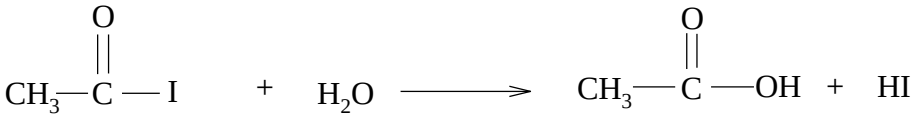

(2.3)

The Monsanto process is an example of a well-studied catalytic process which clearly demonstrates that these processes are based on the repetition of a small set of reaction types such as oxidative addition, its microscopic reverse (reductive elimination) and R-migration or CO–insertion (Foster, 1976:846; Haynes *et al*., 1993:4093 and Parshall & Putscher, 1986:188).

The oxidative addition reaction is the rate-controlling step in many catalytic cycles and it is an important route for incorporating substrate molecules into organometallic complexes (Haynes *et al*., 1996:2187 and Forster, 1976:846). The CO-insertion reaction or R-migration on the other hand plays a vital role in functionalising the substrate, which is already co-ordinated to the metal. The reductive elimination reaction step is also very important since it is the product-forming step and consequently reduces the formal oxidation state of the metal by two units thereby making it susceptible for a further

oxidative addition reaction, continuing the cycle this way. Although the Monsanto process is still widely used, it is further developed to the Cativa process where iridium is employed as the metal centre. Forster's (1976:846) mechanistic studies of iridium-catalysed methanol carbonylation showed many similarities to the rhodium system, but with a larger degree of complexity, due to the participation of both neutral and anionic species. High-pressure IR spectroscopic studies showed that the main species present were the iridium(III) complexes $[IrI_2(CH_3)(CO)_2]^-$ and $[IrI_2(CO)_4]^-$. The latter is inactive and needs to be reduced to $[IrI_2(CO)_2]^-$ before it can further participate in the cycle. A similar inactive species, $[RhI_4(CO)_2]^-$, forms in the rhodium-catalysed reaction but is more easily reduced and is therefore less troublesome. The principal difference between the two processes is a change in the rate-controlling step. Oxidative addition is the rate-controlling reaction step in the Monsanto process whereas CO-insertion is in the Cativa process. Haynes *et al*. (1996:2187) noted that the catalyst in the Cativa process, $[IrI_2(CO)_2]^-$, oxidatively adds organic iodides *ca*. 150 times faster than $[RhI_2(CO)_2]^-$, and CO-insertion on iridium(III) is five to six orders of magnitude slower than the Monsanto process. In contrast to the rhodium system, where specially chosen conditions were required to detect the rhodium-methyl complex, $[RhI_2(CH_3)(CO)_2]^-$, salts of the iridium analogue, $[IrI_2(CH_3)(CO)_2]^-$, are stable and isolable and there is no tendency for spontaneous isomerisation to an acyl complex (Haynes *et al*.,1996:2187). However, adding either methyl or a Lewis acid (SnI_2) can significantly activate the slow CO-insertion for the iridium system.

2.2 GENERAL FEATURES OF MONSANTO TYPE CATALYTIC REACTIONS

2.2.1 Oxidative addition reactions

Low-valent complexes of transition metals, in particular group VIII, IX and X metals, with a d^8 and d^{10} electron configuration prefer the formation of square planar complexes.

These metal ions have the ability to form strong covalent bonds with ligands such as RX, R = alkyl (Hench, 1964:2796; Chock & Halpern, 1966:3511 and Ugo *et al*., 1972:7364), R = aryl (Ugo *et al*., 1972:7364) and X = halide ions; H_2 (Vaska & Diluzio, 1961:2784; 1962:679; Chock & Halpern, 1966:3511 and Ugo *et al*., 1972:7364), O_2 (Vaska *et al*., 1975:2669; Chock & Halpern, 1966:3511 and Ugo *et al*., 1972:7364), I_2 (Vaska *et al*., 1975:2669; Chock & Halpern, 1966:3511) as well as inorganic and organic acids such as HX, X = Cl (Vaska *et al*., 1975:2669), Si-H (Johnson & Eisenberg, 1985:6531), CH_3COBr and CF_3COCl (Oliver & Graham, 1970:243), *etc*., and increase their coordination sphere from 4 to 6 to form hexa-coordinated complexes with a d^6 configuration. These types of reactions are called oxidative addition reactions. It is the simultaneous change in oxidation state and the addition of substrates that give the reaction its name.

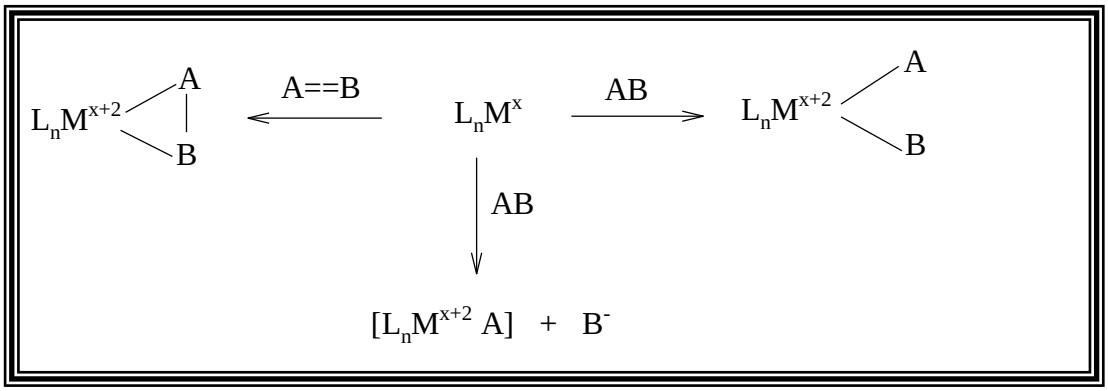

Scheme 2.1 General progress of oxidative addition reactions.

A common example of an oxidative addition reaction is the reaction between Vaska's complex and H_2 which is the key step in the hydrogenation of alkenes and other related reactions, as indicated in Reaction 2.4. A *cis*-dihydrogen Ir(III) complex is produced (Lukehart, 1985:279 and Cross, 1985:197).

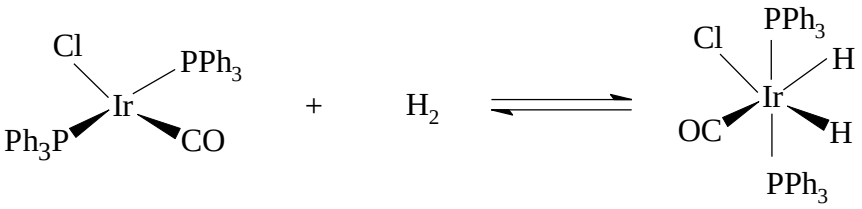

(2.4)

In this reaction the Ir metal centre is oxidised from the +1 oxidation state to the +3 oxidation state. The transfer of the two electrons from the metal to the incoming substrate allows for the dissociation of the H−H bond and two new bonds are subsequently formed with the metal centre. As a result, the complex changes from a co-ordinatively unsaturated $16e^-$ complex to a saturated $18e^-$ complex. Evidence in literature (Fauvarque *et al*., 1981:419), however, indicates that $18e^-$ species can undergo reversible dissociation in solution to give unsaturated $16e^-$ or $14e^-$ complexes which are often highly susceptible to oxidative additions.

For oxidative additions to proceed, the following important characteristic must be present:

1) The metal centre should possess non-bonding electron density. Research also indicates that metal centres in the low oxidation states have a greater tendency to undergo oxidative addition reactions. For example, oxidative addition from Ir(I) to Ir(III) is common but an oxidative addition from Fe(III) to Fe(V), while possible, is generally unlikely.

2) The complex should also be co-ordinatively unsaturated with at least two vacant coordination sites available for the formation of two new bonds with the A or B fractions of the addend substrate molecule. A common example is the oxidative addition of various substrates AB to Vaska's complexes,

$$[IrX(CO)L_2] \quad + \quad AB \quad \rightleftharpoons \quad [IrXAB(CO)L_2]$$

(2.5)

AB = RX, RCOX, R_3SnX, R_3SiX, CH_3HgX (X = Cl, Br, I), RNCS, HCl, RCOOH, and diatoms such as H_2, O_2, I_2 (Cotton & Wilkinson, 1972:774).

3) The metal centre should also be able to change its oxidation state by 2 units and the oxidation states of both the starting and final product have to be relatively stable. Some octahedral platinum(IV) complexes (products of oxidative addition to square planar Pt(II) species) were found to isomerise readily by ligand loss to form five co-ordinate cations (Appleton *et al*., 1974:275).

4) The likelihood of oxidative addition of a substrate A−B to a metal centre, M, depends on the relative strengths of the A−B, M−A and M−B bonds (*http://www.ilpi.com/organomet*). Oxidative addition of an alkane is, for example, much less common than the oxidative addition of an alkyl halide. The reason for this is that the C−H bond in alkanes are fairly strong compared to the M−H and M−R bonds. In the Monsanto process (Chapter 1 Scheme 1.1), methanol is made to react with HI in the iodide cycle to generate CH_3I since it is easier to break the C–I bond compared to that of the C–O bond.

Oxidative additions can be classified according to the nature of the substrate or the mechanism followed or types of complexes involved. Lukehart (1985:276) categorised oxidative addition reactions into three major classes depending on the type of reactant complexes; as five-coordinate d^7-complexes, four-coordinate d^8-complexes and two-coordinate d^{10}-complexes. Square planar four-coordinated $16e^-$ complexes such as Vaska's complexes undergo oxidative addition reactions with a range of substrate molecules such as HCl, H_2 and O_2, and nearly all organic halides. Some of the d^8 metals

and their reactivity towards oxidative addition can be presented in the following order (Lukehart, 1985:278):

$$Os^{0} > Ru^{0} > Fe^{0} >> Ir^{+1} > Rh^{+1} > Co^{+1} >> Pt^{+1} > Pd^{+2} >> Ni^{+2}, Au^{+3} \quad \textbf{(2.6)}$$

The higher oxidation states are usually more stable for the heavier than for the lighter metals (Cotton & Wilkinson, 1972:773). In other words, Purcell & Kotz (1977:943) reported that the lower oxidation states of the heavier metals show the greatest tendency to undergo oxidative addition reactions. In any case, since oxidative addition reactions involve oxidation (losing of electrons) from the metal centre, the more electron-rich the metal is, the more facile the reaction becomes. However, as stated previously, the starting and the final oxidation states must be relatively stable and steric factors have to be considered. Table 2.2 summarises broadly oxidative addition reactions of different substrates to different complexes of Rh(I) and Ir(I).

The table shows the effect of the metal centre, different phosphines and various substrates towards the reaction. For example, the second-order rate constant increases an order of magnitude when Rh in [RhCl(CO)(PPh_3)] is replaced by Ir. The enhancement in reactivity is clearly due to an increase in the Lewis basicity of the Ir metal. Literature by by Purcell & Kotz (1977:944) indicates that Lewis basicity of transition metals increase down the group. For the ligands k (P(*p*-C_6H_4–OMe)$_3$) > k (P(*p*-C_6H_4–Cl)$_3$), though, both have the same metal centre, the rate difference represents a three order of magnitude increase. As expected, a strong donating substituent (like methoxy) on the P-atom increases the electron density or Lewis basicity of the Ir-centre and as result the rate of the reaction enhances. On the other hand, bulky phosphines such as P(*o*-Tol)$_3$ and PCy_3 are found to hinder oxidative addition, particularly the former ligand makes the complex unreactive even toward substrates with the least steric demand, H_2 and O_2. Ligands with a large steric demand can also lead to different products, for example, a study conducted

by Empsall *et al*. (1974:1980) shows the effect of steric crowding on the rate of oxidative addition. This study shows that *trans*-[RhCl(CO){PMe_2(*o*-MeO-Ph)}$_2$] undergoes oxidative addition with a variety of small molecules such as HCl, MeI, CCl_4 and Cl_2 but the more crowded *trans*-[RhCl(CO){$P(t\text{-}Bu)_2$(*o*-MeO-Ph)}$_2$] does not react with them, but rather demethylates with loss of CH_3 and Cl.

Table 2.2 Kinetic data for oxidative addition reactions of [$MX(CO)(PR_3)_2$] in benzene at 25 °C.

M	X	PR_3	Reactant	k, M^{-1} s^{-1}	Ref.
Ir	Cl	PPh_3	H_2	0.67	d
	Cl	P(*o*-Tol)$_3$	H_2	No reaction[a]	e
	Br	PPh_3	H_2	10.5	d
	I	PPh_3	H_2	> 100	d
Ir	Cl	PPh_3	O_2	3.4×10^{-2}	d
	Cl	P(*o*-Tol)$_3$	O_2	No reaction.[b]	e
	Br	PPh_3	O_2	7.4×10^{-2}	d
	I	PPh_3	O_2	30×10^{-2}	d
Ir [c]	Cl	PPh_3	HCl	1.1×10^4	e
		PCy_3	HCl	≤4.0	e
		P(*o*-Tol)$_3$	HCl	0.79	e
Ir	Cl	PPh_3	CH_3I	3.5×10^{-3}	d
	Br	PPh_3	CH_3I	1.6×10^{-3}	d
	I	PPh_3	CH_3I	0.9×10^{-3}	d
Ir	Cl	P(*p*-C_6H_4-OMe)$_3$	CH_3I	3.5×10^{-2}	f
		P(*p*-C_6H_4-Cl)$_3$	CH_3I	3.7×10^{-5}	f
Rh	Cl	PPh_3	CH_3I	12.7×10^{-4}	g
		P(*p*-C_6H_4-OMe)$_3$	CH_3I	51.5×10^{-4}	g

a) No reaction in 3hr at 740mm, in chlorobenzene at 30 °C.
b) No reaction in 18 days at 700mm, in chlorobenzene at 30 °C. c) In benzene at 30 °C.
d) Chock & Halpern, 1966:3511. e) Vaska *et al*., 1975:2669. f) Ugo *et al*., 1972:7364.
e) Douek & Wilkinson, 1964:2604.

Another interesting piece of information from the table is that the rate for O_2 and H_2 addition in terms of the halogen ligand follows the order I > Br > Cl. But the reaction with CH_3I exhibits a somewhat different reactivity pattern, i.e. the dependence of the rate on the halogen ligand follows the reverse order, Cl > Br > I. This pattern is due to steric factors caused by the increase in size of the halide, affecting the nucleophillic attack of the metal d_{Z^2} orbital on CH_3I in order to start the oxidative addition reaction. Pauling's univalent radii for the halides, Cl, Br and I, are 1.81, 1.95, and 2.16 Å respectively (Ball & Norbury, 1974:136). This is indeed direct evidence that oxidative addition of iodomethane to such complexes follows a different mechanism, probably an S_N2 mechanism. The kinetic patterns of the reactions with H_2 and O_2 are very similar, despite the fact that a decrease in k from H_2 to O_2 additions can be noted, reflecting the greater steric requirements of dioxygen in the product.

To conclude, various kinetic studies have shown that strong donor ligands with weak π-acceptor abilities increase the electron density of the metal centre and enhance the rate of oxidative addition reactions (Kubota *et al.*, 1973:195 and Deeming & Shaw, 1969:1802). However, as discussed above, bulky substituents or ligands can retard or even obstruct the reaction. Of importance is that both polar and non-polar species such as dihydrogen, halogens, hydrogen halides, alkyl halides, acyl halides, organotin halides, mercuric halides, organosilicon halides, organosilicon hydrides and other similar compounds can add to these transition metal compounds to produce different products.

2.2.2 Carbonyl insertion reactions

The second important type of reaction in the Monsanto process is the carbonyl insertion reaction with subsequent acyl formation. The mechanism of the formation of the acyl group has long been a contentious issue. The question is whether the process involves the breaking of the CH_3 bond with CO-insertion between Rh and the CH_3 group, or

whether the CH_3 group migrates to CO to afford the acyl group. Broad discussion will be given in the next paragraphs.

In general, insertion reactions are usually characterised by addition of a metal-ligand bond to a substrate molecule such that the coordination number and formal oxidation state of M does not change (Lukehart, 1985:233). These insertion reactions involve a number of steps. The first step generally involves the coordination of an unsaturated ligand, Y, which is then inserted into an adjacent metal–ligand bond (M−X). Consequently another incoming ligand (L') usually occupies the vacant coordination site which is created due to the insertion of Y. Numerous studies have been done in an effort to determine the mechanism of the process. Generally, insertion reactions can be presented as follows:

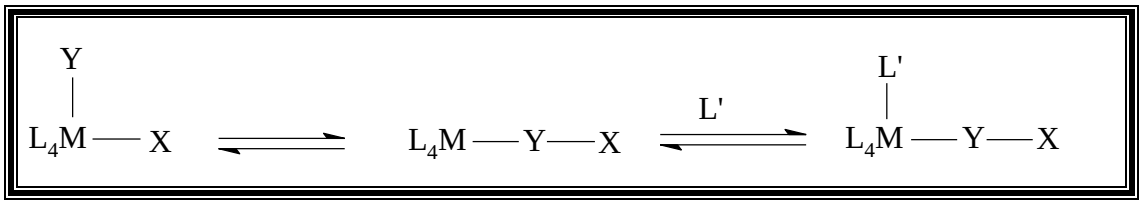

Scheme 2.2 General reaction formula for insertion reactions.

Y = CO, alkenes, alkynes, aryl. L = ligands (including solvents).
X = hydrogen (H), alkyls, aryl. M = transition metal.

Research has shown that carbon monoxide has a strong tendency to insert into metal alkyl bonds to form an acyl complex (Calderazzo & Cotton, 1962:30). This reaction increases the carbon chain of the alkyl by one carbon atom and importantly introduces a carbonyl functional group whereby various organic compounds such as alcohols, acetic acid, acetic anhydrides, aldehydes *etc*. can be produced (Halpern, 1981:11 and Collman *et al*., 1987:681-940).

Three possible mechanistic routes (referred to in the next paragraph), are possible for the formation of the acyl group. Various experimental and theoretical evidence, based on

computational studies, have led to an acceptable mechanism and the uncertainty with the exact nature of the process has been resolved. The best-known and extensively studied mechanistic route of CO-insertion is based on the reaction presented in Scheme 2.3 (Lukehart, 1985:245: Calderazzo 1977:299 and Cotton & Wilkinson, 1972:777).

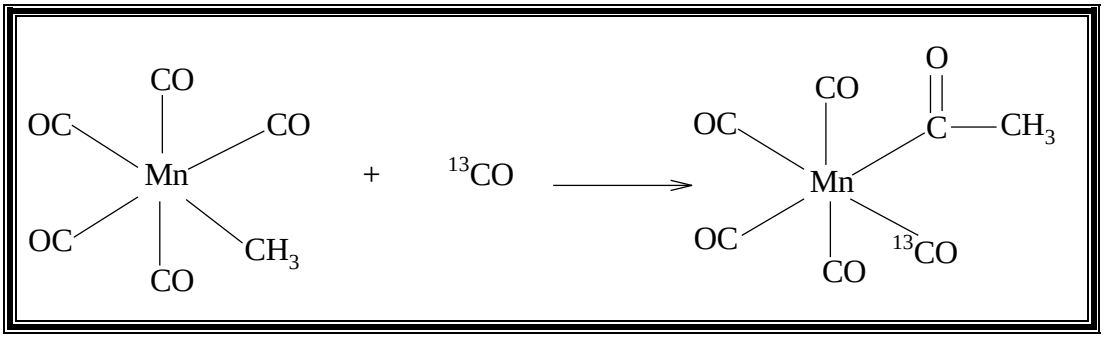

Scheme 2.3 Insertion of CO into Mn–C bond.

The reaction was studied using isotopic labelled ^{13}CO gas as an incoming ligand. Spectroscopic investigations revealed that the product contained the labelled CO *cis* to the newly formed acyl group (Scheme 2.3). This evidence showed that the methyl group migrates to a *cis* co-ordinated CO group, rather than the free CO attacking the Mn–C bond. In other words ^{13}CO occupies the vacant coordination site, which is created by CH_3 migration, to form the octahedral complex.

The mechanism for CO-insertion reactions has also been studied with various theoretical methods such as ab initio molecular orbital (MO) and symmetry arguments. With the ab initio energy gradient method, the structure of a transition state complex as well as the reactant and products can be optimised. The goal of performing a geometry optimisation calculation is to characterise the potential energy minimum of an unknown structure. Sakaki *et al*. (1983:2280) have studied the mechanism of the following reaction with the energy gradient method.

$$[Pt(F)(CH_3)(CO)(PH_3)] \longrightarrow [Pt(F)(COCH_3)(PH_3)] \qquad \textbf{(2.7)}$$

While the structures of the reactant and product are optimised, the geometry of the reaction system was changed in a stepwise fashion in order to simulate the three proposed reaction pathways of CO-insertion, namely:

1) methyl migration
2) CO-migration
3) concerted CO and methyl migration

According to the result obtained, methyl migration was the easiest (lowest potential) and CO-migration was the most difficult process (large potential). Furthermore, Koga and Morokuma (1985:7230 and 1986:6536) have conducted a similar study for a number of d^8 square planar complexes, as indicated in reaction 2.8.

$$[M(CH_3)(H)(CO)(PH_3)] \longrightarrow [M(COCH_3)(H)(PH_3)] \qquad \textbf{(2.8)}$$

M = Pd, Pt

The structure determination with the energy gradient method has shown that the formation of a three-centred transition state is the preferred mechanistic pathway and that the methyl group migrates to the CO group. However, there is an example in the literature that shows how both methyl and CO migration appear to operate. The optically active $[Fe(C_5H_5)(Et)(CO)(PPh_3)]$ was used to determine which of the CO or ethyl group migrates during the reaction (*http://www.ilpi.com/organomet/insertion.html*). The results obtained from the study indicate that the mechanism depends on the solvent used for the reaction. When the reaction was performed in hexamethylphosphoric triamide (HMPA), it was found that the CO ligand migrated to the ethyl group, whereas in a solution of nitroethyl ($EtNO_2$) the ethyl ligand was found to undergo migration. The role of the solvent in the reaction is not yet well known.

A likely explanation for the commonly observed methyl migration in the methanol carbonylation reactions is that the co-ordinated CO is highly unsaturated which makes it highly susceptible to neighbouring nucleophiles. The perceived CO insertion into the M–CH_3 bond takes place *via* a three-centred transition state as intramolecular nucleophilic attack of the alkyl on the CO group proceeds to form the final acyl species. Unlike oxidative addition reactions, intramolecular CO insertion or alkyl migration reactions do not result in the change in formal oxidation state.

2.2.3 Recent developments regarding ligands

Very recently, computational studies such as QM/MM (combined quantum mechanics/molecular mechanics) reported the electronic and steric influences of a variety of ligands on the energy barriers of the migratory carbonyl insertion in complexes like $[RhI_2(CH_3)(CO)(L\text{-}L)]$, where L–L = $PPh_2CH_2P(S)Ph_2$ (dppms), $PPh_2CH_2CH_2PPh_2$, (dppe), and the Monsanto catalyst, *cis*-$[RhI_2(CO)_2]^-$. Calculated energy barriers and the activation energies for the dppms and dppe systems were in excellent agreement. Interesting results were obtained particularly in the case of the dppms system which seems to contradict the belief that electron-donating ligands retard CO-insertion.

The original *cis*-$[RhI_2(CO)_2]^-$ catalyst was developed by Monsanto and later studied by Foster (1976:846). The catalyst was modified then by BP chemicals using the Ir analogue, which is used in the Cativa process (Haynes *et al*., 1996:2187). However, attempts to modify the original catalyst and increase its activity by introducing stronger electron-donating ligands has been unsuccessful, either due to the instability of the complexes under the harsh reaction conditions required for carbonylation or that the reaction conditions under which they were studied were not well suited for the commercial processes (Wegman *et al*., 1987:1891). The studies focused on the modification of the phosphine ligand as well as on several Rh complexes. Complexes utilising various phosphine ligands were synthesised and tested as catalysts. For

example, the catalytic performance using monophosphine, PEt_3 (Rankin *et al*., 1997:1835) diphosphine (dppe) (Moloy & Wegman, 1989:2889) and mixed bidentate phosphines such as dppms (Baker *et al*., 1995:197 and Haynes *et al*., 1999:11233) and $PPh_2CH_2P(NPh)Ph_2$ (dppmn) (Katti *et al*., 1993:5919) were similar to, or better than the original *cis*-$[RhI_2(CO)_2]^-$ catalyst used in the Monsanto process. These results indicate that comparative reaction rates can be achieved in a neutral rhodium(I) complex with appropriate donor ligands.

As mentioned above, all these new ligands enhanced the oxidative addition step in the catalytic process. For example, Haynes *et al*. (1999:11233) found that the oxidative addition of CH_3I with dppms or dppe as ligands is *ca*. 50 times faster than the corresponding reaction of the $[RhI_2(CO)_2]^-$ system but very similar to the rates reported for $[Rh(I)(CO)(PEt_3)_2]$ (Rankin *et al*., 1997:1835). However, the subsequent CO-insertions were retarded for the reactions, except in the case of the dppms complex. A stable methyl product was isolated with $[Rh(I)(CO)(PEt_3)_2]$. Although X-ray characterisation of the product reveals that the methyl group is positioned *cis* to CO which is assumed to favour migration, it only does so under a CO atmosphere. The intermediate, $[RhI_2(CH_3)(CO)(dppe)]$, is relatively stable with a half-life longer than 60 minutes (Baker *et al*., 1995:197). These results can partly be explained by the formation of a stronger than usual $Rh{-}CH_3$ bond as well as an increase in electron density at the metal centre, which leads to stronger back-bonding ($M(d) \longrightarrow CO(\pi^*)$) which in turn increases the electron density on the carbonyl group. That is also thought to inhibit CO-insertion (Cavallo & Sola, 2001:12294).

Interestingly, the migratory CO insertion for the reaction between MeI and the [Rh(I)(CO)(dppms)] system (Haynes *et al*., 1999:11233) is unexpectedly accelerated when compared to the original Monsanto catalyst and to [RhI(CO)(dppe)]. The rate of insertion at 25 ^oC is ~3 orders of magnitude larger than the dppe system. The explanation for the rapid migratory insertion of the dppms system is based on the x-ray

crystallographic result of its Ir-analogue, $[IrI_2(CH_3)(CO)(dppms)]$. The structure shows close contact between the hydrogens of the phenyl and the methyl group which would force it to undergo migratory insertion to release the high degree of steric forces in the complex. Thus, the rate enhancement has a steric origin. The presence of this abnormal degree of steric interaction was the only reason for researchers to explain this large increase in the reaction rate since the general interpretation or belief is that electron-donating ligands in general retard CO-insertion.

Very recently Carles Bo *et al*. (2003:92) utilised modulate computational chemistry to interpret the fast migratory insertion of the dppms system. According to their results the large increase in the rate of the insertion step should be attributed to the different properties of sulfide-phosphine (π–donor) ligands and phosphine (π–acid) ligands. Their molecular orbital calculations showed that the dppms ligand strongly increases the degree of back-bonding to CO as the S atom is situated *trans* to the CO group which favours the orbital overlap between the CO and methyl group (Carles Bo *et al*., 2003:92 and Cavallo & Sola, 2001:12294). The conclusion drawn was that the sulphide-phosphine ligand such as dppms accelerates CO-insertion, due to its π-donor capability rather than steric parameters.

In the same study by Carles Bo *et al*. it was found that the complexes containing the most electron-donating phosphine (with X = Me) react the slowest with regard to CO-insertion and the most electron-withdrawing phosphine group (with X = F) reacts rapidly. Complexes containing the three phosphine substituents studied, reacted in the following order: F >> H > Me. The influence of the ligands is more profound when the phosphine ligand occupies a position *trans* to the CO group. Hence, what seemed to be a contradiction was put into perspective with the realisation that the behaviour of a π–acceptor ligand should not be extrapolated to that of a π-donor ligand such as sulphur.

2.2.4 Reductive elimination

Reductive elimination is in principle the reverse reaction of oxidative addition (Lukehart, 1985:290 and Cotton & Wilkinson, 1972:772). It is frequently the product-releasing reaction step in homogeneous catalytic processes.

$$[M^{n}(L\text{-}L')(CO)(PX_3)] \quad + \quad CH_3I \quad \underset{\text{Red. elim.}}{\overset{\text{Oxd. add.}}{\rightleftharpoons}} \quad [M^{n+2}I(L\text{-}L')(CO)(CH_3)(PX_3)] \qquad \textbf{(2.9)}$$

Whether the equilibrium lies on the reduced or the oxidised side depends on the nature of the metal complex and its ligands, the nature of the addend molecule AB and the M–A and M–B bond formed as well as on the medium in which the reaction is conducted (Cotton & Wilkinson, 1972:774). For example, strong electron donating phosphines make the equilibria to lie further to the M^{n+2} side (Cotton & Wilkinson, 1972:775).

Metal complexes can undergo one or more chemical reactions such as alkyl migration to carbonyl ligands while all the groups are still associated with the same metal centre. In a reversible process the eliminated molecule is then usually different from the molecule that was original oxidatively added to the metal centre (Lukehart, 1985:290).

Reductive eliminations are important steps in the catalytic cycle since various organic compounds can be prepared after these groups have been released from the metal centre. Some common examples are (Crabtree, 1988:309 and Lukehart, 1985:290):

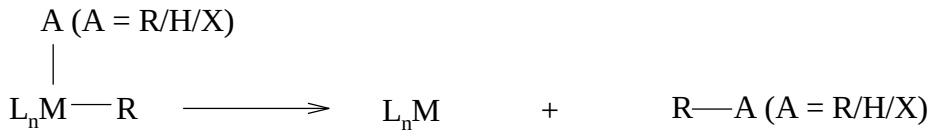

(2.10)

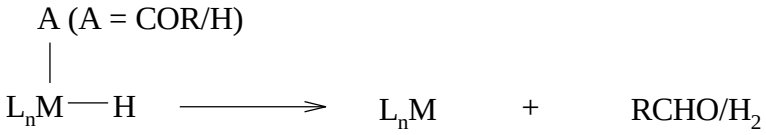

(2.11)

Certain groups are more easily eliminated from the coordination sphere than others. For example, the reductive elimination involving acyl groups seems to be much easier than the elimination of alkyl from the metal complex. This could be due to bulkiness and/or electronic effects. In Reaction 2.12 it can be seen that the cobalt dimethyl complex loses both methyl groups in the reductive elimination reaction with the formation of acetone, instead of ethane, due to the reactivity of the two methyl groups (Bergman, 1980:113).

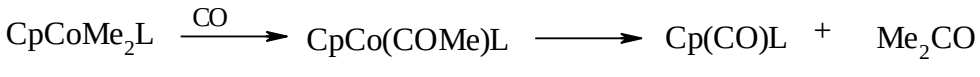

(2.12)

Factors that influence these insertion reactions include the geometry of the groups already attached to the complex, as well as the oxidation state of the metal ion. The geometric requirement for the eliminating groups should be that they are *cis* with respect to each other for a concerted elimination to occur, while *trans* configurations must first isomerise to *cis* before such reactions can occur (Gilli & Stille, 1980:4933; Collman *et al*., 1987:323). As mentioned above, the presence of bulky ancillary ligands is another factor

that favours reductive elimination reactions since the coordination number of the product decreases by two units affording a product with considerably less steric interaction and thus relatively stable (Lukehart, 1985:292). Collman *et al*. (1987:324) found that oxidation of a metal to a higher formal oxidation state frequently also facilitates reductive elimination. This is the reason why oxidations are sometimes used to induce reductive elimination while it would otherwise not occur. A possible explanation for this effect is that changing the oxidation state of the metal often causes a structural change that places the ligands to be eliminated in adjacent coordination sites (Collman *et al*., 1987:324).

2.3 FACTORS INFLUENCING THE RATE OF OXIDATIVE ADDITION REACTIONS

Oxidative addition of organic molecules or organic halides to coordinative unsaturated transition metal complexes are fundamental processes in organometallic chemistry and are also the rate-controlling step in many homogeneous catalysis processes (Parshall & Putscher, 1986:188; Haynes *et al*., 1996:2187). A number of factors influence the rate of these key step reactions and enable further manipulation of not only the oxidative addition, but the catalytic process as well.

2.3.1 Nucleophilicity and oxidation state of the metal centre

Various kinetic studies such as these of Shriver *et al*., (1970:73) indicate that transition metals in a complex act as a nucleophile, particularly in S_N2 reactions. Literature by Purcell & Kotz (1977:943) reported that the heavier transition metals are more basic or nucleophilic than the lighter metals in a given sub-group. A kinetic experiment done by Graham and Hart-Davis (1970:2658) shows the effect of varying the metal in the $[M(\pi\text{-}C_5H_5)(CO)(PPh_3)]$ complex on rates of oxidative addition with methyl and ethyl iodide substrates. Another study also indicates the same effect (Collman *et al*.,

1968:5430). The relative rates of some complexes with different metals are listed in Table 2.3.

Table 2.3 The effect of different metal centres in complexes on the rate of oxidative addition in dichloromethane at 25 °C.

M in [M(C_2H_5)(CO)L]	**Addend molecule**	
	CH_3I	**C_2H_5I**
Co	1.0	2.0 #
Rh	1.4	1.0
Ir	8.0	6.7
[MCl(CO)(PPh_3)$_2$]	**PhN_3** [a]	**4-N_3PhCH_3**[b]
Rh	1.0	1.0
Ir	2.1	1.6

a) In chloroform at 35 °C. b) In chloroform at 30 °C. #. Unexpected order.

It is clear from Table 2.3 (although an unexpected order is observed) that nucleophilicity of the metal centre increases down the group, i.e. from Co to Rh to Ir, and this is manifested in the increased relative second-order rate of the reaction. This order is in agreement with data from literature (Collman & Hegedus, 1980:210 and Purcell & Kotz, 1977:943). Furthermore, oxidative addition of MeI to an iridium(I) anion complex in the Cativa process is found to be *ca*. 150 times faster than the corresponding reaction in the Monsanto process which employs the rhodium analogue (Haynes *et al*., 1996:2187 and Ellis *et al*., 1994:3215).

The oxidation state of a metal centre has also a role to play. Purcell & Kotz, (1977:943) indicate that the largest metals in the lowest oxidation states such as Os(0) and Ir(I) show the greatest tendency to undergo oxidative addition reactions (Eq. 2.6). There are cases where oxidative addition reactions cannot occur because of a metal centre that are already in the highest oxidation state. Ta(V), for example, cannot undergo oxidative addition to give Ta(VII). A sigma-bond metathesis reaction is likely to occur. Sigma-bond

metathesis, which does not change the oxidation state of the metal centre is a common reaction with early transition metals that are in the highest oxidation state (*http://www.ilpi.com/organomet*).

2.3.2 Effects of co-ordinated ligands

In oxidative addition reactions the metal complex can be thought of as functioning as a nucleophile and anything that affects the nucleophilicity of the metal centre therefore influences the course of the reaction. Factors such as the metal centre itself, the electronic properties of the ligands bound to the metal centre as well as the addend molecule all influence the nucleophilicity of the metal complex. The electronic influence of the ligands bound to the metal centre will be the first to be discussed.

A large number of ligands with different nucleophilic properties are known to have the ability to bond to the metal centre. Some of these nucleophiles such as F^-, CN^- and N_3^- have the ability to decrease the nucleophilicity of the metal centre due to their electron withdrawing properties. Ligands such as pyridine, NH_3 and $S(CH_2)_4$ increase the electron density on the metal centre and thereby increase its nucleophilicity toward the addend molecule during oxidative addition.

The phosphine ligand and all its derivatives are an important class of ligands that can be used to control the nucleophilicity of the metal centre. Another important property of these ligands is that not only can they be used to control the electronic properties of the metal centre, but by varying the groups bound to the phosphorus atom, PX_3 (X = Ph, Cy, Et, *t*-Bu, *p*/*o*-toly, *p*-MeO-Ph, *p*-Cl-Ph, *etc*), the steric parameters of the complex can be changed.

2.3.2.1 Electronic effects of phosphines

Electronic and steric properties of a wide range of monodentate phosphines were extensively studied (Tolman, 1970:2953; 1970:2956 and 1977:3). However, very little has been done on the corresponding arsine (AsX_3) and antimony (SbX_3) ligands although these ligands share a number of common characteristics with the phosphine analogue.

Phosphine and arsine ligands have the same general chemical formula PR_3 or AsR_3 where R can be either aliphatic, aromatic, halide or hydride groups (Crabtree, 1988:72). Phosphines and arsines are also two-electron donor groups that bind to the transition metal through these lone pairs of electrons. They also behave, like CO, as π-acids. Concerning the nucleophilicity of group 15 ligands, the Swain-Scott equation is the earliest and most successful equation that relates the reactivity and nucleophilicity of certain ligands such as the halogens, nitrogen donors such as ammonia and pyridine and group 15 donors such as PPh_3, $AsPh_3$ and $SbPh_3$ (Purcell & Kotz, 1977:701). These group 15 ligands show high nucleophilic constants of 8.93, 6.89 and 6.79 respectively. These nucleophilicity values are for substitution reactions towards *trans*-$[Pt(py)_2(Cl)_2]$, py = pyridine. From this study it is expected that PPh_3 ligands release more electron density to the metal centre than $AsPh_3$ and $SbPh_3$ ligands.

Research has shown that the electronic effects of phosphines depend markedly on the nature of the substituent atoms on phosphorus (Tolman, 1970:2953). These substituents also control the extent of the π-back donation from the metal centre, which is bound to the phosphine group. The bonding nature between the ligand and the metal can be described as sigma (σ) donation by the phosphine or arsine to the empty d-orbitals of the metal and subsequently back donation of electron density from the filled metal dπ-orbitals to an empty lower antibonding orbital of the P-atom (Collman *et al*., 1987:69). This back bonding of electron density enable the metal to relieve some of its excess electron density to the P or As atom. In other words, phosphines and most probably arsines are capable of σ-donation and π–accepting. The

following empirical order was found for the different phosphines: (McAuliffe & Levason, 1979 and Crabtree, 1988:72):

$$P(t\text{-}Bu)_3,\ PMe_3,\ PMePh_2,\ \mathbf{PPh_3},\ P(OMe)_3,\ P(NR_2)_3,\ CO,\ PF_3 \qquad \textbf{(2.13)}$$

Ligands on the left of PPh_3 are strong σ-donors and those on the right of it are weak donors or strong π-acceptors. Electron-donating groups bound to the P-atom increase σ-donation capacity of the phosphine ligand, but at the same time weakens the π-acceptor ability of the ligand.

The metal-ligand bond length and the electron density of the metal centre (which affect the reactivity of the complex) are influenced by the σ-donation and π-accepting properties of the ligand. Tertiary phosphines are the most common as well as important ancillary ligands in organotransition metal complexes. The reason is that these ligands constitute one of the few series of ligands in which the electronic and steric properties can be tuned over a wide range by varying the substituents bound to the P atom (Table 2.4). However, as everything has a disadvantage, the usefulness and industrial application of these useful ligands are on the decline because of phosphine degradation during the catalytic process (Garrou, 1985:171). The process involves oxidative addition of the phosphine which deactivates the metal centre.

In most organotransition metal complexes containing carbonyl and phosphine as ligands, good correlation has been found between the carbonyl IR stretching frequency and the reactivity of the complexes. According to this observation, the CO stretching frequency, υ(CO), is a good reflection of the relative electron density/basicity of the complex. Tolman (1970:2953) noticed such a relationship and presented data for 70 monodentate phosphines. He determined that the υ(CO) of the CO group bound *trans* to the different

phosphine ligands gives a good indication of the electron donor–acceptor properties of the different phosphines. These results were obtained from an exhaustive study on $[Ni(CO)_3(PR_3)]$ type of square planar complexes (Table 2.4).

Table 2.4 The relationship between CO stretching frequencies and pK_a values of various phosphine ligands in 0.05M solution of $[Ni(CO)_3(PX_3)]$ in dichloromethane.

Tertiary phosphine	**υ(CO), cm^{-1}**	**pK_a**
With electron donating substituents		
$P(t\text{-Bu})_3$	2056.1	11.40
PCy_3	2056.4	9.65
PMe_3	2064.1	8.65
$P(p\text{-MeOPh})_3$	2066.1	4.57
$P(p\text{-MePh})_3$	2066.7	3.84
$P(m\text{-MePh})_3$	2067.2	3.30
PPh_3	2068.9	2.73
With electron withdrawing substituents		
$P(p\text{-FPh})_3$	2071.3	1.97
$P(p\text{-ClPh})_3$	2072.8	1.30

From these results it is clear that the carbonyl stretching frequency of the CO groups is very sensitive to the substituents bound to the phosphorus atom. A steady increase in υ(CO) is observed with a decrease in the pK_a value of the different ligands. A possible explanation is an increase in metal-phosphine bond strength for the strong electron donating phosphines due to an increase in orbital overlap between the metal and the phosphorous atom. More electron density on the metal enables better back donation towards CO. This results in CO stepping up its σ-donation towards the metal with a consequent weakening of the CO bond strength as reflected in a lower υ(CO) value. This phenomenon can be presented as in Figure 2.1.

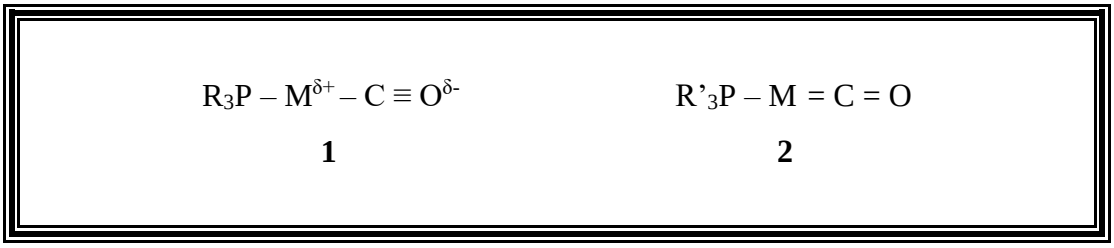

1 **2**

Figure 2.1 Representation of metal-CO bonds, where R = electron withdrawing and R'= electron donating substituents.

An example of the influence of different phosphine ligands is the substantial decrease in bond length from 2.481 to 2.406 Å for the Mo−P bond distance in *trans*-[CpMo(CO)$_2$PPh$_3$] (Bush *et al*., 1971:1003) compared to *trans*-[CpMo(CO)$_2${P(OMe)}$_3$] (Hardy & Sim, 1972:1900). This is due to the fact that the Ph groups are weaker electron donor groups compared to the methoxy groups.

Alternatively, phosphine donating ability is reflected by pK_a values which is a measure of Brϕnsted basicity (Mcauliffe & Levason, 1979:70). It is evident from Table 2.4 that pK_a values of phosphines range widely from 11.4 to 1.03 allowing scientists to adjust or control the electron density on the metal centre by changing the substituent which is bound to the P atom.

Ugo *et al*. (1972:7364) have studied the electronic effects of phosphines on the reactivity of the metal complex. The phosphines used in the study have more or less the same steric properties (Table 2.5). The results obtained only showed a modest influence on the rate of the oxidative addition, but the changes that were observed can solely be interpreted in terms of electron donor-acceptor properties of the phosphine ligand.

It is evident from the results in Table 2.5 that an increase of 10^3 in the oxidative addition rate was obtained by changing the electron withdrawing *p*-ClC_6H_4 group to the electron donating *p*-OMeC_6H_4 group bound to the phosphorus ligand. The electron density of the

metal centre is increased by electron donor ligands such as methoxy and methyl which results in an increase in the metal centre nucleophilicity, which enhances the rate of interaction with methyl halide.

Table 2.5 Rate constants for the oxidative addition of CH_3I to *trans*-$[IrCl(CO)L_2]$ in benzene at 25 °C.

L	pK_a[a]	$\upsilon(CO)$[b], cm^{-1}	10^2k, $M^{-1}\,s^{-1}$
$P(p\text{-}ClC_6H_4)_3$	1.03	2072.8	0.0037
$P(p\text{-}FC_6H_4)_3$	1.97	2071.3	0.015
PPh_3	2.73	2068.9	0.33
$P(p\text{-}CH_3C_6H_4)_3$	3.84	2066.7	1.50
$P(p\text{-}OCH_3C_6H_4)_3$	4.57	2066.1	3.50

a) pK_a value of phosphines in dichloromethane.
b) $\upsilon(CO)$ based on carbonyl mode of $[Ni(CO)_3L]$ in the same solution.

To the contrary, high shortage of electron density at the metal centre decreases the complex's reactivity and can make the complex inert. In Table 2.6 the highly electron withdrawing ligand, $P(C_6F_5)_3$, makes the complex poor in electron density, $\upsilon(CO)$ = 1994 cm^{-1}, and hence inactive towards dioxygen (Vaska & Chen, 1971:1080).

2.3.2.2 Steric aspects of phosphines and the effect on reactivity

In the earlier days the reactivity of organotransition metal complexes was almost exclusively contributed to the electronic effects of the ligands bound to the metal centre. Little was known concerning the steric effects of the different ligands. In 1970 Tolman (1970:2956) introduced the ligand cone angle (θ) concept, a parameter which quantifies the steric demand of phosphines. This became necessary when the inability of bulky

phosphorous ligands to compete for the coordination position on a Ni(0) compound (Reaction 2.14) could not be explained in terms of their electronic character.

$$[Ni(CO)_4] \quad + \quad L \quad \longrightarrow \quad [Ni(CO)_3L] \quad + \quad CO \qquad \textbf{(2.14)}$$

Results have, however, shown that steric effects are equally important as electronic effects, particularly, in those reactions where bulky ligands such as triphenyl phosphine are bound to transition metal complexes which are often used as catalysts. In general, bulky ligands tend to promote lower coordination numbers and often unusual reactivity such as cyclometallation is observed (Collman *et al*., 1987:298), whereas small ligands exert less steric hindrance towards the attainment of higher coordination numbers. The steric demand of a ligand is not simply about the size of the ligand but rather an indication of its spatial requirement in the metal coordination sphere.

Steric and electronic effects of phosphine ligands in complexes are often interrelated which makes it difficult to separate the contribution of each of these factors. Both these effects were quantified separately by Tolman (1970:2953; 1970:2956 and 1977:3). He quantified the steric effects of the different phosphines on measurements made using atomic models. The idea is that each ligand in a complex will subtend some solid angle as viewed from the centre of the metal atom. Tolman however used the measurement of the apex angle of a cone centred on the metal. The measurement used is large enough to enclose the Van der Waals radii of the outermost atoms of that ligand (Figure 2.2). The metal used to construct this model was Ni(0), but it can be applied to other transition metals and oxidation states.

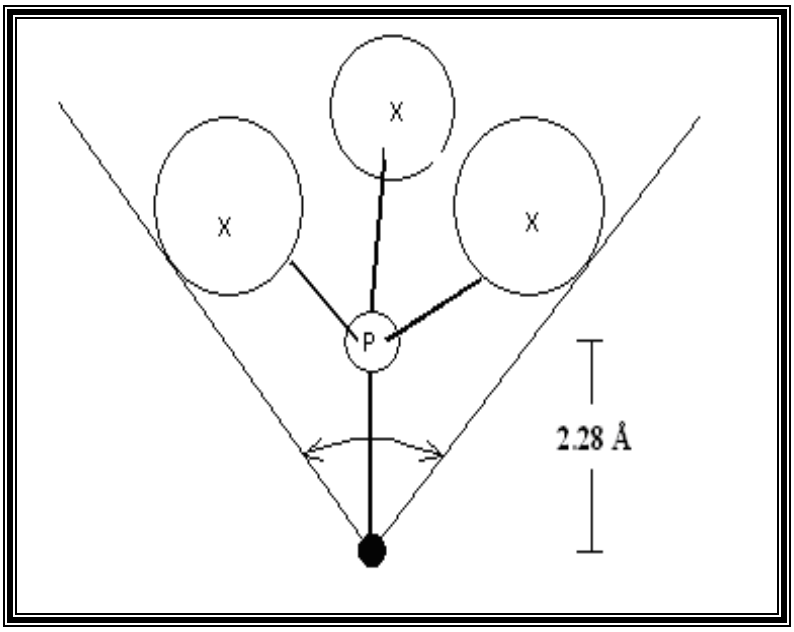

Figure 2.2 Representation of the calculation of the cone angles in symmetrical phosphines. The Tolman cone angle shown by double headed arrow, Ni^0–P = 2.28 Å (the big black circle denotes Ni and X = substituent on a P-atom).

The value of the Tolman cone angle (θ) for unsymmetrical phosphine ligands can be calculated from their corresponding half-angles (θ/2) by using the equation below (Tolman, 1977:3):

$$\theta_T = \frac{2}{3}\sum_{i=1}\left(\frac{\theta}{2}\right)_i \qquad \textbf{(2.15)}$$

For example, the θ value for $PMePh_2$ is two-thirds of the way between PMe_3 (118°) and PPh_3 (145°) which is 136°.

Despite some shortcomings, the cone angle concept remains a valuable semi-quantitative approach to steric demand of ligands, i.e. almost all steric effects of monodentate ligands are measured by this model. Crystallographic data are still

considered as the best information for the calculation of steric size of a ligand. Once again, steric size of ligands should be viewed as a spatial requirement in the coordination sphere and not necessarily the size. As discussed earlier, the steric demand of arsine ligands is expected to be relatively lower than the corresponding phosphine ligands in the same complex.

Tolman (1970:2956) suggested that the concept of the cone angle could be applied or extended to other ligands. Otto (1999:159) has roughly calculated the steric demand of some arsine, stibine and silyl ligands using Vaska's type of *trans*-[Rh(CO)(Cl)L_2] complexes, where L = PPh_3, $AsPh_3$, and $SbPh_3$. Results obtained from his research gives average effective cone angles (avg. θ_E) of the three group 15 donor ligands, PPh_3, $AsPh_3$, and $SbPh_3$, as 146.8, 140.4 and 133.9º respectively. The value obtained for PPh_3 (145 ± 2º) is in excellent agreement with the Tolman value of 145º. The correctness of the values can be obtained from Tolman's model itself (1977:3). This model predicts that an increase in the bond length of M−L or L−C (metal ligand or ligand carbon) by 0.1 Å decreases the cone angle by 3 to 5º. The longer bond length in the corresponding arsine complexes is thus responsible for the decrease in cone angle of the corresponding arsine ligand.

Bulky tertiary phosphines such as PPh_3 P(*t*-Bu)$_3$, P(*o*-tol)$_3$, *etc* with cone angles of 145, 182 and 194º respectively are able to distort the normal coordination geometry of the surrounding ligands and shield the metal from the addend molecule. This crowding of the metal ion makes it difficult for the addend molecule to interact with the metal centre which has a large effect on the rate of the reaction. The steric attributes of phosphines can be adjusted by changing the substituents, which are bound to it. These ligands exhibit a large steric size with cone angles ranging from 87 to 212º, which makes it possible to tune the reactivity of the complexes (Tolman, 1977:3). Research has shown that phosphines with less steric demand and more electron donating properties favour oxidative addition reactions. Excessive steric effects inhibit the reactivity of complexes

and can even make it inert towards reactions as can be seen from the results in Table 2.6 (Shaw & Stainbank, 1971:3716; 1972:23).

Table 2.6 Rate and equilibrium constants for the reaction between *trans*-[IrCl(CO)L_2] and O_2 (Vaska & Chen,1971:1080).

L	Cone angle (θ)	υ(CO), cm^{-1} (Nujol)	10^2 k, $M^{-1}s^{-1}$	10^3 K, M^{-1}
$P(C_2H_5)_3$	132	1948	33.8	215
$P(n\text{-}C_4H_9)_3$	132	1937[a]	26.1	66.9
$P(C_6H_5)_3$	145	1956	9.93	7.14
$P(Cy)_3$	170	1934	0.127	0.217
$P(o\text{-tol})_3$	194	1948	No reaction [b]	No reaction
$P(C_6F_5)_3$ [c]	184	1994	No reaction	No reaction

a) Measured in the same solvent and the rest in *trans*-[IrCl(CO)L_2] in Nujol.
b) At 30 °C, no reaction in 18 days at 700nm. c) Included to indicate steric and electronic effects.
d) $K=k_1/k_{-1} = [O_2IrCl(CO)L_2]/[IrCl(CO)L_2][O_2]$.

The results in Table 2.6 above clearly show the steric influence on the reactivity of metal complexes. The bulkier ligand (L), which is represented by the large cone angle of 194°, has a remarkable effect on the rate of the reaction. The sterically hindered *trans*-[IrCl(CO)$P(o\text{-tol})_2$] does not undergo reaction even with small molecules such as H_2. The lack of its reactivity is explained by the steric effect of the $P(o\text{-Tol})_3$ groups. Results obtained from crystal and molecular determination indicated that the two *ortho*-methyl groups are orientated in such away that they shield the metal to react with incoming addend molecules (Vaska *et al*., 1975:2669). The inactivity of $P(C_6F_5)_3$ towards the reaction is mainly due to electronic factors which was discussed in Section 2.3.2.1, although it is believed that the large cone angle (184°) has some influence in rendering the complex inactive towards oxidative addition.

2.3.2.3 Steric *vs* electronic

Steric and electronic properties of phosphines are usually viewed separately, but they do not operate in isolation and both are operative during coordination to the metal centre or

during oxidative addition reactions. A change in the steric effect can result in a change in the electronic properties of the ligand and *vice versa*. An increase of the angle between substituents, for example, will decrease the percentage of s-character in the phosphorus lone pair. Changing the electronegativity of atoms can also affect bond distance and angle. It is therefore important to remind that the electronic and steric effects are intimately related and difficult to separate in any pure way. A quantitative measure of the steric and electronic effects in transition metal complexes is normally based on a measurement that is made using atomic models and CO stretching frequencies respectively.

The relative dominance or importance of one of the factors largely depends on the nature of the substituents bound to the P-atom (Deeming & Shaw, 1969:1753). A kinetic study done by Miller and Shaw (1974:480) indicates that under certain conditions the steric effects can be overshadowed by electronic factors (Table 2.7).

Table 2.7 Reaction rates for oxidative addition between iodomethane and *trans*-[IrCl(CO)$(L)_2$], in toluene at 25.3 ºC.

L	**Tolman cone angle (θ)**	**10^2k, M^{-1} s^{-1}**
$PPhMe_2$	122	4.7(1)
P(*p*-MeOPh)Me_2	≈129	6.75(20)
P(*o*-MeOPh)Me_2	>129[a]	530(25)

a) Slightly greater than 129º.

From the result in Table 2.7 it is clear that in spite of a relatively larger cone angle for the *ortho*-methoxy phosphine, its rate of reaction is about 100 times faster than the other two. This pronounced rate increase is a direct result of electron donation from the methoxy oxygen to the iridium centre. An X-ray structural study performed on [$RhCl_3${$AsMe_2$(*o*-OMePh)}$_2$] by Graziani *et al*. (1969:1236) has shown that the oxygen of an *ortho*-methoxy group is co-ordinated to Rh, similar to what was found in the structure of *trans*-[IrCl(CO)(*o*-$MeOPh)_2$] (op. cit. Graziani *et al*. 1969:1236), Figure 2.3.

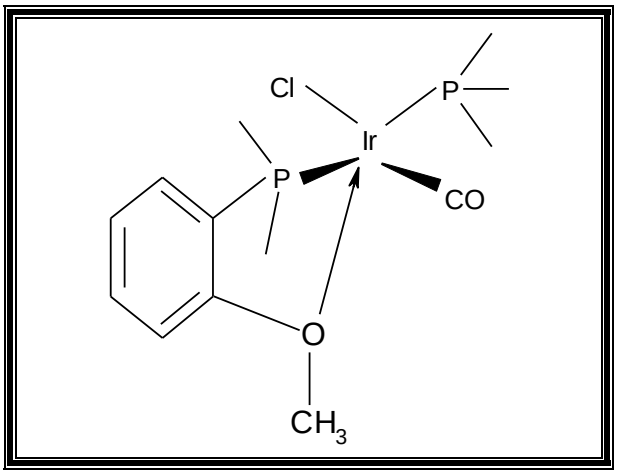

Figure 2.3 Structure of *trans*-[IrCl(CO)(*o*-MeOPh)$_2$].

Studies where the electronic effects overshadow the geometric effects can also be found elsewhere in the literature. Phosphines with good σ-donating capacities such as $P(Bu^t)_2Et$, $P(Bu^t)_2Pr^n$ (Shaw & Stainbank, 1971:3716 and 1972:23) and P(*o*-tol)$_3$ (Vaska *et al*., 1975:2669) *etc*. are observed to give inert complexes. This inactivity is solely attributed to the excessive bulkiness (cone angle of 194° for the latter) of the substituents on the phosphine which overrides the favourable electron density on the metal centre.

It is also known that excessive bulkiness of the ligands bound to the metal complex can distort the idealised coordination geometries of the complexes and hence influence the reaction rates enormously. Wilkinson's catalyst, [$RhCl(PPh_3)_3$], has for example a non-planar geometry in the solid state rather than a square planar geometry as expected for d^8 Rh(I) complexes (Bennett & Donaldson, 1977:655 and Hitchcoc *et al*., 1969:1367). [$Ir(CH_3)\{P(C_6H_5)_2\}_4$] (Clark *et al*., 1975:375) has a tetrahedral arrangement due to the steric interaction within the complex while an extreme case where complete planarity lost was found with [$CoCl(PPh_3)_3$] (Aresta *et al*., 1975:375). Its tetrahedral arrangement obtained from magnetic and spectral studies is rather unusual for a d^8 ML_4 complex. This unusual configuration may be due to the fact that the three large phosphines cannot be

readily accommodated in a planar manner around the relatively small cobalt atom. A consequence of this geometry is that the complexes react very slowly with incoming groups and as a result both complexes, $[Ir(CH_3)\{PC_6H_5)_2\}_4]$ and $[CoCl(PPh_3)_3]$, are found to be unreactive, even towards small molecules such as O_2 or CO and O_2 or H_2 respectively (Tolman, 1977:3).

2.3.2.4 Cupferron as bidentate ligand

Cupferron, the ammonium salt of N-nitrosophenyl hydroxyl amine, was used as bidentate ligand for this study. General features such as aromatic behaviour of the chelate ring and uses will be discussed in the paragraphs below. The cupferrate ligand can be presented as in Figure 2.4.

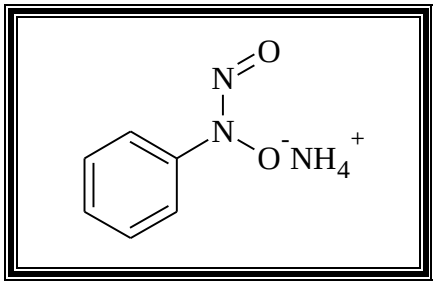

Figure 2.4 The cupferrate bidentate ligand.

The cupferrate ions can form chelate complexes with different metals centres, which are very similar to tropolonato type of β-diketonato complexes. Unlike β-diketonato complexes such as acac and hfaa which form six-membered chelate rings, the tropolonato and cupferrate ions form five-membered chelate rings and the bond distance and bite angle are smaller than that of the correspondning β-diketonato complexes. This is evident in the Rh(I) cupferrate complexes which offer a substantial smaller bite angle ($\theta = 76.6(3)^o$), even smaller than the tropolonato analogue, (77.8(3) ^{o}), (Basson *et al.*, 1986:L45).

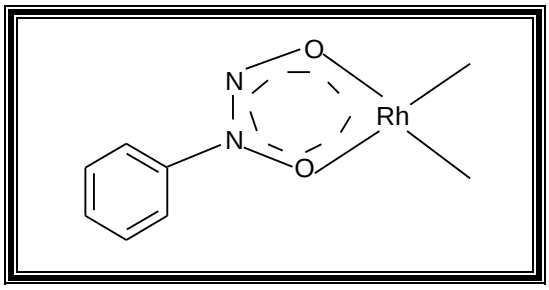

Figure 2.5 Chelate ring of cupferrate.

The aromatic character of the chelate in Rh(I) cupferrate complexes is manifested in the O−N and N−N bond distances which are roughly equal, which is prove that delocalization of π-electrons takes place in the ligand during bonding with the metal ion (Basson *et al*., 1986:L45). The same article reported that the N−N bond has a 80% double bond character which is confirmed by the actual N−N bond distance found crystallographically, which corresponds with the calculated bond order. The sp^2-hybridised character of the chelate ring is further demonstrated by the planarity of the ring.

Cupferrate can be used in diverse areas such as gas chromatography, in solvent extraction as NMR shift reagents, in laser technology and in the polymer industry. It can also be used as chelating reagents in analytical chemistry, chelate chemistry and radiochemistry (Mehrotra, 1978). An example is the chelating of manganese in urine with a good detection limit (50 ppb). Cupferron is also found to be suitable for the fluorimetric determination of Fe(II) with a detection limit of 30 ppb (Jan & Shah, 2002).

2.3.2.5 Manipulating the bidentate lgand

Bonati and Wilkinson (1964:3156) were the first to show that the carbonyl group in $[Rh(L\text{-}L')(CO)_2]$, where L-L' = monocharged bidentate ligand, can be substituted by olefins such as cyclo-octa-1,5-diene and by neutral ligands such as phosphines, arsines and stibines. Different studies on a number of [Rh(L-L')(CO)X] complexes enable

researchers to determine the relative thermodynamic *trans* influence of the bonding atoms in the bidentate ligands (Leipoldt *et al*., 1991;193).

The thermodynamic *trans*-influence is a ground state phenomenon which can be described as the ability of a ligand to weaken the metal-ligand bond *trans* to itself (Pidcock *et al*., 1966:1707). The ligand with the weakest bond in the square planar complex will be substituted by the incoming molecule. The thermodynamic *trans*-influence of a bidentate ligand is determined by the relative strength of the two Rh–C bonds in the dicarbonyl complexes (Leipoldt *et al*., 1982:113). The kinetic *trans*-effect depends on the electron attracting power of one or both substituents of the bidentate ligand. The difference between these two properties is that the thermodynamic *trans*-influence determines the specific isomer that will be formed when the dicarbonyl reacts with the phosphine or arsine while the kinetic *trans*-effect determines the rate of the substitution reaction.

Previous studies done in the laboratory showed that the *trans*-influence of the L-L' atoms in the bidentate ligand (where L-L' = combination of O, N or S atoms) follows the reverse electronegativity range, i.e. S > N > O (Leipoldt *et al*., 1991:193 and Botha *et al*., 1987:25). This means that the carbonyl *trans* to the sulphur will preferably be substituted compared to nitrogen and oxygen. Recent quantum mechanics (QM) calculations on the P,S and P,N ligand combination indicated that the geometry with the CO *trans* to the S or N atom is favoured energetically relative to the geometry with the CO *trans* to the P atom by 25 and 48 kJ/mol for the P,S and P,N ligands combinations respectively (Cavallo & Sola, 2001:12294). These computational results agree well with the above X-ray crystallographic *trans*-influence order. The electronic preference for geometries with CO *trans* to S or N can be explained by means of the different *trans*-influence of these ligands. The large *trans*-influence of the sulphur donor atom weakens the carbonyl bond *trans* to it more than that of the nitrogen donor atom with the subsequent substitution at the CO *trans* to the sulphur atom.

It was proposed that the thermodynamic *trans*-influence was purely of electrostatic nature. However, Roodt & Steyn (2000:1) observed an unexpected substitution pattern in the solid state chemistry of the type [Rh(L-L')(CO)(PPh_3)] of complexes where L-L' = N,S such as macsm, cacsm and stsc. In these complexes the CO ligand *trans* to the nitrogen atom was replaced by PPh_3. This unexpected substitution mode was found to be due to excessive steric demand of the methyl and cyclohexyl groups on the nitrogen atom in the macsm and cacsm ligands and the salicylate on stsc respectively. This was confirmed by replacing the more bulky methyl or cyclohexyl in macsm and cacsm with a hydrogen which gave hacsm (Figure 2.5). The less steric complex has undergone the expected electronic substitution pattern, i.e. the CO *trans* to S was replaced by PPh_3. These results clearly show that the thermodynamic *trans*-influenc can also be influenced by the steric demand of the substituents.

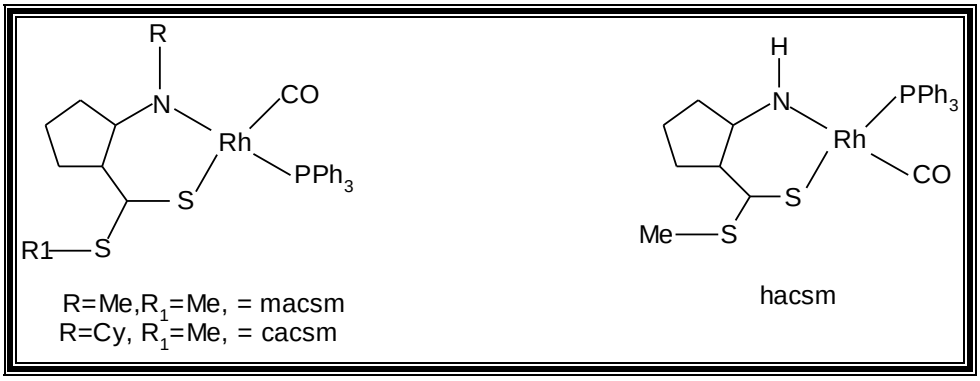

Figure 2.6 Steric influence on the type of product formed.

In a study performed by Basson *et al*., (1986:L45) on cupferrate complexes, it was found that only one isomer of [Rh(cupf)(CO)(PPh_3)] crystallises which implies that the donor capability of the two oxygen atoms in cupferrate is not equal. If the two oxygens were equivalent, two isomers would have been expected (one *trans* to L and the other to L') at comparable ratios (Roodt & Steyn, 2000:1 and Treciak & Ziolkowski, 1985:15). These results indicate that cupferrate is an asymmetrical mono anionic bidentate ligand, even though the two donor atoms are the same type. The CO groups *trans* to the nitroso

oxygen atom in the [Rh(cupf)$(CO)_2$] was substituted by PPh_3 indicating the greater *trans*-influence of this oxygen compared to that of the second oxygen atom (Basson *et al*., 1986:L45).

Another parameter which can be used to measure the thermodynamic *trans*-influence is the M–P bond length that is found in the different complexes. Studies done by Leipoldt *et al*., (1991:193) and Roodt *et al*., (1992:3477) have shown that the Rh–P bond distance in the [Rh(L-L')(CO) (PPh_3)] type of complexes is an accurate indicator of the *trans*-influence of the donor atoms in the bidentate ligand. It was observed that the Rh−P bond distance increase in the order of O < N < S which shows the increasing order of the *trans*-influence of the donor atoms. The trend is clearly shown in Table 2.8.

Table 2.8 The average Rh–P bond length in [Rh(L-L')(CO)(PPh_3)] type of complexes (Damoense, 2000).

	Rh−P bond length, Å	
Donor atom L-L'	**5-membered chelate ring**	**6-membered chelate ring**
O,O	2.232(2)	2.244(2)
N,O	2.260(2)	2.278(2)
S,O	2.278(1)	2.291(2)

Another important observation can be made from the results in Table 2.8. From these results, it is also clear that the Rh−P bond length increases from the five to six-membered chelate groups, meaning that the *trans*-influence is larger for the six-membered chelate compared to the same donor pair in the corresponding five-membered systems. An explanation for this observation is that the overlapping between the ligand σ-orbital and the dsp^2 orbital of the Rh metal centre is less effective for the five-membered chelate with a bite angle of *ca*. 80º (Roodt *et al*., 1992:3477). Better orbital overlap can be obtained when the bite angle of the bidentate ligand approaches 90º because the interacting metal orbitals are more or less perpendicular to

each other. Hence six-membered chelates with a bite angle of *ca*. 90^{o} show a greater *trans*-influence than the corresponding five-membered chelates.

2.3.2.6 The *trans*-influence of phosphine and arsine ligands

The relative *trans*-influence of PPh_3 and $AsPh_3$ was crystallographic studied using the [Rh(DBDTU)(CO)(XPh_3)] type of complexes, where X = P (Roodt *et al*., 1994:39) and X = As (Kemp *et al*., 1966:17). As expected both the group 15 ligands occupy the position *trans* to the S-atom which is in agreement with the large *trans*–influence of the S-atom compared to the oxygen atom of the bidentate moiety. However, shortening of the Rh–S bond was observed from 2.307(1) to 2.290(1) Å, when P is interchanged by an As atom. Although it is not safe to generalise, it seems that $AsPh_3$ has a weaker *trans*-influence than PPh_3, or at least in these complexes. determination of Fe(II) with a detection limit of 30 ppb (Jan & Shah, 2002).

2.3.2.7 Bidentate ligands and reactivity

Bidentate ligands can also affect the reactivity and the mechanism of the reaction and thus the final product formed. An increase in the reaction rate by two orders of magnitude was observed when one of the oxygens in [Rh(cupf)(CO)(PPh_3)] was replaced by a sulphur donor atom in [Rh(macsh)(CO)(PPh_3)]. This is attributed to the large electron donating ability of the sulphur atom (Roodt *et al*., 1993:25). Steric factors, however can also have a large influence on the rate of the reaction. For example, a 4 to 5 fold increase in the k_1 rate constant was observed from [Rh(anmeth)(CO)(PCy_3)] (Preston, 1993) to the corresponding complex with L-L' = stsc. A further increase in the reactivity of the metal complex was found when the donor atom pair was replaced with a P,S atom combination. Very recent reports indicate that Rh(I) complexes containing P,S donor atoms such as *cis*-[RhI(CO){$Ph_2PCH_2P(S)Ph_2$}] (Baker *et al*., 1995:197) and [Rh($SC_6H_4PPh_2$)($CO)_2$] (Dilworth *et al*., 1995:1579) are almost 4-8 times faster in catalysing the carbonylation of methanol compared to *cis*-[$RhI_2(CO)_2]^-$.

The role of the bite angle of the bidentate ligand (L-L') may be illustrated by the thermodynamic stability of the five-membered chelate ring relative to the corresponding six-membered chelate ring. Table 2.9 also shows the influence of bite angle on the rate of oxidative addition.

Table 2.9 Kinetic data for iodomethane oxidative addition to [Rh(L-L')(CO)(PX_3)] type of complexes in $CHCl_3$ at 25 °C.

Complex[a]	**L-L'**	**Ring size**	**Bite angle**	**10^2k_1, $M^{-1}s^{-1}$**	**K_1[c],M^{-1}**	**Ref**
[Rh(stsc)(CO)(Pcy_3)]	S-N	5	81.9(3)	0.71(2)	71	d
[Rh(cacsm)(CO)(PCy_3)	S-N	6	93.5(1)	0.002(1)	0.15	e
[Rh(anmeth)(CO)(PPh_3]	O-S	5	83.4(2)	4.2(3)	0.6	f
[Rh(sacac)(CO)(PPh_3)]	O-S	6	91.7(1)	4(1)	0.4	g
[Rh(Ox)(CO)(PPh_3)]	O-N	5	80.0(2)	3.02(4)	600[b]	h
[Rh(dmav)(CO)(PPh_3)]	O-N	6	87.4(2)	23(1)	58[b]	i
[Rh(cupf)(CO)(PPh_3)]	O-O	5	76.6(3)	0.12(2)	200	j
[Rh(acac)(CO)(PPh_3)]	O-O	6	87.9(2)	2.4(3)	3.3	k

a) See list of abbreviations. b) In acetone. c) esd's ca.10%, but for the Sacac complex 20%.
e) Roodt & Steyn, 2000:1. f) Preston, (1993). g) Leipoldt *et al*., (1990:215). i) Damoense, (2000).
j) Basson *et al*., (1987:31). k) Basson *et al*.,(1984:167).

It is clear from the results in Table 2.9 that a decrease in the K_1 value is consistently observed from the five to six-membered chelates. The approximately 10 degrees decrease in bite angle from the six to five-membered chelate could be the prime reason for the increase in the thermodynamic stability of the alkyl product or intermediate.

The type of binding atoms of the bidentate ligand or the nucleophilicity of the ligand in a complex can influence the final product. An acyl complex (Leipoldt *et al*., 1993:11) is formed when one or both of the donor atoms are sulphur atoms. For L-L'= β-diketonato (Basson *et al*., 1984:167), cupferrate (Basson *et al*., 1987:31), or

8-hydroxyquinoline (Leipoldt *et al*., 1991:369) where the donor atoms are oxygen, the final product is the alkyl isomer. A possible explanation for such behaviour could be the capability of the donor atoms to stabilise the Rh(III)-acyl bond, i.e. relative to the alkyl the acyl complex seems to be stabilised by more nucleophilic donor atoms such as sulphur of the bidentate ligand.

2.3.2.8 Substituent effect

Leipoldt *et al*. (1988:223) studied the electronic effect of various substituents on β-diketonato for the oxidative addition of iodomethane to [Rh(β-diketone){$P(OPh_3)_2$}]. The results obtained are listed in Table 2.10.

Table 2.10 Second order rate constants for the reactions between [Rh(β-diketone){$P(OPh_3)_2$}] and CH_3I in acetone at 25 °C.

β-diketonato	**Substituent on β-diketonato**		**pK_a**	**10^2k, $mol^{-1}dm^3s^{-1}$**
	R_1	**R_2**		
Acac	CH_3	CH_3	8.94	9.6(2)
Ba	CH_3	C_6H_5	8.70	3.42(5)
Dbm	C_6H_5	C_6H_5	9.35	1.49(3)
Tfaa	CH_3	CF_3	6.30	0.56(1)
Tfba	CF_3	C_6H_5	6.30	0.263(5)
Hfaa	CF_3	CF_3	4.35	0.0024

It is evident from these results that electronegative substituents such as CF_3 on the β-diketonato retarded the reactivity of the complexes towards oxidative addition reactions. The hfaa-system, for example, is deactivated by a factor of over 1000 as compared to the acac system. The inhibitory effect of strong electron withdrawing ligands on reaction rates is due to the decrease of electron density on the metal centre making it a weaker Lewis base.

2.3.3 Effect of solvent

Polar solvents generally enhance the rate of oxidative addition reactions, though in some cases the observed solvent effects do not change parallel with solvent polarity (Masel:2001:802). The effect of solvents on the rate of oxidative addition reactions is illustrated in Table 2.11.

Table 2.11 Solvent effects on the relative second order rate for the oxidative addition of iodomethane to the complexes listed (R/r = relative second order rate).

Complex	**Solvent**	**Є, Dn**[a]	**R/r**
***trans*-[IrCl(CO)(PPh_3)$_2$]**[b]	Benzene	2.3, 0.1	1.0
	Chlorobenzene	5.6, -	2.2
	THF	7.6, 20.0	2.8
	Acetonitrile	38, 14.1	6.0
	DMF*	36.1, 26.6	8.0
[Rh(cupf)(CO)(PPh_3)][c]	Ethyl acetate	6, 17.1	1.0
	Acetone	20.7, 17.0	5.3
	Methanol	32.6, 19	10.9
	DMSO	45, 29.8	34.0
[CoC_5H_5(CO)L][d]	THF	7.6, 20.0	1.0
	Acetone	20.7, 17.0	3.7
	Dichloromethane*	8.6, 4	4.2
	Acetonitrile	38, 14.1	*ca*.10
[Rh(Sacac)(CO)(PPh_3)][e]	1,2- Dichloroethane	10.1, -	1.0
	Chloroform*		1.6
	Acetonitrile	38, 14.1	1.8
	Nitromethane	35.9, 2.7	3.3

a) ϵ = dielectric constant. Dn = donocitiy power. R/r = relative rate.
*Unexpected order according to solvent parameters. b) Ugo *et al*., 1972:7364.
c) Basson *et al*., 1987:31. d) Shriver *et al*., 1970:73. e) Venter *et al*., 1991:2207.

It can be seen from these results that polar solvents with a few exceptions (denoted by an asterisk) increase the rate of the reaction. The drastic influence of the solvent is clearly evident from the [Rh(cupf)(CO)(PPh_3)] reaction. The donocity of ethylacetate and methanol, for example, is nearly the same but the increase in polarity of about five times leads to a ten times increase in the rate of the reaction. This pronounced activation

however, cannot only be accounted for by solvent polarity differences. Results for the sacac system indicate that solvent variation, even for the highly polar nitromethane, did not show any significant increase in reaction rate. The role of the solvent in these reactions can be summarised as follows:

1) Solvent may remain as an inert medium or could have an insignificant effect (Venter *et al*., 1991:2207).

2) It may also act as a nucleophile to ease charge separation and ion-pair formation in the reaction intermediates, forcing the reaction to proceed *via* a linear transition state and consequently influence the mechanism of a reaction (Basson *et al*., 1987:31 and Venter *et al*.,1991:2207).

2.3.4 Nature of the substrate

Thermodynamically, R−X and H−H oxidative additions are favourable whereas R−H and R–R additions are least favourable (Collman *et al*., 1987:284). Non-polar molecules such as H_2 oxidatively add in a stereoselective way to form the more stable *cis*-dihydride isomer (Cross, 1985:197). Substrates with a better leaving group like R−X, H−X, (X = halogen) and RCN, are relatively more reactive in S_N2 reactions because the leaving group can detach easily from the linear transition state complex. Common substrates are listed in Table 2.12.

Table 2.12 Common substrates in oxidative addition reactions.

Nonpolar/low polar	**Electrophilic**	**Other substrates***
H_2, R_3SiH, RH, ArH, RSH, R_3SnH, $(SCN)_2$	HX, X_2, RX, ArX, ArCN, $CHCl_3$, HgX_2, R_3SnCl, RCHO, HCHO, RCO_2H, $SnCl_4$, $GeCl_4$, R_3PbCl.	O_2, S_2, Se_2, Cyclopropane.

*Substrates where both atoms remain bonded. R = alkyl, X = halide. (Collman *et al*., 1987:282 and Lukehart, 1985:275).

Collman and Murphy (1974:3019) studied the neighbouring group effect during oxidative addition of various organic substrates to macrocyclic rhodium(I) complexes. The substrates included $CH_3(CH_2)_3X$ (X = I, Br), $(CH_3)_2CHBr$, and $X(CH_2)X$ (X = Br, I, Cl), *etc*. A substrate dependence of methyl > ethyl > secondary > cyclohexyl was obtained for the oxidative addition reaction and the order for the halides is as presented in Table 2.13.

Table 2.13 The effect of different substrates on the rate of oxidative addition with different complexes (R/r = relative second order rate).

Complex	**Substrate**	**R/r**
$[Rh(C_5H_5)(CO)(PPh_3)]$[a]	$PhCH_2Cl$	1.0
	$PhCH_2Br$	*ca*.470
	$PhCH_2I$	*ca*.7000
	*RCl	1.0
	*RBr	*ca*.10.0
	*RI	*ca*.100.0
Trans-$[IrCl(CO)(PPh_3)_2]$[b]	$PhCH_2Br$	1.0
	$PhCH_2Cl$	1.2
	CH_3I	33.0
$[Rh(acac)(CO)(PPh_3)]$[c]	C_2H_5I	1.0
	CH_3I	*ca*.120

* R = C_3H_5 (allyl). a) Hart-Davis & Graham, 1971:8. b) Chock & Halpern, 1966:3511. c) Ugo *et al*., 1972:7364.

The results in Table 2.13 clearly illustrate the effect of a leaving group and the R-group. Alkyl or aryl iodides react faster while the bromide and chloride analogue react progressively slower. The order for the halogens is Cl << Br < I (Chock & Halpern, 1966:3511 and Hart-Davis & Graham, 1971:8). This may be due to the lower carbon-iodine dissociation energy, which makes the iodide a better leaving group and hence increasing the electrophilic character of the carbon compared to the other halides and thereby facilitating the nucleophilic attack of the metal atom at the carbon atom of the substrate. The results also show that the alkyls are relatively more

reactive than the corresponding aryls while the less steric alkyls in turn are more reactive than the steric alkyls.

2.4 FACTORS GOVERNING CO−INSERTION REACTIONS

CO insertion reactions, being part of the catalytic cycle, is the next important reaction type under discussion. Like other chemical reactions, the rate and the yield of these reactions are not free from the influence of parameters such as electron density at the metal centre, the solvent employed and the ligands bound to the complex.

CO-insertion reactions are very sensitive to high electron density at the metal centre. In this case, however the effect is opposite to that of oxidative addition. In the iridium-catalysed carbonylation of methanol using the $[IrI_2(CO)_2]$, the rate of oxidative addition is significantly enhanced as compared to its Rh-analogue, but the insertion step is deactivated by a factor of *ca*. 10^{-5} to 10^{-6} (Haynes *et al*.,1996:2187). One consequence thereof is that iridium-alkyl complexes are very stable and salts of $[IrI_3(CH_3)(CO)_2]^-$ can be isolated while the corresponding Rh-alkyl complexes are highly unstable and hence undergo rapid insertion to give the acyl isomer (Foster, 1976:846 and Labinger & Osborn, 1980:3230). The stability of the former can be attributed to the relative strength of the Ir–C bond.

Various studies indicate that the rates of CO-insertion reactions are influenced by the nature of solvents (Flood, 1981:4410), which can be quite large in some cases. Butler *et al*. (1967:2070) studied the insertion reactions of $[MoCp(CO)_3CH_3]$ with PPh_3 as incoming ligand using THF, benzene and chloroform as solvents. From this study, it was evident that the effect of the solvent is not to stabilise the co-ordinatively unsaturated complex, but it attacks the metal centre directly as alkyl migration occurs. These migrations are, in other words, solvent assisted or solvent catalysed CO insertions. In

contrast to these studies, no or only a small solvent effect was observed for the carbonylation of [FeCp(CO)$_2$R] in DMSO (Nicholas *et al*., 1974:133).

$$[FeCp(CO)_2R] \xrightarrow[DMSO]{L} [FeCp(CO)(COR)(DMSO)^{\#}] \xrightarrow{L} [FeCp(CO)(COR)L] \quad \textbf{(2.16)}$$

In this reaction, the effect of the solvent may be described as a stabilisation of the transition state by solvation around its coordination sphere. The DMSO molecule is very tightly bound in the transition state that makes it very difficult for L to displace it in the final step. Generally, it is believed that polar solvents promote the rate of the migratory insertion when they attack directly at the metal centre (Butler *et al*., 1967:2070). However, if the solvent stabilises the intermediate by means of solvation the rate decreases dramatically.

Another factor which influences CO-insertion is the type of migrating group. A study shows that the migratory aptitude of alkyl groups follows the order Me > Ph > benzyl *(http://www.ilip.com/organomet/insertion.html)*. The incoming ligand (Anderson & Cross, 1984:67) and the strength of M−C, M−CO bonds (Micheal & Bergman, 1981:7028) also play a vital role. The configuration of the migrating group relative to the carbonyl is another factor that influences the rate, with migrating groups in adjacent positions favouring the process (Collman & Hegedus, 1980:271). Relative to oxidative addition, CO-insertion is not well studied. The reason may be due to the fact that the oxidative addition reaction is usually the rate-controlling step.

2.5 METHODS OF DETERMINING A REACTION MECHANISM

In many chemical reactions the reactants are normally not instantly transformed into products. Even the simplest type of reaction takes place *via* a series of elementary

reactions to give the overall reaction. This progression of events from reactants to products in a chemical reaction is called the reaction mechanism. A reaction mechanism shows whether a given chemical reaction occurs in a single molecular process (in which case it is called an elementary reaction) or in several. These elementary reactions combine together in parallel or competitive, consecutive and/or opposing reactions to constitute a proposed mechanism (Connors, 1990:59). In parallel reactions, a reactant undergoes two or more concurrent reactions to give different products. Consecutive reactions are those in which the product of one reactant is the reactant of the next reaction.

A chemical kinetic study does not fully determine a reaction mechanism. The proposed mechanism, however, must be consistent with kinetic evidence, i.e. with its empirical rate law. In addition to kinetic information the scientist normally uses information obtained from scientific sources and techniques to propose a mechanism. Even then a mechanism is not conclusively solved. That is why Espenson (1995) defined a reaction mechanism as a scientific postulate that is open to revision when new data, new insights or new theories of reactivity emerge. Some of these parameters (Connors, 1990:3) are discussed below.

2.5.1 Stereochemical methods

In determining the stereochemistry of the overall reaction the structure of both the reactant and product (if possible the intermediate as well) and the course of a reaction may give valuable information about the mechanism of a reaction (Bock *et al*.,1974:2814). Methods to characterise the stereochemical pathway of the reaction and to help with elucidating the mechanism include techniques such as IR, NMR and X-ray crystallography. However, it should be noted that product geometry alone is not a definitive way in establishing the mechanistic route and the geometry of the final complex can be misleading (Cross, 1985:209).

Generally, it is believed that oxidative addition of homonuclear molecules such as H_2, O_2, and I_2 in non-polar solvents result in product formation where the two addend fractions are added as bound to one another. This can be shown by H_2 addition to Vaska's complex (Cross, 1985:209):

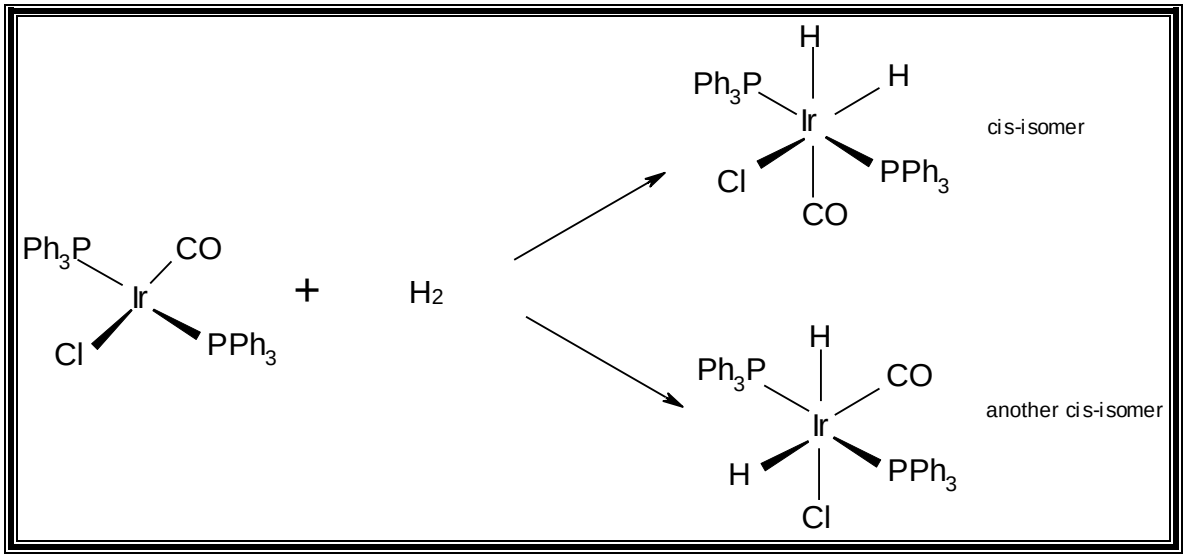

Scheme 2.4 Possible formation of *cis*-isomers.

Addend molecules containing polar properties normally result in *trans*-addition of the substrate fractions (Collman & Sears, 1968:27; Morarskiy & Stille, 1981:4182 and Strope & Shriver, 1974:2652), but *cis*-addition of such molecules as well as hydrogen halides (Hayde & Shaw, 1975:765 and Vaska, 1966:5325) and silanes (Johnson & Eisenberg, 1985:6531) have also been recorded. The oxidative addition of iodomethane to square planar Rh(I) and Ir(I) complexes can occur *via cis* or *trans* addition, depending on the mechanism that is followed during the reaction. If, as might be expected, the L ligands remain *trans*, then only two isomers are possible (Hayde & Shaw, 1975:765 and Cross, 1985:209).

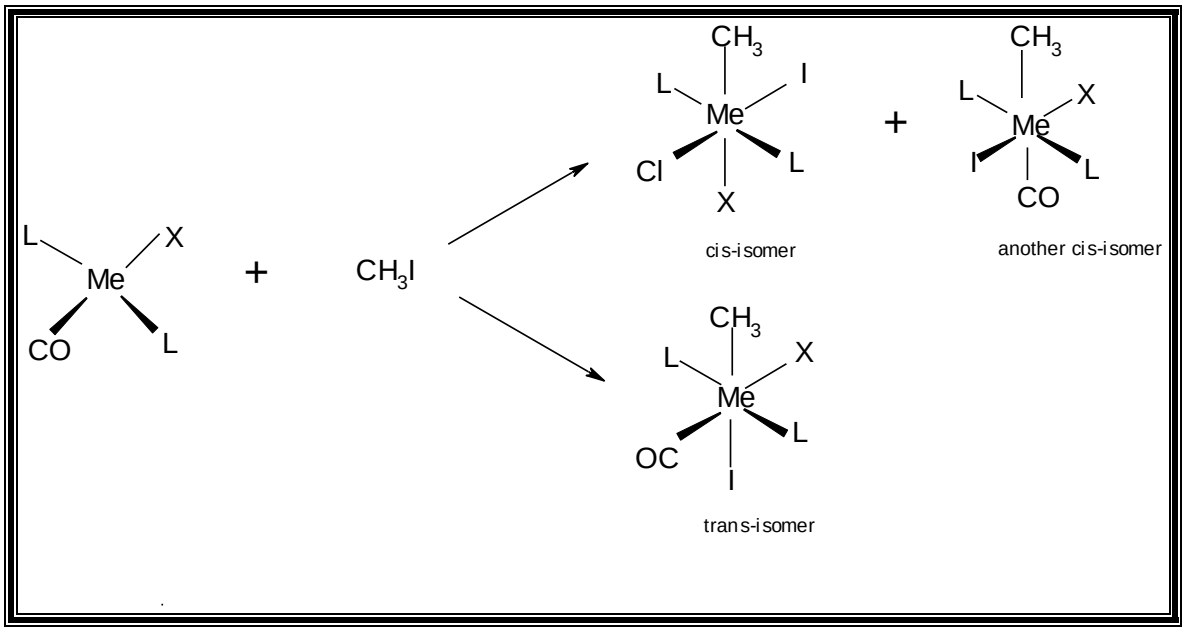

Scheme 2.5 Possible formation of isomers, L = Phosphines, X = Cl and Me = Rh(I), Ir(I).

Crystallographic and kinetic studies have been used to illustrate that the majority of oxidative addition reactions lead to the formation of the *trans*-isomer as the final product (Pearson & Muir, 1970:5519; Collman & Maclaury, 1974:3019 and Terblans *et al*., 1995:1748). The formation of this *trans*-isomer might be the result of isomerisation of the initial *cis* oxidative addition product. This kind of rearrangement was experimentally observed by Leipoldt *et al*. (1986:75; 1987:35). The study found that the oxidative addition of I_2 to [Rh(β-diketonato){$P(OPh_3)_3$}$_2$] resulted in the formation of the *trans*-isomer as the final product only after the isomerisation of the initially formed *cis*-analogue. The kinetic and structural determinations of the oxidative addition of methyl iodide to [Rh(cupf)(CO)(PPh_3)] indicated that the final oxidative addition adduct results in a product with the *cis*-configuration (Basson *et al*., 1987:31).

2.5.2 Factors governing the stereochemistry of the adduct

It is difficult to identify the factors that govern or influence the addition mode for a particular reaction, but it mainly depends on the mechanism followed during the reaction.

Kinetic studies show that an S_N2 two-step mechanistic route usually leads to *trans*-addition *via* a linear polar transition state (Griffin *et al*., 1996:3029 and Pearson & Muir 1970:5519). In cases where the reaction takes place *via* a three-centred concerted transition state, the formation of the *cis*-adduct is normally observed (Cross, 1985:209).

The nature of binding atoms of a bidentate ligand is one of the major factors that affect the configuration of the final product. Kinetic studies performed on the reaction between the oxidative addition of CH_3I to $[Rh(L\text{-}L')(CO)(PX_3)]$, X = Ph, *p*-ClPh, *p*-MeOPh, *etc.*, depend on the incoming group and nucleophilicity of the bidentate ligand in the metal complex. The results indicate that β-diketones containing two oxygen atoms such as cupferron lead to the formation of the alkyl complex as the final product *via cis*-alkyl formation (Basson *et al*., 1987:31) and *trans*-alkyl formation for β-diketonato ligands such as acac (Basson *et al*., 1986:35), substituted acac (Basson *et al*., 1984:167), 8-hydroxyquinolinato (Leipoldt *et al*., 1991:369), and dmvak (Purcell *et al*., 1995:14). As mentioned earlier, the inclusion of a sulphur donor atom in the bidentate chelate resulted in the rapid formation of the acyl complex. Leipoldt *et al*. (1993:11) characterised such a Rh(III)-acyl complex. The tendency could be related to a possible *trans*-labilisation effect of coordinated sulphur. In previous discussions it was emphasised that the rate-controlling step in the alkyl-acyl cycle is the alkyl formation, allowing for the isolation of both the alkyl complex as well as the subsequent acyl product in the final step. In the reaction involving these β-diketones containing the sulphur ligand, the rate-controlling step becomes acyl formation which results in the isolation of only the final product.

Another factor which affects the stereochemistry of the adduct is the steric effect of the ligands involved. Generally, it appears that less crowded complexes give a higher percentage of the *cis*-isomers and *vice versa*. Studies recently conducted by Verstuyft and Nelson (1975:150) on $[PdX_2L_2]$, L = PMe_2-*p*-C_6H_4Y or $PMe(p\text{-}C_6H_4Y)_2$, show that the *trans/cis* ratio is favoured by the following influences:

1) Making L more bulky
2) Changing X from N^{-3} to Cl^- to I^-
3) Making Y more electronegative.

In some cases the reaction media (solvents) can also affect the configuration of the adduct. Evidence from kinetic studies done by Vaska (1966:5325) as well as Blanke and Kubota (1970:989) of the oxidative addition of HX to $[IrX(CO)L_2]$, (X = Cl, Br, I and L = PPh_3) indicated *cis*-addition when non-polar solvents were used. In the presence of more polar solvents such as methanol, acetonitrile, water and DMSO, a mixture of the *cis* and *trans* isomers was formed.

The nature of the substrate, which oxidatively adds to a complex, can also affect the stereochemistry of the final product. Homonuclear molecules such as H_2 and O_2 lead to *cis*-addition in non-polar solvents (Cross, 1985:209), while the oxidative addition of I_2 to Rh(I) complexes give *trans*-isomers *via* isomerisation of the *cis*-adduct (Leipoldt *et al*., 1986:75; 1987:35). A possible explanation for isomerisation could be the result of steric requirements of I_2 as compared to H_2 and O_2.

The factors mentioned were those that influence the stereochemistry of the adduct. Moreover, the stereochemistry of the edduct can have an effect on the stereochemistry of the adduct. For example, studies indicate that an axial approach of CH_3I to Rh(I) and Ir(I) complexes is more favourable than a side-on approach (Griffin *et al*., 1996:3029) hence square planar complexes should be the favoured geometry of the edduct.

2.5.3 Volume of activation

The determination of the volume of activation (which can be obtained using Eq. 2.17) of a reaction is a powerful tool to determine the nature of the transition state and very helpful in proposing the reaction mechanism. Plots of ln k *vs* P gives a straight line with

a negative slope of $\frac{\Delta V^{\#}}{RT}$. The value of $\Delta V^{\#}$ may be zero, positive or negative. A negative value of the volume of activation implies bond formation in the transition state, as one would expect from an associative mechanism with the transition state occupying a smaller volume than that of the combined reactants. Hence a negative $\Delta V^{\#}$ could indicate that bond formation and/or charge creation must play a vital role on forming the transition state.

$$\ln k = \ln k^{\circ} - \frac{\Delta V^{\#}}{RT} P \qquad \textbf{(2.17)}$$

The magnitude of $\Delta V^{\#}$ is the sum of two independent components, $\Delta V^{\#}_{intrinsic}$ and $\Delta V^{\#}_{solvating}$. The former is the change in volume due to change in bond lengths and bond angles during the formation of the activated complex and the latter, $\Delta V^{\#}_{solvating}$, is the change in volume due to changes in solvation, e.g. electrostriction during the formation of the activated complex (Venter *et. al.*, 1991:2207). Interpretation of the observed activation volume is important not only to identify the contribution of the components but also to identify the mechanistic route of reactions.

In a study conducted by Venter *et. al.* (1991:2207) it was shown that the cupferrate system gave a large negative $\Delta V^{\#}$ value (*ca.* -25.0 $cm^3\ mol^{-1}$) in more polar solvents such as acetonitrile, indicating that this oxidative addition most probably proceeds *via* the linear transition state. Electrostriction effects play no role or have a small contribution since the marked negative $\Delta V^{\#}$ value did not correlate well with the smaller q_p values for the solvents employed.

2.5.4 Detection of intermediates

A reaction mechanism is difficult to determine, particularly when intermediates (if formed) go undetected or are not isolated. The least energetic intermediates, those

with the slowest reactions, can directly be detected during the course of a reaction. These intermediates are often free radicals, ion-radicals or ions, and could be detected either by spectroscopic or by chemical means. The results from these techniques could help with the determination of the composition of the intermediate and possibly its structure by trapping these intermediate and then identify or propose the product.

2.5.5 Isotopic substitution

Isotopes can be employed in several ways, the most direct of which is the tracer method, wherein the isotope is used merely as a label to keep track of a specified atom or group throughout the course of the reaction. CO-insertion into the M–R bonds is a good and relevant example where the mechanism was studied using isotopically labelled CO gas as incoming ligand (Scheme 2.3). The method confirmed that CH_3 migrates into the co-ordinated CO and the isotopic labelled ^{13}CO occupied the site where CH_3 initially occupied. Additional parameters include activation energies such as $\Delta S^{\#}$, $\Delta H^{\#}$, kinetic isotope effect and Linear Free Energy Relations (LFER).

2.6 MECHANISTIC ROUTES OF OXIDATIVE ADDITION REACTIONS

One of the main aims of this study is to determine the mechanism of oxidative addition reactions studied. The definition and methods of determining mechanistic routes are already presented in the previous section. This paragraph will present a discussion of the various types of mechanisms observed in oxidative addition reactions. These mechanisms were proposed, depending on kinetic patterns, X-ray crystallographic characterisations, NMR studies and theoretical approaches such as geometry optimisation and orbital symmetry theory (Koga & Morkuma, 1991:823). Research has shown that oxidative addition reactions can occur *via* a number of possible mechanisms. These mechanisms include the S_N2, three-centred, free radical and ionic pathways and will be discussed in the following paragraphs.

2.6.1 The S_N2 two-step mechanism

The S_N2 mechanism which is analogue to the Menschutkin-type (Baker, 1936:1448) reaction mechanism employs the metal centre as a nucleophile (Lewis base) and attacks the carbon of the adding halide molecule (Basson *et al*., 1984:167; Graffin *et al.*, 1996:3029 and Baker 1936:1448). This allows for the formation of a linear polar ionic transition state. Subsequently the iodide detaches itself from the methyl fraction to produce an ionic species (Oliver & Graham, 1970:243), which is stable in the case of the iridium complex, but collapses rapidly due to coordination of the halide ion to the coordination sphere in the case of the rhodium and cobalt complexes.

$$[Rh- - - \ CH_3^{\delta+} - - - I^{\delta-}]^{\#}$$

Figure 2.7 Linear transition state.

On the basis of orbital symmetry, these reactions are interpreted as the overlap between the donor orbital of the metal (probably the filled d_{z2}), and the acceptor p_z orbital where both have the same symmetry along the z-axis (Cross *et al*., 1985:197).

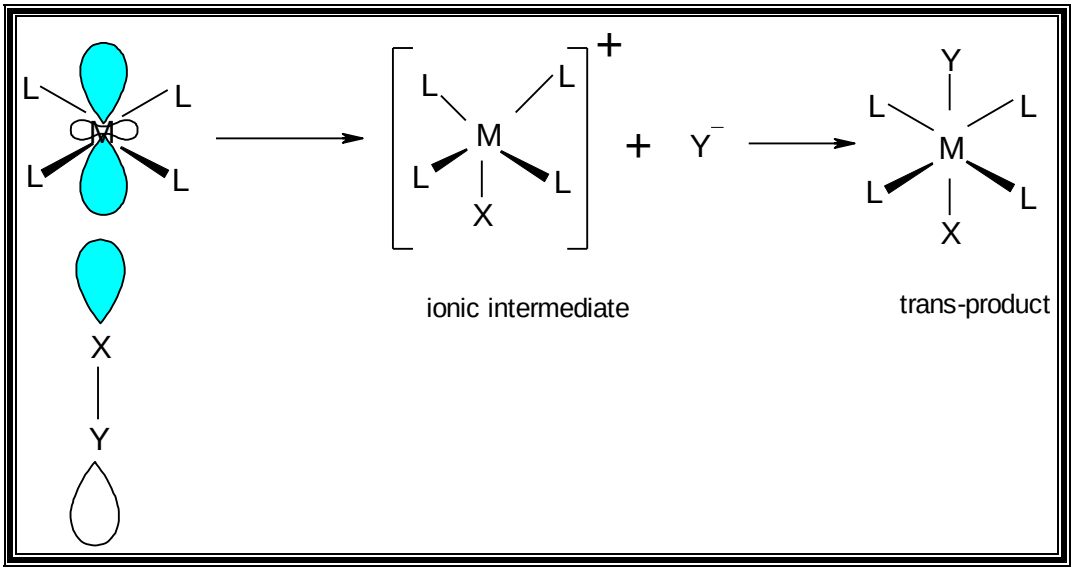

Scheme 2.6 Two-step S_N2 mechanistic route.

Kinetic and crystallographic studies propose a linear polar transition state for reactions that lead to a *trans*-configuration (Collman & Maclaury, 1974:3019 and Collman & Murphy, 1973:2687), but *cis*-addition has also been observed (Basson *et al*., 1987:31). Thus, 'X' and 'Y' fragments may end up *cis* or *trans* to one another in the final product.

S_N2 mechanisms are often proposed for oxidative addition reactions that have been performed with polar addend molecules such as methyl, allyl, and benzyl halides to complexes such as those of Vaska and related complexes. Recent reports (Haynes *et al*., 1996:3029) based on computational work have also presented experimental and theoretical evidence that support the same mechanism. Ab initio molecular orbital calculations for the addition of CH_3I to *cis*-$[MI_2(CO)_2]^-$, (M = Rh, Ir) as well as computed secondary α-Deuterium kinetic isotope effects (α-D KIEs) for the classical S_N2 mechanism are in excellent agreement with the experimental results. Haynes *et al*., for example, found excellent agreement between theoretical KIEs and experimental values, giving good evidence for an S_N2 inversion mechanism in these reactions. Additionally, orbital symmetry considerations (Labinger *et al*., 1970:612) do not exclude a two-step mechanism for the reaction of d^8 complexes with halides.

The same article by Haynes *et al*. clearly demonstrated that the methyl iodide substrate approaches the complex in two ways. An axial approach that leads to a linear transition state, with iodine directed away from the metal, is presumed to proceed with inversion of configuration at carbon. Retention of configuration results from a side-on approach of methyl iodide to the complex. Both mechanisms follow the S_N2 reaction. However, computational and experimental results indicate that a linear transition state is strongly favoured over the bent geometry.

2.6.2 The three-centred mechanistic route

It has already been mentioned that oxidative addition of a nonpolar addend such as H_2 and O_2 usually results in *cis*-addition. The reaction tends to proceed *via* a

three-centred transition state or intermediate as shown below. This can be illustrated by the oxidative addition of H_2 to Vaska's complex (Cross, 1985:209).

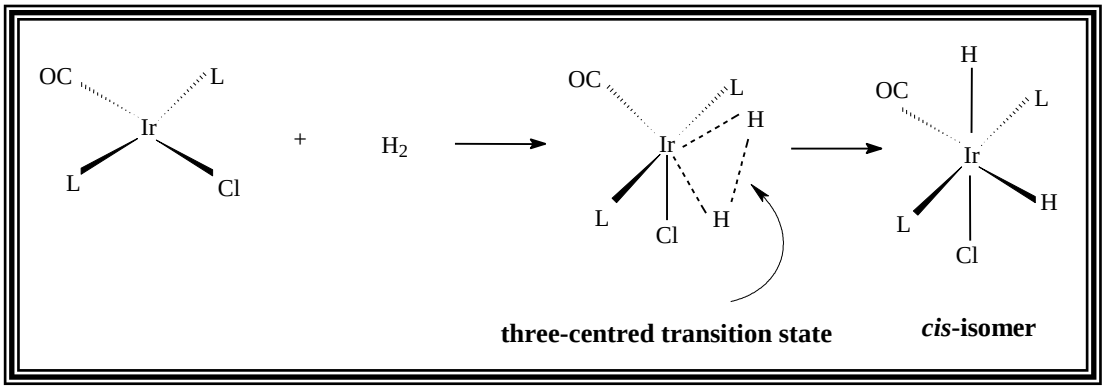

Scheme 2.7 Three-centred transition state.

A *cis*-isomer is usually formed, but subsequent rearrangement can give the *trans*-isomer as in the case of I_2 addition (Leipoldt *et al.*, 1986:75 and 1987:35). On the basis of orbital symmetry arguments, concerted *trans*-additions are symmetry-forbidden whereas *cis*-addition is allowed. According to the theory, the filled d_{xz} or d_{yz} orbital of the metal overlap with an empty σ*-orbital of the addend molecule as illustrated below.

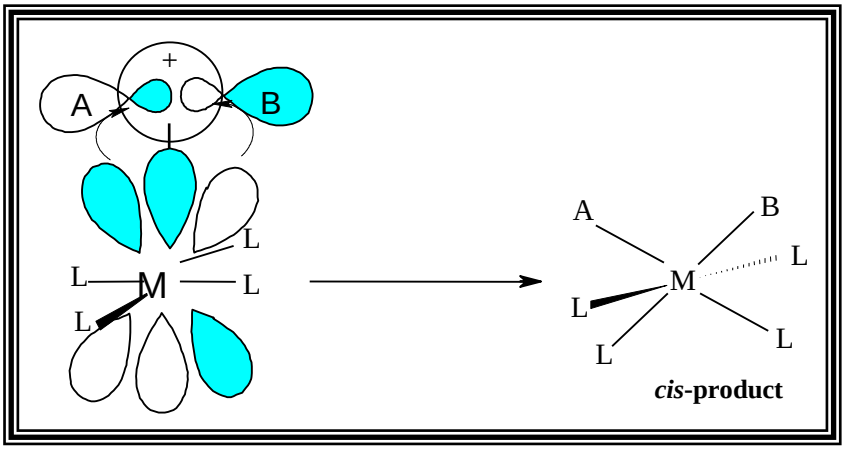

Scheme 2.8 The two-way electron flow in a concerted mechanism.

2.6.3 The radical mechanism

These pathways are often observed in odd electron systems such as Co(II) d^7 or Mn(0) d^7, although it can even occur in even electron systems like Ir(I) d^8. It was found that higher alkyl substrates such as propyl prefer such a mechanism (Labinger & Osborn, 1980:3230 and Haynes *et al*., 1994:3215). The radical chain mechanism requires radical initiators like traces of air/O_2, impurities, light (hυ), and in some cases the RX substrate itself initiates the reaction.

These parameters may initiate a radical pathway for a reaction that otherwise would have followed a non-radical mechanism such as S_N2. Reaction steps in the radical chain mechanism are widely available in literature (Lukehart, 1985:290). Evidence for such a mechanism includes trapping of $R^{\bullet}$ by scavengers, and the ability to initiate or inhibit the reaction with peroxides, light and oxygen. Radical mechanisms can be prevented by controlling the factors such as light, oxygen and impurities *etc* that lead to such mechanism.

2.6.4 The ionic mechanism

A solution of dissociated hydrogen halides largely favours such a mechanistic route. The complex, which acts as a Lewis base, is protonated first and then followed by the anion which bonds to the metal complex to give the final product. The opposite case is observed too, where the metal centre acts as an electrophile (Crabtree, 1988).

$$[Pt(PPh_3)_4] + H^+ + Cl^- \xrightarrow{-PPh_3} [HPt(PPh_3)_3]^+ + Cl^- \xrightarrow{-PPh_3} [HPtCl(PPh_3)_2] \quad \textbf{(2.18)}$$

Generally, only a few reactions proceed *via* the radical and ionic mechanisms. Some studies indicate the presence of two competing mechanisms, a S_N2 (or possibly three-centred) and a radical chain path (Still & Lau, 1977:434).

References

Anderson, G.K., Cross, R.J., *Acc. Chem. Res.*, (1984), **17**, 67.

Appleton, T.G., Clark, H.C., and Manzer, L.E., *J. Organomet. Chem.*, (1974), **65**, 275.

Aresta, M., Rossi, M., and Sacco, A., *Inorg. Chim. Acta*, (1975), **3**, 375.

Baker, J.W., *J. Chem. Soc.*, (1936), 1448.

Baker, M.J., Giles, M.G., Orpen, A.G., Taylor, M.J., and Watt, R.J., *J. Chem. Soc. Chem. Commun.*, (1995), 197.

Ball, M.C., and Norbury, A.H., *Physical Data For Inorganic Chemists*, 1st- edition, 1974, William Clowes and Sons. 136.

Barnett, K.W., and Treichel, P.M. *Inorg. Chem.*, (1967), **6**, 294.

Basson, S.S., Leipoldt, J.G., Roodt, A. and Venter, J.A., *Inorg. Chim. Acta*, (1987), **128**, 31.

Basson, S.S., Leipoldt, J.G., Roodt, A., and Venter, J.A., *Inorg. Chim. Acta*, (1986), **118**, L45-L47.

Basson, S.S., Leipoldt, J.G., Roodt, A., Venter, J.A., and Van der Walt, T.J., *Inorg. Chim. Acta*, (1986), **119**, 35.

Basson, S.S., Leipoldt, J.G., and Nel, J.T., *Inorg. Chim. Acta*, (1984), **84**, 167-172.

Bennett, M.J., Donaldson, P.B., *Inorg. Chem.*, (1977), **16,** 655.

Bergman, R., *Acc. Chem. Res.*, (1980), **13**, 113.

Blanke, D.M., Kubota, M., *Inorg. Chem.*, (1970), **9**, 989-991.

Bonati, F., and Wilkinson, G., *J. Chem. Soc.*, (1964), 3156.

Botha, L.J., Basson, S.S., and Leipoldt, J.G., *Inorg. Chim. Acta*, (1987), **126**, 25.

Bibler, J.P., and Wojeieki, A., *Inorg. Chem.*, (1966), **5**, 889.

Bock, P.L., Boschetto, D.J., Rasmussen, J.R., Demers, J.P., and Whitesides, G.M., *J. Am. Chem. Soc.*, (1974), **96**, 2814-2821.

Bush M.A., Hardy A.D.U., Manojlovic-Muir Lji., and Sim G.A., *J. Chem. Soc., A.* (1971), 1003.

Butler, I.S., Bosolo, F. and Pearson, R.G., *Inorg. Chem.*, (1967), **6**, 2070-2079.

Calderazzo, F., *Ang. Chem. Int. Ed.*, (1977), **16**, 299.

Calderazzo, F., and Cotton, F.A., *Inorg. Chem.*, (1962), **1**, 30-36.

Camel, E.J., and Anderson, J.A.M., *J. Organomet. Chem.*, (2000), **604**, 7-11.

Cavallo, L., and Sola, M., *J. Am. Chem. Soc.*, (2001), **123**, 12294-12302.

Cheng, C-H., Spivack, B.D., and Eisenberg, R., *J. Am. Chem. Soc.*, (1977), **99**, 3003.

Chock, P.B., and Halpern, J., *J. Am. Chem. Soc.*, (1966), **88**, 3511.

Clark, G.R., Skelton, B.W., and Waters, T.N., *J. Organomet. Chem.*, (1975), **85**, 375.

Collman, J.P., Hegedus, L.S., Norton, J.R., Finke, R.G., *Principles And Application Of Organotransition Metal Chemistry*, 1987, University Science Books, CA., 584.

Collman, J.P., Hegedus, L.S., Norton, J.R., Finke, R.G., *Principles And Application Of Organotransition Metal Chemistry*, 1987, University Science Books, CA., Part III *Application to Organic Synthesis*.

Collman, P.J., Hegedus, L.S., *Principles And Application Of Organotransition Metal Chemistry*; University Science Books, CA., 1980, 271-281.

Collman, J.P., Kubta, M., Vastine, F.D., Sun, J.Y., and Kang, J.W., *J. Am. Chem. Soc.*, (1968), **90**, 5430.

Collman, J.P., and Maclaury, M.R., *J. Am. Chem. Soc.*, (1974), **96**, 3019.

Collman, J.P., Murphy, D.W., and Doketti**,** G., *J. Am. Chem. Soc.*, (1973), **95**, 2687.

Collman, J.P. and Maclaury, M.R., *J. Am. Chem. Soc.*, (1974), **96**, 3019-3020.

Collman, J.P., and Sears, C.R., *Inorg. Chem.*, (1968), **7**, 27.

Connors, K.A., *Chemical Kinetics (The Study Of Reaction Rates)* VCH Publisher, 1990, USA. 59.

Cotton, J.D., Crisp, G.T. and Daly, V.A., *Inorg. Chim. Acta*, (1981), **47**, 165-169.

Cotton, J.D., Crisp, G.T. and Latif, L. *Inorg. Chim. Acta*, (1981), **47**, 171-176.

Crabtree, R.H., *The Organometallic Chemistry Of The Transition Metals*, Wiley-Interscience, USA, 1988, 309.

Cross, R.J., *Chem. Soc. Rev.*, (1985), **14**, 209.

Cross, R.J., *Chem. Soc. Rev.*, (1985), **14**, 197-223.

Damoense, L., (2000), Ph.D. Thesis, Free State University, Bloemfontein, South Africa.

Damoense, L.J., Purcell, W., and Roodt, A., *Rhodium Express*, (1995), **6**, 14.

Daura-oller, E., Poblet, J.M., and Carles Bo., *J. Chem. Soc., Dalton. Trans.*, (2003), 92.

Deeming, A.J., and Shaw, B.L., *J. Chem. Soc. (A)*, (1969),1802.

Dierkes, P., and P.W.N.M. van Leeuwen, *J. Chem. Soc., Dalton Trans*., (1999), 1519.

Douek and Wilkinson, *J. Chem. Soc. (A)*, (1964), 2604.

Ellis, P.R., Pearson, J.M., Haynes, A., Adams, H., Bailey, N.A., Maitlis, P.M., *Organometallics*, (1994), **13**, 3215.

Empsall, H.D., Hyde, E.M., Jones, C.E., and Shaw, B.L.,*J. Am. Chem. Soc., Dalton. Trans*. (1974), 1980.

Espenson, J. H., *Chemical Kinetics And Reaction Mechanism*, 2nd-edition, McGraw-Hill Series, 1995, USA.

Fauvarque, J.F., Pfluger, F., and Troupel, M., *J. Organomet. Chem*., (1981), **208**, 419.

Flood, T.C., Jensen, J.E., Statler, J.A., *J. Am. Chem. Soc*., (1981), **103**, 4410-4414.

Foster, D., *J. Am. Chem. Soc*., (1976), **98**, 846.

Garrou, P.G., *Chem. Rev*., (1985), **85**, 171.

Gilli, A. and Stille, J.K., *J. Am. Chem. Soc*., (1980), **102**, 4933.

Gonsalvi, L., Adams, H., Sunley, G.J., Ditzel, E., and. Hayens, A., *J. Am. Chem. Soc*., (1999), **121**, 11233.

Graham, D.E., Lamprecht, G.J., Potgieter, I.M., Roodt, A., and Leipoldt, J.G., *Transition Met. Chem*., (1991), **16**, 193.

Graziani, R., Bombieni, G., Volpani, L., Panatheni, C., and Clark, R.J.H., *J. Chem. Soc.(A)*, 1969, 1236.

Griffin, T.R., Cook, D.B., Haynes, A., Pearson, J.M., Monti D., and Morris, G.E., *J. Am. Chem. Soc*., (1996), **118**, 3029.

Halpern, J., and Wong, C.S., *J. Chem. Soc. Chem. Commun*., (1973), 629.

Halpern, J., *Inorg. Chim. Acta*, (1981), **50**, 11-19.

Hardy A.D.U. and Sim G.A, *J. Chem. Soc. Dalton Trans*., (1972), 1900.

Hart-Davis, A.J., and Graham, W.A.G., *Inorg. Chem*., (1971), **10**, 8.

Haynes, A., Mann, B.E., Morris, G.E., Maitlis, P.M., *J. Am. Chem. Soc*., (1993), **115**, 4093.

Hench, R.F., *J. Am. Chem. Soc*., (1964), **86**, 2796.

Hitchcoc, P.B., Mcparflin, M., Mason, R., *Chem. Commun*., (1969), 1367.

Hongyu, Xu., and Li Jia, *Organic Lett*., (2003), **5**, 3955-3957.

Hussey, A.S., and Yakeuchi, Y., *J. Org. Chem*., (1970), **35**, 643.

Hyde, E.M., and Shaw, B.L., *J. Chem. Soc*., *Dalton Trans*., (1975), 765.

Jonathan R. Dilworth, John R.Miller, Nigel Wheatley, Micheal J.Baker and J.Glenn Sunley, *J. Chem. Soc. Chem. Commun*., (1995), 1579.

Johnson, C.E., and Eisenberg, R., *J. Am. Chem. Soc*., (1985), **107**, 6531-6540.

Katti, K.V., Santarsiero, B.D., Pinkerton, A.A., and Cavell, R.G., *Inorg. Chem*., (1993), **32**, 5919.

Kemp, G., Roodt, A., and Purcell, W., *Rhodium Express*, (1996), **16**, 17-22.

Koga, N., and Morokuma, K., *Chem. Rev*., (1991), **91**, 823-842.

Koga, K. and Morokuma, K., *J. Am. Chem. Soc*. (1985), **107**, 7230.

Koga, K. and Morokuma, K., *J. Am. Chem. Soc*., (1986), **108**, 6536.

Kubota, M., Kiefer, G.W., Ishikawa, R.M., and Bencala, K.E., *Inorg. Chim. Acta*, (1973), **7**, 195.

Labinger, J.A., Branus, R.G., Dolphin, D., and Osborn, J.A., *J. Chem. Soc. Chem. Commun*., (1970), 612.

Labinger, J.A. and Osborn, J.A., *Inorg. Chem*., (1980), **19**, 3230.

Leipoldt, J.G., Steynberg, E.C. and Van Eldik, R ., *Inorg. Chem*., (1987), **26**, 3068.

Leipoldt, J.G., Basson, S.S. and Botha, L.J., *Inorg. Chim. Acta*, (1990), **168**, 215.

Leipoldt, J.G., Basson, S.S., Schlenbusch, J.J.J., and Grobler, E.C., *Inorg. Chim. Acta*, (1982), **62**, 113-115.

Longat, B., Morandini, F., Bresadola, S., *Inorg. Chim. Acta*, (1980), **39**, 27-34.

Lukehart, C.M., *Fundamental Transition Metal Organometallic Chemistry*, Brooks/Cole Pub. Co., CA., 1985, 405.

Maitlis, P.M., Haynes, A., Sunley, G.J., and Howard, M.J., *J. Chem. Soc*., *Dalton Trans*., 996, 2187-2196.

Mawby, R.J., Bosolo, F., Pearson, R.G., *J. Am. Chem. Soc*., (1964), **86**, 3994-3999.

Mcauliffe, C.A., and Levason; W., *Phosphine, Arsine and Stibine Complexes of Ttransition Elements*; Elsevier Scientific Publishing Company, 1979, Netherlands.

Mehrotra, R.C., Bohra, R., and Gaur, D.P., *Metal β-Diketones and Allied Derivatives*, 1978, Academic Press, London, Chapter 1.

Mehrotra, R.C., Bohra, R., and Gaur, D.P., *Metal β-Diketones and Allied Derivatives*, 1978, Academic Press, London, Chapter 6.

Micheal, W., and Bergman, R.G., *J. Am. Chem. Soc*., (1981), **103**, 7028-7030.

Miller, E.R., and Shaw, B.L., *J. Chem. Soc., Dalton Trans*., (1974), 480.

Moloy, K.G., and Wegman, R.W. *Organometallics,* (1989), **8**, 2889.

Morarskiy, A., and Stille, J.K., *J. Am. Chem. Soc*., (1981), **103**, 4182.

Nicholas, K., Raghu, S., Rosenblum, M., *J. Organomet. Chem*., (1974), **78**, 133-137.

Oliver, A.J., and Graham, W.A.G., *Inorg. Chem*., (1970), **9**, 243.

Otto, S., *Structural and Reactivity Relationship in Platinum(II) and Rhodium(I) Complexes*, Ph.D. Thesis, Free State University,1999.

Parshall, G.W., and Putscher, R.E., *J. Chem. Educ*., (1986), **63**, 188-109.

Pearson, R.G., and Muir, W.R., *J. Am. Chem. Soc*., (1970), **92**, 5519.

Pidcock, A., Richards, R.E., and Vegans, L.M., *J. Chem. Soc. (A)*, (1966), 1707.

Preston, H., (1993), Ph.D. Thesis, Free State University, Bloemfontein, South Africa.

Rankin, J., Poole, A.D., Benyei, A.C., Cole-Hamilton, D.J., *J. Chem. Soc. Chem. Commun*., (1997), 1835.

Rasul, M., Shah, J. and Ali, M. *Application Note*, 2002, Pakistan.

Roodt, A., and Steyn, G.J.J., *Rec. Res. Inorg. Chem*., (2000), **2**, 1-23.

Roodt, A., Leipoldt, J.G., Koch, K.R., and Matoetoe, M., *Rhodium Exp*., (1994), **7/8**, 39.

Sakaki, S., Kitaura, K., Morokuma, K., Ohkubo, K., *J. Am. Chem. Soc*., (1983), **105**, 2280.

Scott, R.N., Shriver, D.F., and Lehman, D.D. *Inorg. Chim. Acta*., (1970), **4**, 73.

Shaw, B. L., and Stainbank, R.E., *J. Chem. Soc*., (A), (1971), 3716.

Shaw, B.L., and Stainbank, R.E., *J. Chem. Soc., Dalton. Trans*., (1972), 223.

Shriver, D.F., Scott, R.N., and Lehman, D., *Inorg. Chim. Acta*., (1970), **4**,73.

Singer, H., and Wilkinson, G., *J. Chem. Soc. (A),* (1968), 2516.

Steyn, G.J.J., Roodt, A., and Leipoldt, J.G., *Rhodium Express,* (1993), **0**, 11-15.

Steyn, G.J.J., Roodt, A., and Leipoldt, J.G., *Inorg. Chem*., (1992), **31**, 3477-3481.

Steyn, G.J.J., Roodt, A., and Leipoldt, J.G., *Rhodium Express*, (1993), **1**, 25.

Stille, J.K., and Lau, K.S.Y., *Acc. Chem. Res*., (1977), **10**, 434.

Strope, D., and Shriver, D.F, *Inorg. Chem*., (1974), **13**, 2652.

Terblans, Y.M., Basson, S.S., Purcell, W., and Lamprecht, G.J., *Acta, Cryst*., (1995), C51, 1748.

Thorn, D.L. and Hoftamn, R., *The olefine insertion reaction, J. Am. Chem. Soc*., (1978), **100**, 2079-90.

Tolman, C.A., *J. Chem. Ed*., (1968), **63**, 199.

Tolman, C.A., *Chem. Rev*., (1977), **77**, 3.

Tolman, C.A., *J. Am. Chem. Soc*., (1970), **92**, 2953.

Treciak A.M., and Ziolkowski J.J., *Inorg. Chem. Acta*, (1985), **96**, 15.

Ugo, R., Pasini, A., Fusi, A., and Cemini, S., *J. Am. Chem. Soc*., (1972), **94**, 7364.

Van Aswegen, K.G., Leipoldt, J.G., Potgieter, I.M., Roodt, A., and Van Zyl, G. J., *Trans Met. Chem*., (1991), **16**, 369.

Van Zyl, G.J., Lamprecht, G.J., Leipoldt, J.G., and Swaddle, T.W., *Inorg. Chim. Acta*, (1988), **143**, 223.

Van Zyl, G.J., Lamprecht, G.J., and Leipoldt, J.G., *Inorg. Chim. Acta*, (1986), **122**,75.

Van Zyl, G.J., Lamprecht, G.J., and Leipoldt, J.G., *Inorg. Chim. Acta*, (1987), **129**, 35.

Van Zyl, G.J., Lamprecht, G.J., Leipoldt, J.G., and Swaddle, T.S., *Inorg. Chim. Acta*., (1988), **143**, 223-227.

Vaska, L., *J. Am. Chem. Soc*., (1966), **88,** 5325.

Vaska, L., and Chen, L. S., *Chem. Commun*., (1971),1080.

Vaska, L., Brady, R., Decamp, W.H., Flynn, B.R., Schneider, M.L., Scott, J.D., and Werneke, M.F., *Inorg. Chem*., (1975), **14**, 2669-2675.

Vaska, L., and Diluzio, J., *J. Am. Chem. Soc*., (1961), **83**, 2784 and (1962), **84**, 679.

Venter, J.A., Leipoldt, J.G., and Van Eldik, R., *Inorg. Chem*., (1991), **30**, 2207-2209.

Verstuyft, A.W., and Nelson, J.H., *Inorg. Chem*., (1975), **14**, 150.

Wegman, R.G., Abatjoglou, A.G., and Harrison, A.M., *J. Chem. Soc. Chem. Commun*., (1987), 1891.

CHAPTER 3

SYNTHESIS AND CHARACTERISATION OF Rh(I) CARBONYL COMPLEXES CONTAINING ARSINE AND CUPFERRATE

3.1 INTRODUCTION

It has already been stated in chapter 2 that square planar Rh(I) carbonyl complexes, being coordinatively unsaturated, undergo oxidative addition reactions with various organic and inorganic molecules. These reactions can proceed via different reaction pathways. It is thus essential to characterise reactants and products in order to propose a suitable reaction mechanism.

This chapter describes the various methods and materials (chemicals and instruments) used in synthesising and characterising the compounds used in this study. The identification and characterisation of the complexes and the reaction products are necessary to ensure that the right type of the reaction is investigated. At the end, correlation between IR and ^{1}H NMR data is reported and discussed. With regard to X-ray

analysis, the phosphine analogue, [Rh(cupf)(CO)(PPh_3)], of the arsine complex studied, was previously characterised by Basson *et al*., (1986:45) and isomorphism is commonly observed in analogous complexes.

3.2 GENERAL OBSERVATIONS ON SUBSTITUTION REACTIONS

The substitution reaction of the carbonyl group in the [Rh(L-L'-BID)($CO)_2$] type of complexes, with L−L' = O−O, N−O or N−S anionic bidentate ligands, by PR_3 or AsR_3 seems to depend on the donor properties of L−L' and the incoming ligand. In principle, with L−L' a non-symmetrical bidentate ligand, two isomers could be formed. Non-symmetrical β-diketones such as benzoylacetone(BAC), trifluoroacetylacetone(TFA), benzoyltrifluoroacetone(BTA) and naphthoyltrifluoroacetone (NTA) are known to indicate the presence of two isomers in solution (Trzeciak & Ziolkowski, 1985:15).

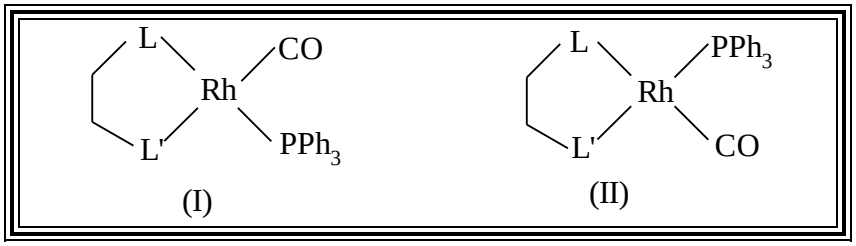

Figure 3.1 Possible isomer formation during the substitution reaction between [Rh(L-L'-BID)($CO)_2$] and PPh_3 (L-L' = bidentate ligand).

Solution studies employing ^{1}H, ^{13}C, and ^{31}P NMR clearly showed the presence of two isomers in solution (Trzeciak & Ziolkowski, 1985:15, Cherkasova, Osetrava & Varshavsky, 1993:8 and Cherkasova *et al*., 1993:21). However, crystallographic studies on various [Rh(L-L'-BID)(CO)(PPh_3)] complexes for example L-L' = Pic (Leipoldt, Lamprecht & Graham, 1985:123), Sacac (Botha *et al*., (1987:25) and dmavk (Purcell *et. al*., 1994:10) revealed that only one isomer crystallised from the solution.

These results showed that the thermodynamic most stable isomer in the solid state is that in which substitution takes place *trans* to the atom of the bidentate ligand which exerts the larger *trans* influence.

As mentioned in chapter 2 the *trans* influence order for oxygen, nitrogen and sulphur donor atoms is S > N > O, i.e. the least electronegative atom exerts the largest *trans* influence. However, in [Rh(N-S-BID)$(CO)_2$] type of complexes where N-S = macsm (Steyn *et al*., 1992:3477), cacsm and stsc (Roodt & Steyn, 2001:1) an unexpected substitution pattern was observed, i.e. the CO ligand *trans* to nitrogen atom was substituted. This unexpected substitution mode was found due to the much larger steric demand of bulky substituents which showed that substitution modes can also be sterically controlled.

Spectroscopic investigations has confirmed that if the donor capabilities of L and L' are similar, two isomers are formed in comparable ratio. Familiar examples of these include the asymmetrical β-diketones, [Rh($R^1COCHCOR^2$)(CO)(PR_3)], where $R^1 \neq R^2$ such as (CH_3, Ph) or (CH_3, CF_3) (Trzeciak & Ziolkowski 1985:15). However, in some cases solvents play an important role in the determination of the ratio of the two isomers present in a solution. Varshavsky *et al*. (1993:8, 1993:14 & 1993:17) studied the reaction between [Rh(AVK)$(CO)_2$] and PPh_3 in benzene and chloroform, using ^{31}P and ^{13}C NMR techniques and detected two [Rh(AVK)(CO)(PPh_3)] isomers in a 10:1 ratio i.e. P-*trans*-N and P-*trans*-O respectively. However, as expected, the former isomer crystallised in the solid state that indicates its relative thermodynamic stability. So far, the unique case where two isomers crystallise in the same unit cell was found with [Rh(BA)(CO)(PPh_3)], BA = benzoylacetonato (Purcell *et al*., 1995:153).

With regard to cupferrate complexes, reactions of [Rh(cupf)$(CO)_2$] with equimolar PPh_3 substituted one carbonyl group. This was expected and further confirmed by X-ray crystallographic study of the monocarbonyl product, [Rh(cupf)(CO)(PPh_3)]

(Basson *et al*., 1986:45). The structure showed that PPh_3 positioned *trans* to the nitroso oxygen, in other words the CO ligand *trans* to that oxygen was replaced by the phosphine. Perhaps two isomers might have formed in solution, i.e. one with PPh_3 *trans* and the second *cis* to nitroso oxygen. However, as explained above, the thermodynamic most stable isomer crystallises out. The substitution of one carbonyl group of the parent complex, $[Rh(L\text{-}L'\text{-}BID)(CO)_2]$, by PX_3 (X= Ph, Cy, *etc*) has been successfully used to determine the relative *trans* influence of the two oxygen atoms of non-symmetrical β-diketones or cupferrate oxygen atoms. Hence one can say, in $[Rh(cupf)(CO)(PPh_3)]$ the nitroso oxygen of the cupferrate's ligand atom has the greater *trans* influence and the second oxygen nearest to the phenyl is more electron deficient, thus exerting a smaller *trans* influence.

These substitution reactions are also dependent on the incoming ligand. The carbon monoxide groups can be completely replaced by COD (Bonati & Wilikinson, 1964:3156), PF_3 (Collman *et al*., 1987:71), diphosphine ligands like dppm (Cano *et al*., 1994:1563) and partially by triphenyl phosphine (Purcell *et al*., 1995.153) arsines and stibines (Bonati & Wilikinson 1964:3156). It is interesting to note that the reaction with triphenyl phosphite produced $[Rh(\beta\text{-diketone})\{P(OPh)_3\}_2]$ or $[Rh(\beta\text{-diketone})(CO)=\{P(OPh_3)\}]$ depending on the amount of the phosphite used (Trzeciak & Ziolkowski 1985:15). In contrast, when Basson *et al*., (1990:1324) added excess (about 10 fold) PPh_3 to $[Rh(cupf)(CO)(PPh_3)]$, the reaction did not lead to substitution of the remaining carbonyl group, but instead a penta co-ordinated complex, $[Rh(cupf)(CO)(PPh_3)_2]$, was formed.

The fact that only one CO group is substituted by PPh_3 and both by $P(OPh)_3$ may be explained in two ways:

1. The weaker donor and better π-acceptor properties of the phosphite weakens the remaining Rh-CO bond in the respective monocarbonyl, with the result that it is also substitutable with excess $P(OPh)_3$.

2. Or it may be the result of the smaller cone angle of the phosphite compared to that of phosphine, 130 *vs* 145°, respectively (Tolman 1977:3).

Since PPh_3 has an almost comparable electronic property as the corresponding arsine ligand (at least both possess σ-donor and π-acceptor ability, though the magnitude of the ability is still in contention), a similar substitution mode is highly expected, i.e. like PPh_3, the $AsPh_3$ ligand would also replace the CO ligand *trans* to nitroso oxygen. The bulkier size of arsenic atom (covalent radius of 1.20Å *vs* 1.10 Å , for As and P respectively (Ball & Norbory, 1974), is very unlikely to play a role, but would slow down the substitution reaction relative to phosphine. The subject will be discussed in more detail in the following chapter.

3.3 EXPERIMENTAL

3.3.1 Instruments and starting reagents

The complexes prepared were characterised by means of IR and ^1H NMR spectroscopy. The CO stretching frequencies of the complexes were obtained from infrared spectra recorded on a DIGILAB FTS 2000 spectrophotometer in the wavenumber range 600 to 2200 cm^{-1}, and the liquid infrared spectra in the range (2100-1650 cm^{-1}) in dry organic solvents in a NaCl cell. The ^1H NMR spectra were obtained in $CDCl_3$/acetone solution on a 300 MHz Bruker spectrometer. All chemical shifts are reported in ppm.

The chemicals used in the study, Rh(III) tricholoride ($RhCl_3.3H_2O$), ammonium salt of N−nitrosophenyl hydroxyamine (cupferron), triphenylarsine ($AsPh_3$) and diphenyl-methylarsine ($AsMePh_2$) are all commercially available. Rhodium-μ-dichloro-dicarbonyl dimer was synthesised from Rh(III) tricholoride as will be described in the following section. All the chemicals were of analytical reagent grade and when necessary, were recrystallised to increase purity.

3.3.2 Synthesis of the complexes

3.3.2.1 Preparation of Rh(I) dicarbonyl

Both dicarbonyl complexes, $[Rh(cupf)(CO)_2]$ and $[Rh(cupf.CH_3)(CO)_2]$, were synthesised by refluxing 0.30g of $RhCl_3.3H_2O$ in 25ml of DMF for about 25 minutes until the colour changed from red to orange yellow (Goswami & Singh, 1980:83). A small amount of distilled water (2-3 drops) was added before refluxing to enhance the solubility of the ionic compound. To the resulting yellow solution of rhodium-μ-dichloro-dicarbonyl dimer, a slight excess of cupferron was added and stirred. The overall reactions can be presented as follows:

$$RhCl_3.3H_2O \xrightarrow[\Delta]{DMF} [Rh(CO)_2Cl]_2 + COCl_2 + H_2O \qquad \textbf{(3.1)}$$

$$[Rh(CO)_2Cl]_2 + 2cupf \longrightarrow 2[Rh(cupf)(CO)_2] + 2Cl^- \qquad \textbf{(3.2)}$$

Adding ice-cold water precipitated the complex formed in reaction 3.2, firstly dropwise to initiate crystal growth and then in larger quantities to facilitate complete precipitation of the product. The resulting yellow precipitate was suction filtered to isolate the product. The average yield was 68%. Recrystalisation to increase the purity (for example from acetone) did not yield crystals. Spectroscopic characterisation of the product is given below and the spectra is presented in Figures 3.3, 3.4 and 3.5 (pages 95 - 97).

$[Rh(cupf)(CO)_2]$

IR: $\upsilon(CO) = 2009.8, 2087.2\ cm^{-1}$

^1H NMR: 7.6 ppm

$[Rh(cupf.CH_3)(CO)_2]$

IR: $\upsilon(CO) = 1996.9, 2087.8\ cm^{-1}$

^1H NMR: 7.3 ppm and 2.3 ppm

As expected, both dicarbonyls, [Rh(cupf)$(CO)_2$] and [Rh(cupf.CH_3)$(CO)_2$], gave two CO stretching frequencies corresponding to the two CO groups. Morever, both gave multiplets in the region 7.3-7.6 ppm which are associated with the cupferron ligand. The cupf.CH_3 gave an addition peak at 2.3 ppm, integrating to 3 protons for the CH_3 group bound to the cupferrate ligand.

3.3.2.2 Preparation of [Rh(L-L')(CO)($AsPh_3$)] (L-L' = cupf and cupf.CH_3) and [Rh(cupf)(CO)($AsMePh_2$)]

To a solution of [Rh(cupf)$(CO)_2$] (0.20 g, 0.675 mmoles) in about 20 ml acetone, slight excess of triphenylarsine ($AsPh_3$) was added slowly. The substitution of the CO from the coordination sphere was clearly visible with the formation and subsequent liberation of CO gas from the reaction mixture. The substitution reaction with $AsPh_3$ can be illustrated as follows:

$$[Rh(L\text{-}L')(CO)_2] + AsPh_3 \longrightarrow [Rh(L\text{-}L')(CO)(AsPh_3)] + CO \quad \textbf{(3.3)}$$

The complex formed was isolated by adding ice cold water and stirring it for about 45 minutes to enhance precipitation. The resulting yellow precipitate was collected by suction filtration. Characterisation resulted in the following:

[Rh(cupf)(CO)($AsPh_3$)]

IR: $\upsilon(CO) = 1978.8\ cm^{-1}$

^1H NMR: 7.6 & 8 ppm

[Rh(cupf.CH_3)(CO)($AsPh_3$)]

IR: $\upsilon(CO) = 1976.5\ cm^{-1}$

[Rh(cupf)(CO)($AsMePh_2$)]

IR: $\upsilon(CO) = 1965.5\ cm^{-1}$

^1H NMR: 1.7 ppm

The IR of the products formed showed only one sharp carbonyl peak corresponding to one CO group. These results, in addition to the liberated CO from the reaction mixture confirmed replacement of one CO group by the arsine ligand. The ^{1}H NMR of [Rh(cupf)(CO)($AsPh_3$)] gave multiplets at 7.6 ppm indicating the presence of phenyl protons, which is attributed to the presence of $AsPh_3$. The [Rh(cupf)(CO)($AsMePh_2$)] gave additional signals at δ =1.7 ppm which is assigned to the methyl protons of the $AsCH_3Ph_2$ ligand.

The reaction of [Rh(cupf)$(CO)_2$] with $AsPh_3$ was also followed by means of IR spectroscopy. The spectra obtained for this reaction is successively presented in Figure 3.2. The spectra clearly indicate the simultaneous disappearance of the two Rh(I)-dicarbonyl CO peaks (2009.8 and 2087.2 cm^{-1}) accompanied by the appearance of the Rh(I)-monocarbonyl CO peak at 1975.1 cm^{-1}. As a result the stretching frequency of the unsubstituted CO group shifts to a lower wavenumber as one of the CO groups is displaced out of the coordination sphere by the incoming triphenylarsine ligand. More electron density on the rhodium centre as a result of the arsine ligand's σ-donation ability leads to more back-donation from rhodium to carbon. A stronger Rh-CO bond and a weaker carbon-oxygen bond with a lower stretching frequency follows.

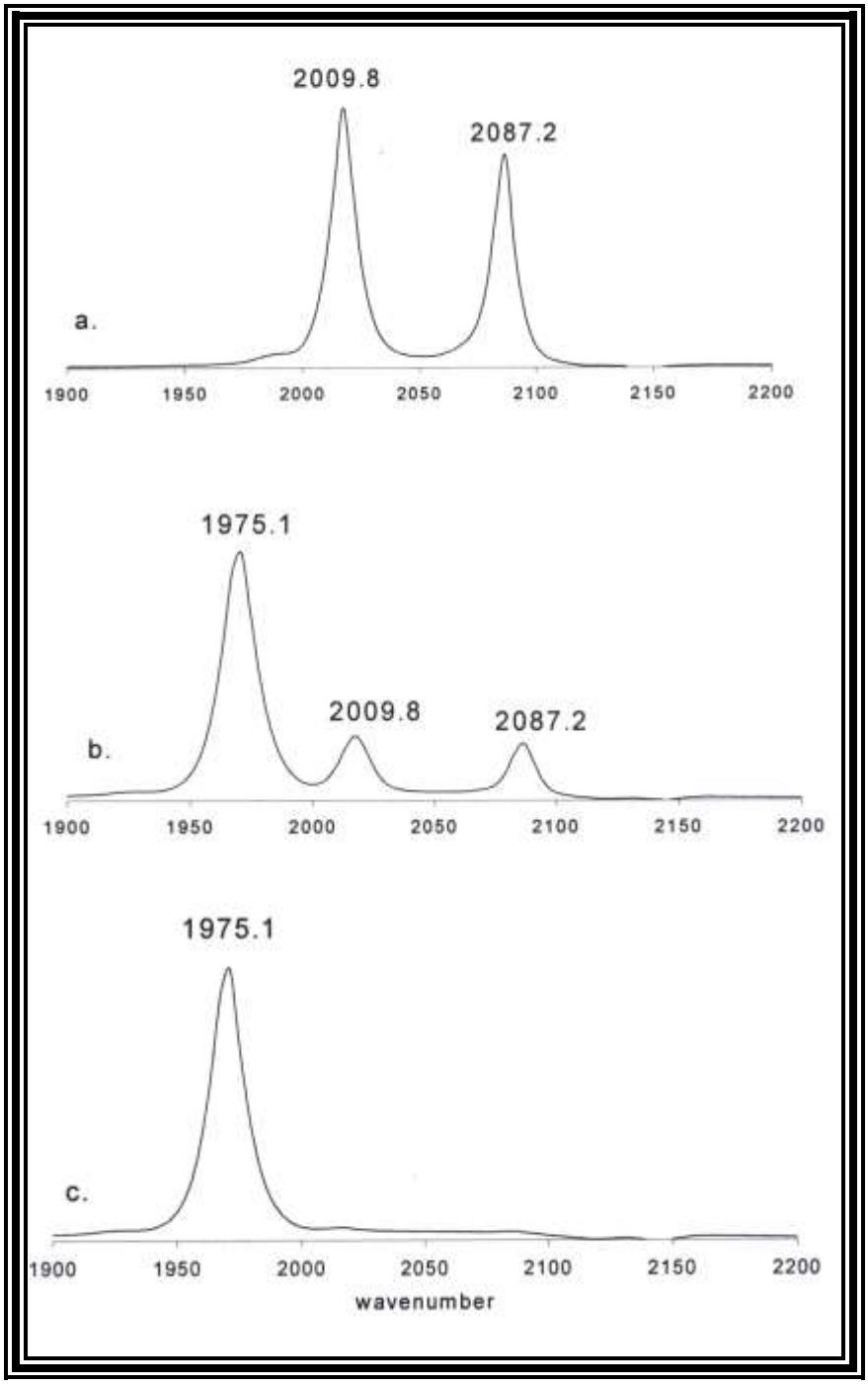

Figure 3.2 The progress of substitution reaction between [Rh(cupf)$(CO)_2$] and $AsPh_3$ ligand. (a) shows the complex in solution of acetone, i.e before addition of any ligand, (b) when *ca*. 90% of the ligand was added and (c) when slight excess of the ligand was added to the solution in (b).

3.3.2.3 Preparation of [RhI(cupf)(CH_3)(CO)($AsPh_3$)]

The title complex, the oxidative addition product, was prepared by adding 0.335 g (0.1475 ml) CH_3I to 0.125 g of [Rh(cupf)(CO)($AsPh_3$)] which was already dissolved in *ca*. 3 ml of acetone. The solution was covered with a plastic film for about 25 minutes, then opened to allow evaporation of the red orange solution to give yellow crystals, which were unfortunately not suitable for an X-ray crystal structure analysis.

IR: Rh(III)-CO, υ(CO) = 2040.2 cm^{-1}

^1H NMR: could not be done due to instability of the complex in several solvents.

3.4 DISCUSSION

The two sharp peaks around 2000 cm^{-1} (refer Fig. 3.3) in the IR spectra of the dicarbonyl complex confirmed the existence of two carbonyl groups in the complex. The spectra of the reaction products between Rh(I) dicarbonyl complex and the triphenylarsine and diphenylmethylarsine ligands showed only one sharp carbonyl peak (corresponding to one CO group) at 1978.8 and 1965.5 cm^{-1} respectively. This confirms that, as expected, only one CO group was replaced by the arsine ligands. The reaction progress for [Rh(cupf)($CO)_2$] with triphenyl arsine ligand is illustrated in Figure 3.2.

The complexes prepared in this study were further characterised using ^1H NMR techniques. The dicarbonyl and monocarbonyl, [Rh(cupf)($CO)_2$] and [Rh(cupf)(CO)($AsPh_3$)], gave multiplets at 7.6 ppm indicating the presence of phenyl protons. Complexes [Rh(cupf.CH_3)($CO)_2$] and [Rh(cupf)(CO)($AsMePh_2$)] gave additional signals at about 2.3 ppm and 1.7 ppm respectively, i.e. the methyl protons of the former complex resonate more down-field than the latter as a result of the inductive effect of the phenyl group. The collection of these signals confirms the presence of phenyl and methyl groups, which indicate that the compounds were correctly prepared with regard to phenyl and methyl containing cupferrate complexes.

3.5 CONCLUSION

The arsine complexes, [Rh(cupf)(CO)($AsPh_3$)], [Rh(cupf.CH_3)(CO)($AsPh_3$)] and [Rh(cupf)(CO)($AsMePh_2$)], have been successfully synthesised and characterised by IR and ^{1}H NMR spectroscopy. Both types of spectra showed that the desired products were synthesised. The observed decrease in the υ(CO) value with σ-donor ligands such as triphenylarsine might have mechanistic implication for the oxidative addition of organic substrates such as iodomethane to the metal centre where an increase in Lewis basicity is expected to enhance the rate of nucleophilic attack by the Rh-atom on the substrate. Furthermore, Rh(I) arsine complexes are expected to be less steric demanding than their corresponding phosphine complexes. This is believed due to a longer Rh-As bond length and slightly smaller cone angle of a corresponding phosphine ligand. However, electronic factors also play an important role in such reactions. These aspects will be addressed in the next chapter where the experimental kinetic results of the various complexes are discussed in detail.

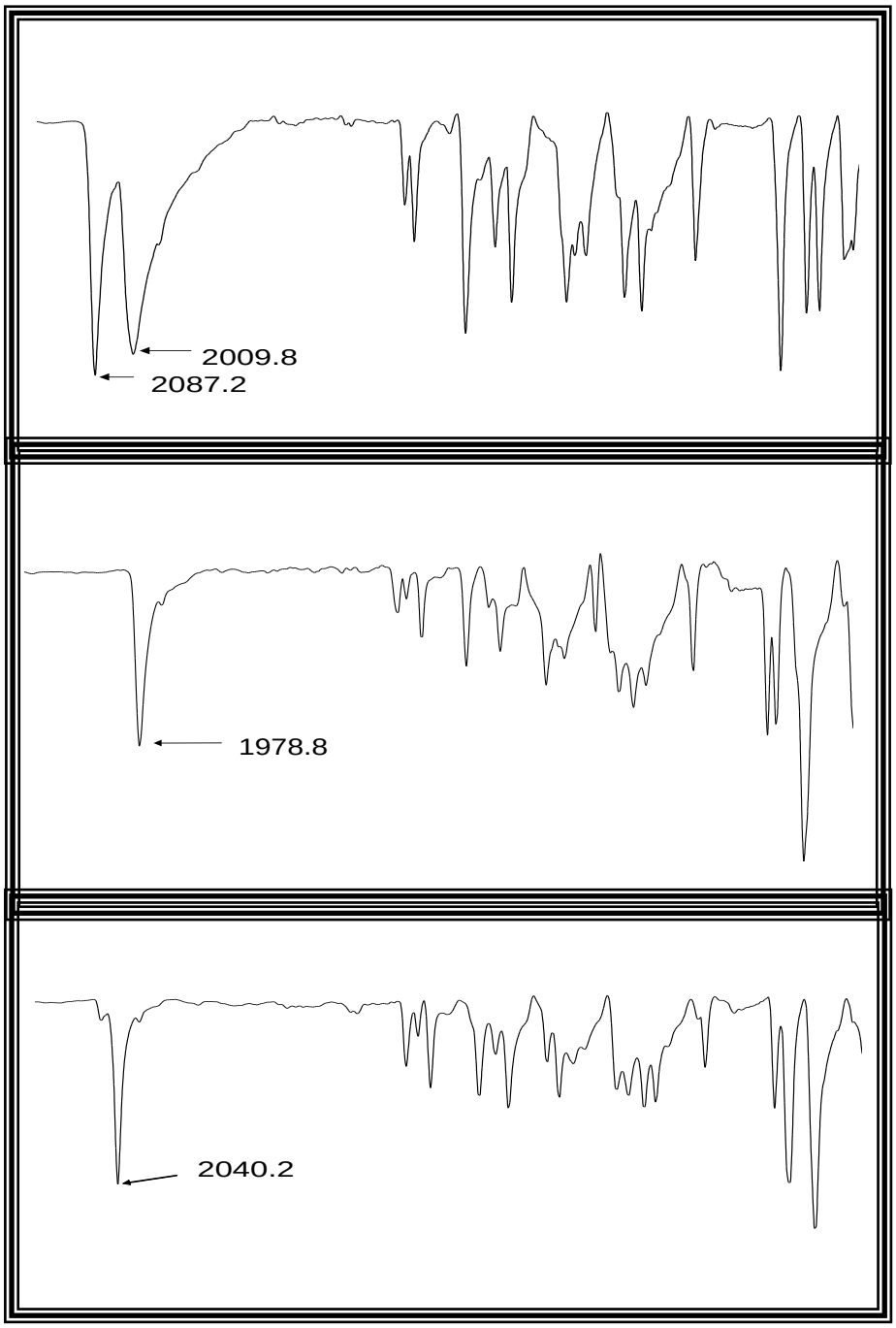

Figure 3.3 From top to bottom: IR Spectra of [Rh(cupf)$(CO)_2$], [Rh(cupf)(CO)$(AsPh_3)$] and [RhI(cupf)(CO)$(CH_3)(AsPh_3)$] in solid state respectively, in the range of 600 cm^{-1} to 2200 cm^{-1}.

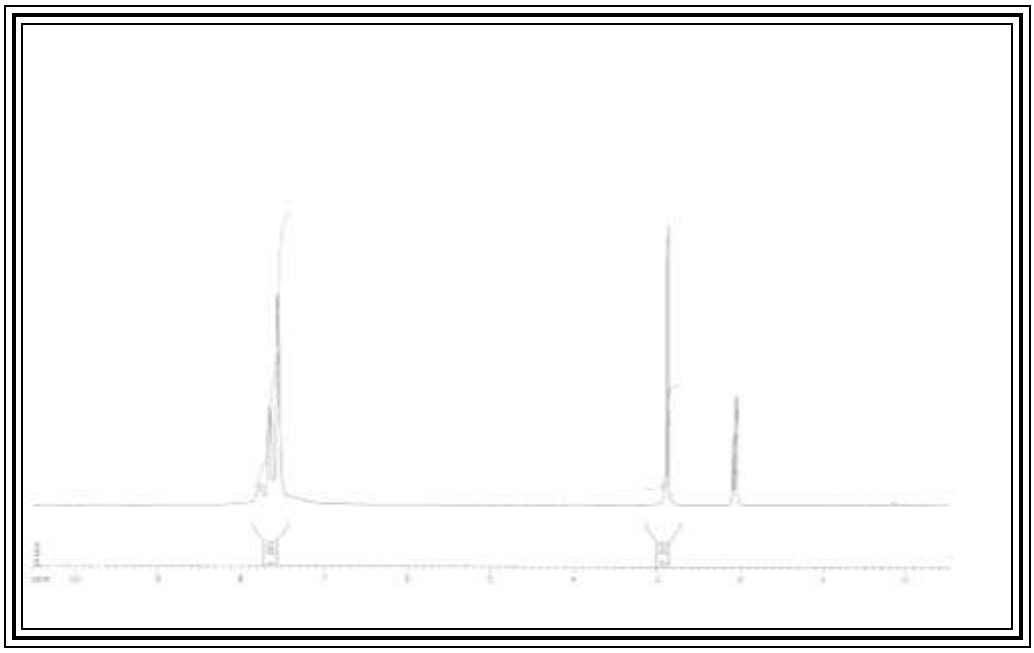

Figure 3.4 ^{1}H NMR spectrum of the dicarbonyl complex, [Rh(cupf)$(CO)_2$].

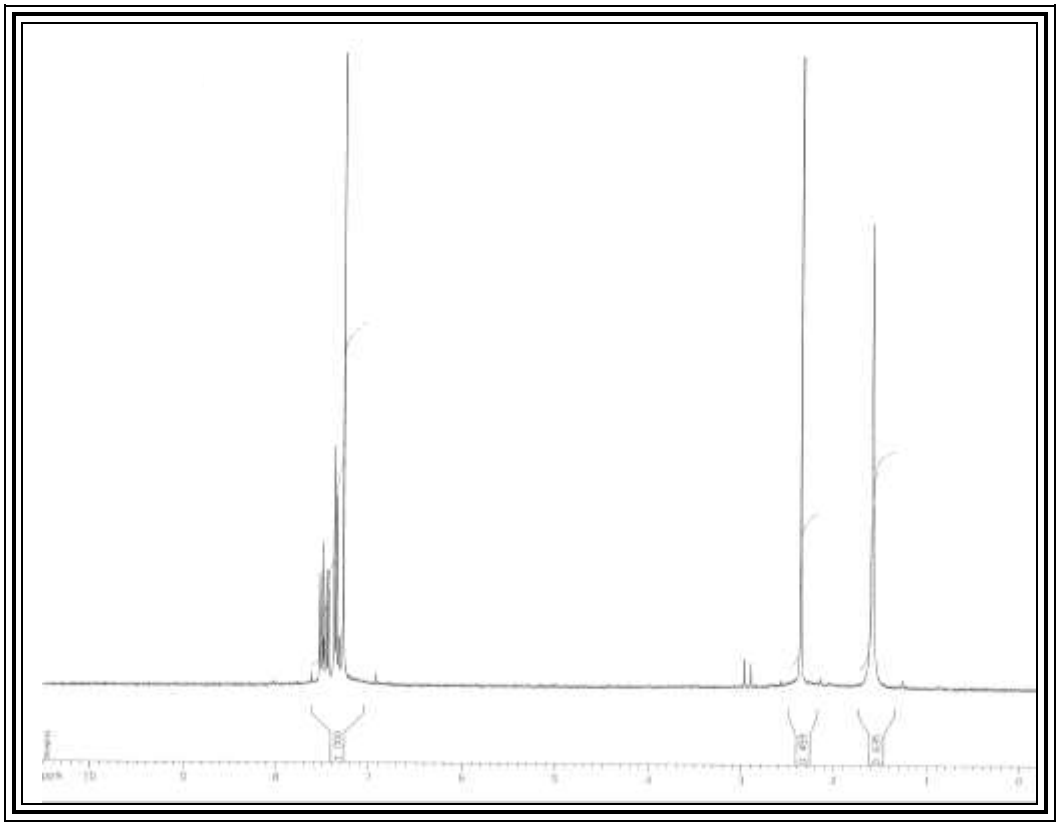

Figure 3.5 ^{1}H NMR spectrum of the dicarbonyl complex, [Rh(cupf.CH_3)$(CO)_2$].

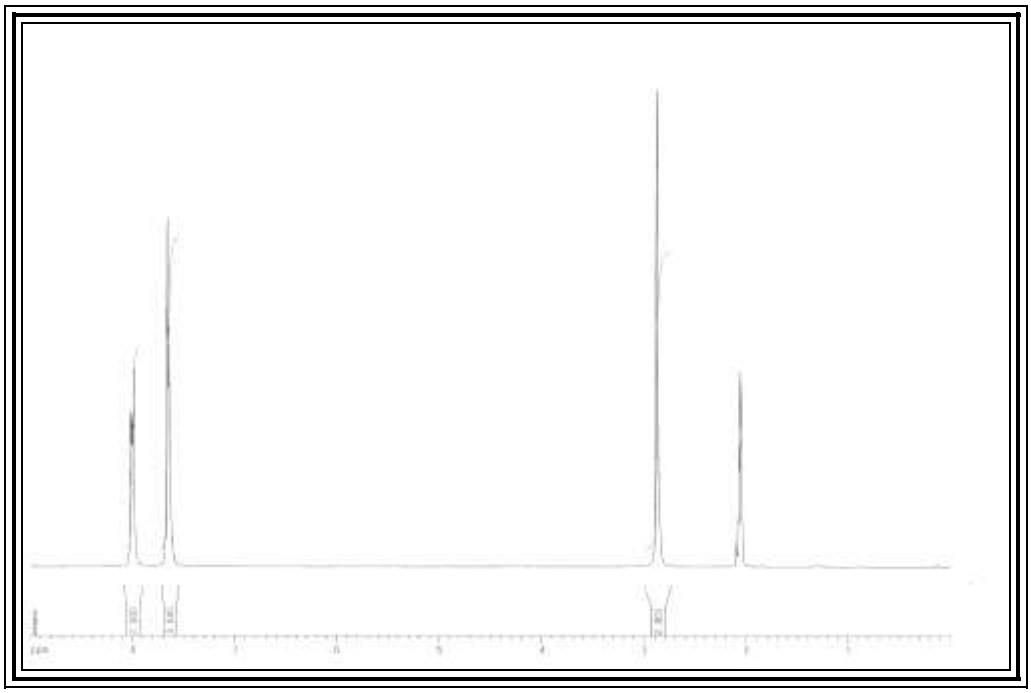

Figure 3.6 ^{1}H NMR spectrum of the monocarbonyl complex, [Rh(cupf)(CO)($AsPh_3$)].

References

Ball, M.C., and Norbory, A.H., *Physical Data For Inorganic Chemists*, Longman Group Limited, 1974, London.

Basson, S.S., Leipoldt, J.G., and Venter, J.A., *Acta*. *Cryst*., (1990), **C46**, 1324.

Basson, S.S., Leipoldt, J.G., Roodt, A., and Venter, J.A., *Inorg*. *Chim*. *Acta*, (1986), **118**, L45.

Bonati, F., and Wilikinson, G., *J*. *Chem*. *Soc*., (1964), 3156.

Botha, L.J., Basson, S.S., Leipoldt, J.G., *Inorg*. *Chim Acta*, (1987), **126**, 25.

Cano, M., Heras, J.V., Lobo, M.A., Pinilla, E., and Momge, M.A., *Polyhedron* (1994), **13**, 1563-1573.

Cherkasova, T.G., Osetrava, L.V., and Varshavsky, Y.S., *Rhodium Express,* (1993), **1**, 8.

Cherkasova, T.G., Varshavsky, Podkorytov, I.S., and Osetrava, L.V., *Rhodium Express*, (1993), **0**, 21.

Cherkasova, T.G., Galding, M.R., Osetrava, L.V., and Varshavsky, Yu.S., *Rhodium Express*, (1993), **3**,

Collman, J.P., Hegedus, L.S., Norton, J.R., Finke, R.G., *Principles And Application Of Organotransition Metal Chemistry*, 1987, Part I, University Science Books, 71.

Damoense, L.J., Purcell, W., Roodt, A., and Leipoldt, J.G., *Rhodium Express,* (1994), **5**, 10.

Galding, M.R., Cherkasova, T.G., Osetrava, L.V., and Varshavsky, Yu. S., *Rhodium Express*, (1993), **1**, 14.

Goswami, K., and Singh, M.M., *Trans*. *Met*. *Chem*., (1980), **5**, 83.

Langford, C.H., Gray, H.B., *Ligand Substitution Process*, W.A. Benjamin Inc., New York, 1966.

Leipoldt, J.G., Lamprecht, G.J., and Graham, D.E., *Inorg. Chim*. *Acta*, (1985), **101**, 123.

Leipoldt, J.G., Basson, S.S., Schlebusch , J.J.J, and Grobler, E.C., *Inorg*. *Chim*. *Acta*, (1982), **62**, 113-115.

Leipoldt, J.G., Basson, S.S., Lamprecht, G.J., Bok, L.D.C., and Schlebusch, J.J.J., *Inorg. Chim*. *Acta*, (1980), **40**, 43.

Purcell, W., Basson, S.S., Leipoldt, J.G., Roodt, A., and Preston, H., *Inorg. Chim. Acta*, (1995), **234**, 153.

Roodt, A., and Steyn, G.J.J., *Inorg. Chem.*, (2001), **2**, 1-23.

Steyn, G.J.J., Roodt, A., and Leipoldt, J.G, (1992), **31**, 3477.

Tolman, C.T., *Chemical Rev.*, (1977), 77, 3.

Trzeciak, A.M., and Ziolkowski, J.J., *Inorg. Chim. Acta*, (1985), **96**, 15.

CHAPTER 4

KINETIC STUDY OF IODOMETHANE ADDITION TO Rh(I) CUPFERRATE ARSINE COMPLEXES

4.1 INTRODUCTION

The kinetics and mechanism of oxidative addition reactions of transition metal complexes with d^8 electronic configuration such as Rh(I) complexes with iodomethane have been extensively reported. In particular, Basson *et al*., (1987:31) have studied oxidative addition of CH_3I to [Rh(cupf)(CO)(PX_3)], cupferron having a small bite angle 76.6(3) deg. and X = Ph, *p*-PhCl, *p*-PhOMe. As an extension of these results this study manipulates electron density and steric demand of [Rh(L-L')(CO)(AsX)] (L-L' = cupf and cupf.CH_3, X = Ph_3 and $MePh_2$) complexes for the first time. Steric manipulation was accomplished by interchanging $AsPh_3$ with the $AsMePh_2$ ligand. In fact, this change would possibly lead to a steric as well as an electronic effect since the methyl is more electron donating than the phenyl group. Pure electronic manipulation was achieved by introducing the electron releasing methyl substituent group on the phenyl ring of the cupferron (2-methyl cupferrate). This study also utilised the Rh(III)-alkyl intermediate, [RhI(cupf)(CO)(CH_3)($AsPh_3$)], as starting complex to investigate solvent effects on its CO-insertion reaction.

Hence in this chapter the kinetics of some Rh(I) arsine complexes and solvent effects in CO-insertion reactions are reported and discussed. The kinetic effect of the substrates employed, such as CH_3I, CH_3Br and CH_3CH_2I, and data interpretation are presented as well. Kinetic data or results obtained are presented in five sections. Each section is accompanied by a broad discussion and conclusion where data are correlated with each other as well as with related systems reported in the literature. As we know, determination or proposal of a reaction mechanism is a major objective of chemical kinetics and therefore a possible reaction mechanistic route will be proposed from the results of this study.

4.2 GENERAL REACTION MECHANISM

The reaction route for the oxidative addition of iodomethane to various complexes of the type [Rh(L-L')(CO)(PX_3)], (L-L') = monocharged bidentate ligands, has been studied in this laboratory using techniques such as X-ray crystallography, IR, UV/VIS and ^1H , ^{31}P-NMR and can generally be presented as follows:

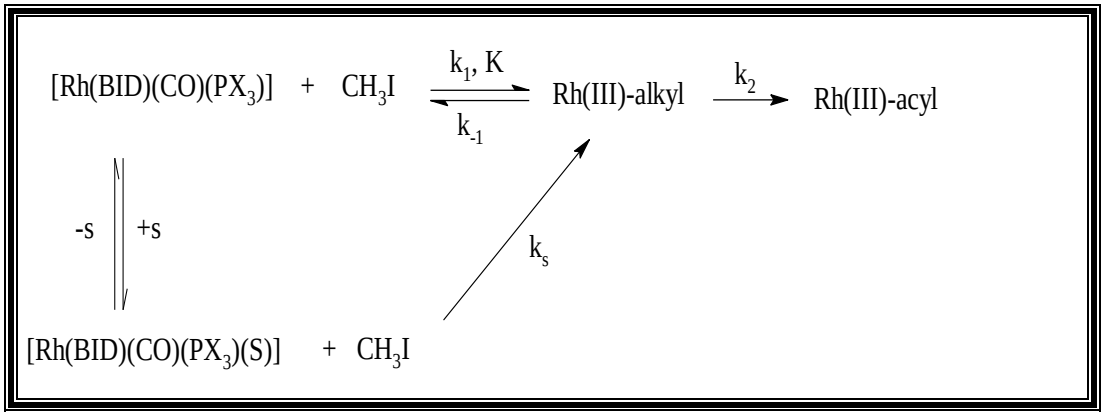

Scheme 4.1 General reaction scheme: iodomethane oxidative addition to [Rh(BID)(CO)(PX_3)] complexes. (BID = bidentate ligand and S denotes solvent and k_s = solvent path).

Various kinetic studies postulated the above scheme and in cases detected or isolated the alkyl intermediate which further depletes by parallel or consecutive CO-insertion pathways to a final Rh(III)-acyl product (Roodt *et al.*, 2000:1 and Basson *et al*., 1984:167). However, the final outcome towards alkyl or acyl complexes are dependent on the type of L-L' ligand or its nucleophilicity. If L-L' = O-S, N-S, or S-S the acyl complex is stabilized (Leipoldt *et al*., 1990:215 and Eisenberg *et al*., 1977:3003). In the case of L-L'= β-diketone such as acac (Basson *et al*., 1984:167) and hydroxyquinolinate (Leipoldt *et al*., 1991:369) the final products were alkyl complexes. The effect of coordinated sulphur is discussed in Chapter 2.

The above general route becomes more complex due to solvent pathways observed in few oxidative addition reactions. For instance, Basson *et al*., (1987:31) observed substantial solvent interaction in the reaction between CH_3I and [Rh(cupf)(CO)(PPh_3)], i.e. highly polar solvents like acetonitrile and DMSO have greatly enhanced the rate-controlling reaction step. Hence the respective mechanism was proposed to include a solvent pathway. Furthermore, in the reaction between iodomethane and corresponding complexes with L-L' = N-S bidentate ligands such as cacsm, solvent variation resulted in significant changes in the rate of oxidative addition, but a separate solvent pathway could not be detected (Roodt *et al*., 2001:1).

4.3 EXPERIMENTAL PROCEDURE

The preparation and spectroscopic characterization of the complexes kinetically investigated were described in Chapter 3. All chemicals were of reagent grade materials. Iodomethane, iodoethane and bromomethane were used as purchased. The complexes were characterised by IR measurements of the Rh(I)−CO wavenumbers and ^1H NMR. The reaction was followed spectrophotometrically with UV/VIS radiation using a CARY 50 Conc Spectrophotometer equipped with a thermostated cell compartment (± 0.2 °C) by measuring the rate of formation of Rh(III)-alkyl complexes. The

concentration of the metal complex was 1.7×10^{-4} M and the concentration of CH_3I was in large excess (0.2 - 1.0 M), i.e. all reactions were monitored under pseudo-first-order conditions. Known volumes of thermostated solutions of the complex and the reagents were mixed in a 1 cm cell placed in the thermostated cell compartment of the instrument. From the recorded visible spectra such as Figure 4.1, a suitable wavelength was chosen and the kinetics of the reactions were followed by recording the change in absorption as a function of time.

All IR measurements were done on a DIGILAB Spectrophotometer in the region 600 to 3000 cm^{-1}. IR kinetic measurements were performed in a thermostated (± 0.2 °C) cell of NaCl optics. Most spectra were done in chloroform and acetone at *ca*. 25 °C. Some of the spectra are presented in Figures 4.3, 4.8.1 and 4.8.2. From the recorded IR-multi-scanned spectra, the disappearance of the reactant, [Rh(cupf)(CO)($AsPh_3$)] and the formation of the product, [RhI(CH_3)(cupf)(CO)($AsPh_3$)], obeyed first-order kinetics. Pseudo-first-order rate constants of the reactions were then calculated from the slopes of the linear plots of $\ln(|A_\infty - A_t|)$ *vs* time obtained from kinetic runs at a definite CH_3I concentration.

Kinetic data analysis were conducted by means of Microsoft Excel 97 (1997), Microsoft Excel XP (2002) for the IR data and Micro Math Scientist (1990) for the UV/VIS data. Kinetic least-squares curve fitting was done using Equation 4.1, where A_t and A_∞ are absorbance after time t and infinite respectively. Infinite time was considered approximately $10t_{1/2}$. The activation enthalpy and entropy were determined using the Eyring equation (Equation 4.2).

$$A_t = A_\infty - (A_\infty - A_0)\, e^{k_{obs}.t} \qquad \textbf{(4.1)}$$

$$\ln\left(\frac{k}{T}\right) = \ln\left(\frac{k_B}{h}\right) + \left(\frac{\Delta S^{\#}}{R}\right) - \left(\frac{\Delta H^{\#}}{RT}\right) \quad \textbf{(4.2)}$$

A graph of $\ln\left(\frac{k}{T}\right)$ against $\frac{1}{T}$ should be linear with slope = $\left(\frac{-\Delta H^{\#}}{R}\right)$ and y-intercept = $\frac{\Delta S^{\#}}{R} + \ln\left(\frac{k_B}{h}\right)$. Thus the slope gives $\Delta H^{\#}$, the standard enthalpy change of activation, and the intercept gives $\Delta S^{\#}$, the standard entropy change of activation.

4.4 PRELIMINARY INVESTIGATION OF THE REACTION BETWEEN IODOMETHANE AND [Rh(Cupf)(CO)(AsPh$_3$)]

The kinetics of the oxidative addition reaction of iodomethane to various [Rh(L-L')(CO)(PX$_3$)] complexes (where L-L' = monocharged bidentate ligands and X = different substituents on the phosphorous atom) was studied in this laboratory and summarised in Chapter 1. As a continuation of this research, the present study has the objective of varying the electron density and specifically steric properties of Rh(I) complexes by introducing cupferron, a bidentate ligand with a significant smaller bite angle as well as triphenylarsine ligands. The combined effects of these two manipulations thus form the basis of this study. Preliminary work focused on the progress and outcome of Eq. 4.3 through spectrophotometric measurements.

$$[Rh(cupf)(CO)(AsPh_3)] + CH_3I \underset{k_{-1}}{\overset{k_1}{\rightleftharpoons}} [RhI(cupf)(CO)(CH_3)(AsPh_3)] \quad \textbf{(4.3)}$$

Overlay scans of the above reaction was recorded in the visible region from 340–600 nm (Fig. 4.1). These overlay scans are used to select an optimum wavelength

for the study of absorption change as a function of time. The formation of a product was observed at a wavelength of about 400 nm in acetone. This product was later identified by virtue of IR spectra as the oxidative addition product, [RhI(cupf)(CO)(CH_3)($AsPh_3$)] (refer Fig.4.3).

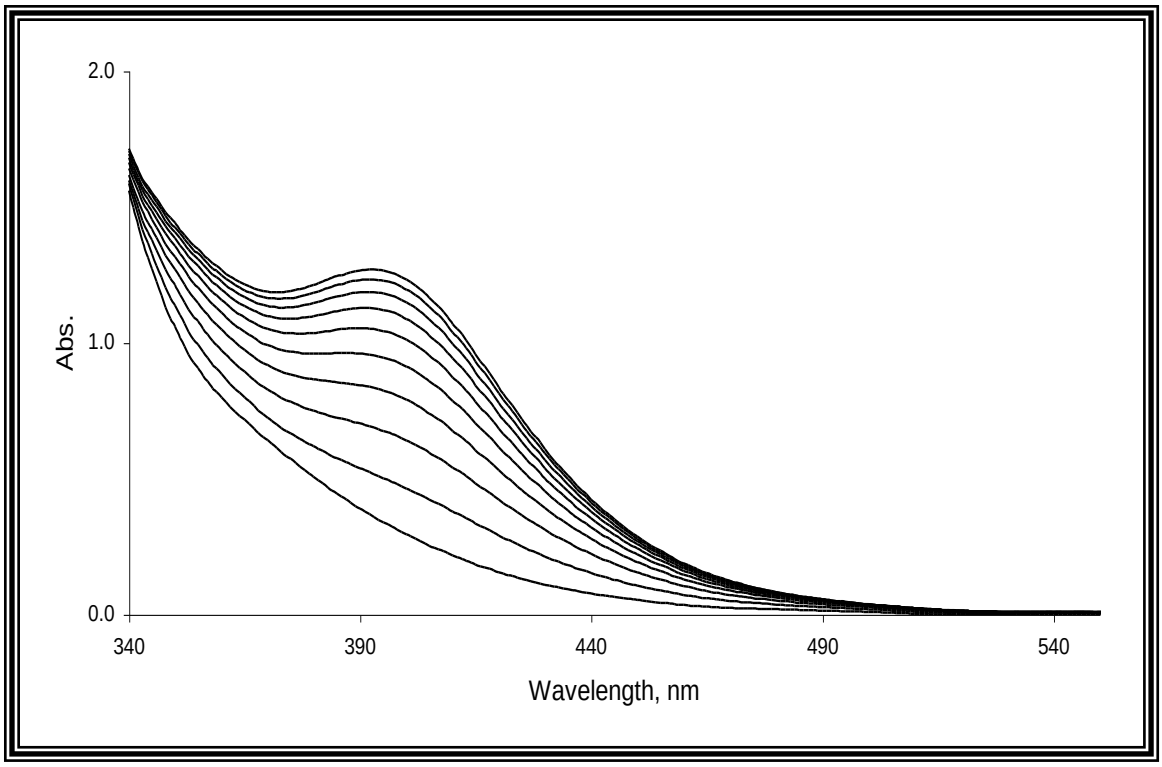

Figure 4.1 UV/VIS multi-scans (every 10 minute) for the oxidative addition of CH_3I to [Rh(cupf)(CO)($AsPh_3$)] in acetone at 25.8 °C. [complex] = 4.8×10^{-4} M, [CH_3I] = 0.088 M

An initial fast increase and later a progressively slower increase in absorbance as the reaction proceeded showed that the reaction should be first-order, which was confirmed by the linearity of plots of $\ln(|A_\infty - A_t|)$ *vs* time. Furthermore, the spectra in acetone appeared to indicate the formation of a single product without biphasic behaviour, i.e. no second reaction or formation of another product was observed or detected even after 10 half-lives of the reaction (15 hours of scanning). Overlay scans for the same reaction in chloroform and ethyl acetate gave similar spectra as in acetone, with absorption maxima

at *ca*. 395 nm and 400 nm respectively. However, the multi-scans in more polar solvents than acetone (ε = 20.7), namely acetonitrile (ε = 38.0) and methanol (ε = 32.6) were found to be different. Initially a fast increase was observed and later a decrease in absorbance followed (refer Fig. 4.2). This difference in spectra or the decrease in absorbance in the latter solvents is due to a subsequent reaction as revealed from absorbance-time (Fig. 4.2) and IR multi-scanned spectra (Fig. 4.3) as well. The second reaction was identified as CO-insertion and/or isomerization from the IR-multi-scanned spectra.

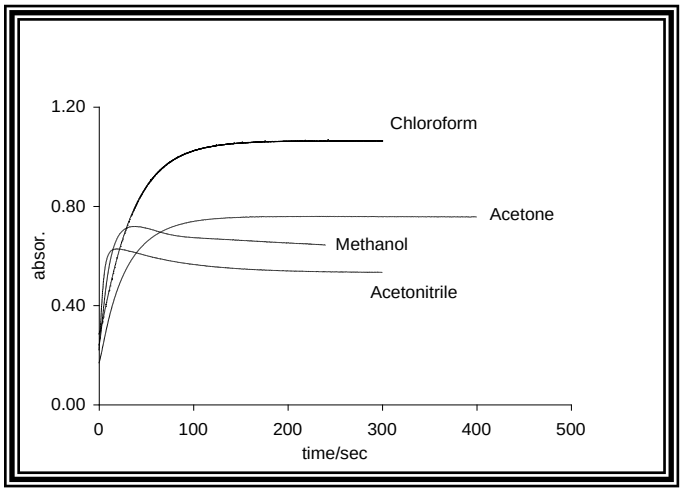

Figure 4.2 Monophasic and biphasic absorbance-time plots for oxidative addition of CH_3I (1.0M) to [Rh(cupf)(CO)($AsPh_3$)] (1.7×10^{-4} M) in different solvents at 24.8 °C. λ_{max} = 400nm (acetone), λ_{max} = 395nm (chloroform), λ_{max} = 390nm (methanol), λ_{max}= 400nm (acetonitrile).

Absorbance-time traces of the reactions were scanned at maximum absorption, λ_{max} = 400, 395 and 390 nm in acetone or acetonitrile, chloroform and methanol respectively, and showed biphasic kinetics in more polar solvents and monophasic behaviour in acetone and chloroform. As confirmed from IR spectra and presented in Figures 4.3, 4.8.1 and 4.8.2, the first curve in the biphasic plot corresponds to the Rh(III)-alkyl formation and the second to acyl formation and isomerisation. It was also

determined that the monophasic curve in acetone corresponded to a Rh(III)-alkyl formation.

One can easily notice by looking at the curves that the first reaction's rate enhancement is influenced by the polarity of the solvents. It follows the sequence of acetone < chloroform < methanol < acetonitrile which is the polarity order for these solvents. However, this order must be proved by kinetic calculations. IR-analysis of the reaction in terms of the Rh(I)-CO peak in the starting complex and the formation of either or both Rh(III)-alkyl or Rh(III)-acyl complexes provided efficient means of tracing the progress of the reaction and collecting kinetic data on these grounds.

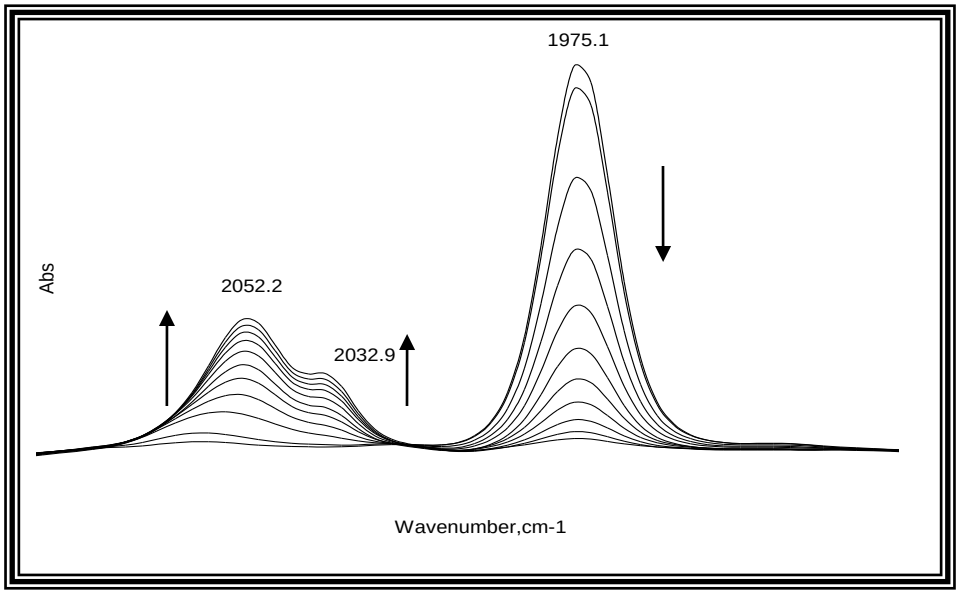

Figure 4.3 IR-multi-scans of the reaction between CH_3I and Rh(cupf)(CO)($AsPh_3$) in acetone at 25.0 °C, scanned every 12 minutes. ([complex] = 2.73×10^{-3} M, [CH_3I] = 0.2 M).

The above multi-scanned spectra of the reaction showed that the Rh(I)-CO peak (1975 cm^{-1}) disappeared and simultaneously two new CO peaks were formed at about 2052 (1^{st}-species) and 2033 cm^{-1} (2^{nd}-species), both of which grew progressively at the cost of depletion of the reactant. The species formed, particularly the former, should be

Rh(III)-alkyl complex since the oxidative addition product in acetone medium are expected to give υ(CO) values in the range of 2050-2060 cm^{-1} (Basson *et al*., 1987:31). Although two new CO-peaks are formed, it can be seen from the figure that the reaction is thermodynamically favoured towards the first species, with higher υ(CO).

Though two oxidative addition products are observed in the solution, the IR spectrum of the isolated solid product showed only one Rh(III)-alkyl species at υ(CO) = 2040.2 cm^{-1}. With regard to which complex crystallises, it is safe to say that the thermodynamically favoured product (with higher stretching frequency) was isolated since the crystallised isomer gave the same CO stretching frequency of 2052 cm^{-1} when redissolved in acetone, i.e. υ(CO) = 2040.2 cm^{-1} (in solid) becomes υ(CO) = 2052 cm^{-1} in acetone.

It is worth asking what the two simultaneously formed species are. The study tried to present possible reasons for the formation of two CO-peaks observed in Figure 4.3. Most likely the two species formed should be Rh(III)-alkyl isomers based on their υ(CO) values. Though cupferron is an unsymmetrical bidentate ligand, the donor properties of the two binding oxygen atoms (O,O) are not that different, like for example, with a (S,O) combination of ligand atoms and hence upon addition of $AsPh_3$ to [Rh(cupf)$(CO)_2$], two isomers of Rh(I) monocarbonyl complexes may have been formed in the solution similar to those found by Purcell *et al*., (1995:153). These two starting Rh(I) complexes in turn could have produced their corresponding Rh(III)-alkyl species. However, as presented in Chapter 3, X-ray crystallographic studies of its phosphine analogue, [Rh(cupf)(CO)(PPh_3)], detected or analysed only one isomer.

Furthermore, the reaction appears to be irreversible, i.e. it can be seen from the figure that Rh(I) disappears almost completely to Rh(III) species. Another evidence that supports the irreversibility of the system comes from the IR-multi-time-scans of the isolated Rh(III)-alkyl intermediate, of which the solution scanned in acetonitrile, chloroform and THF only gave the Rh(III)-isomer in the range of υ(CO) = 1710-1720 cm^{-1}, i.e. back

reaction towards Rh(I)-CO was not observed. The reaction pattern/sequence of oxidative addition of iodomethane to [Rh(cupf)(CO)($AsPh_3$)] in acetonitrile, chloroform and 1,2-dichloroethane as reaction medium, where no absorption in the IR region between 1650-2100 cm^{-1} occurred, gave the same results and are discussed in Paragraph 4.5.3.

These were some preliminary investigations of the reaction done before performing kinetic measurements and collecting data. The next sections are the main body of the kinetics performed on these complexes.

4.5 RESULTS AND DISCUSSION

In this section the results of the kinetic study will be presented with discussion, interpretation and integration with related studies done previously. The kinetic investigations were divided into different sections based on the type of the complex and the results obtained. The first is the reaction of iodomethane with [Rh(cupf)(CO)($AsPh_3$)] and the effect of the bidentate ligands, the second is the influence of electronic and steric factors on Rh(I) complexes containing arsine ligands and the third deals with a presentation of an appropriate reaction mechanism based on the data collected and the type of spectra obtained. Substrate effects such as CH_3I, CH_3Br and C_2H_5I are discussed in the fourth section and lastly the study of solvent effects on CO-insertion reactions will be presented. Activation parameters were determined at four different temperatures in acetone.

4.5.1 Oxidative addition of CH_3I to [Rh(cupf)(CO)($AsPh_3$)]

The reaction of iodomethane with [Rh(cupf)(CO)($AsPh_3$)] was studied in toluene, ethyl acetate, acetone, chloroform and in more polar solvents such as methanol and acetonitrile. As noted in Chapter 1, one of the aims of the project was to investigate and determine the reactivity of this complex and to investigate the degree of polarity of the

transition state in order to suggest an appropriate mechanism for the reaction. As stated earlier, each reaction was studied at different CH_3I concentrations, ranging from 0.2 to 1.0 M to ensure good pseudo-first-order conditions.

As noted in Section 4.4, kinetic measurements (absorbance–time scanning) to determine rate of reactions showed monophasic and biphasic kinetics. Moreover, it was analysed from the IR-spectra that the first curve in both represents oxidative addition with the Rh(III)-alkyl as product and the second subsequent absorbance change corresponds to CO-insertion and reactions like intramolecular rearrangement (isomerisation). It was decided to determine the rate of Rh(III)-acyl formation using IR-multi-scanned spectra in chloroform and acetonitrile at definite $[CH_3I]$. The variation of $[CH_3I]$ was not necessary since it was proved (Fig. 4.4 and 4.8) that the graph of k_{obs} *vs* $[CH_3I]$ was linear with small intercepts. It was also shown in previous studies and in the present study that both UV/VIS and IR techniques give comparable results. For example, the first-order rate constants of the reaction obtained for the formation of the Rh(III)-alkyl complex in acetone from infrared spectroscopy compared well (within experimental error), with the first-order rate constant obtained using visible spectroscopy at $[CH_3I]$ = 0.2 M, i.e. 0.00028(5) *vs* 0.000302(1) respectively. Therefore both techniques can give reliable kinetic values. However, a few kineticists argue that kinetic results obtained from UV/VIS spectroscopy are more reliable because reactions are studied at a constant wavelength. It seems true, but the IR kinetics performed in the current study was followed by measuring the decay or appearance of narrow (approximately constant wavelength) CO-absorption bands (refer Figure 4.3 and 4.8).

The kinetic data were collected by UV/VIS spectroscopy and analysed by means of the Micro Math Scientist package for Windows, i.e. data were fitted to Eq. 4.1 to determine k_{obs}. Plots of observed pseudo-first-order rate constants *vs* variable concentration of CH_3I gave linear relationships and fitted Eq 4.4 well, with insignificant intercepts except in

acetonitrile indicating reverse or concurrent reactions such as the solvent path detected in previous studies. The constants k_1, k_{-1} and K_1 obtained from Eq. 4.4. or Fig. 4.4 are presented in Table 4.1.

$$k^{OA}_{obs} = k_1[CH_3I] + k_{-1} \quad \textbf{(4.4)}$$

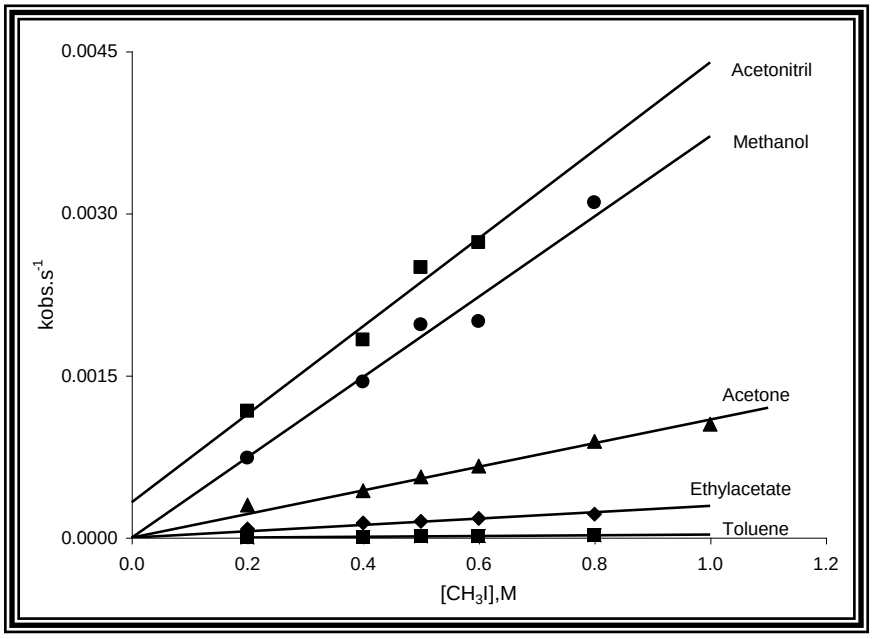

Figure 4.4 Solvent dependence of the pseudo-first-order rate constants for the formation of [RhI(cupf)(CO)(CH_3)($AsPh_3$)] generally at 24.8 °C. (Supplementary data Table ST.1).

The formation of the Rh(III)-alkyl complex in various solvents, as shown in Figure 4.4, shows a direct relationship of the pseudo-first-order rate constant on [CH_3I] at least up to 0.8 M, with methanol and toluene having zero intercepts, in ethyl acetate and acetone zero within experimental error but in acetonitrile quite a significant intercept was observed. Generally, the rhodium complex containing triphenyl arsine reacted at rates comparable to its corresponding phosphine, for example in acetone k_1 are $0.97(4) \times 10^{-3}$ and $1.22(2) \times 10^{-3}$ M^{-1} s^{-1} respectively (refer Tables 4.1 and 4.2).

Furthermore, Figure 4.4 and Table 4.1 showed quite reasonable correlation between solvent parameters (polarity and donocity) and the second-order rate constants. Like its phosphine analogue, the second-order rate constants increased significantly from the non-polar (toluene) to moderately polar (acetone) and to highly polar (acetonitrile). Factor variations of *ca*. 20 and 4 were observed from ethyl acetate to acetonitrile and from acetone to acetonitrile respectively. According to literature, Masel (2001:802) and Scott *et al*. (1907:73), solvent polarity measured by dielectric constant (ε) plays an important role during S_N2 reactions. Comparison of the rates in acetonitrile and methanol showed comparable second-order rate constants and a pronounced increase in K for methanol. This could be evidence to suggest that solvent donocity has a certain role to play. However, this suggestion needs further proof to be a reliable conclusion. It can be confirmed by comparing the rates in acetone and ethyl acetate both having almost the same donocity value (Dn) but a large difference in polarity. In order to make a sensible comparison and to suggest the contribution of Dn, let's consider the ratio of ε {ε(acetone)/ε(ethyl acetate), 20.7/6 = 3.45} and k_1 {k(acetone)/k(ethylacetate), $0.97\times10^{-3}/0.22\times10^{-3} = 4.41$}. The increment in k_1 thus almost parallels the increment of ε. In a similar sense, the rate enhancement observed in methanol may be interpreted as a result of increasing polarity over acetone (Table 4.1), since the donocity of methanol is not that different from ethyl acetate and acetone. Methanol, however, is a protic solvent and a good solvating agent, having the ability of hydrogen bond formation and therefore H-bonding is expected to form in the transition state. Since the reaction proceeds by an associative mechanism, this bond formation should favour (enhance) the rate of the reaction, thereby making the transition state complex more associative due to additional bond formation that originated from the solvent, in this case methanol.

Table 4.1 Rate constants for the oxidative addition of CH_3I to [Rh(cupf)(CO)($AsPh_3$)], at 24.8 °C (Standard deviation in parentheses).

Solvent	ε	Dn	$10^3k_1(M^{-1}s^{-1})$	$10^4k_2(s^{-1})$	$K= k_1/k_2$
Toluene	2.4	---	0.035(3)	≈0.0*	VL#
Ethyl acetate	6.0	17.1	0.22(1)	0.39(6)	5.6
Acetone	20.7	17.0	0.97(4)	0.8(2)	12.1
Methanol	32.7	19.0	3.8(2)	≈0.0*	VL
Acetonitrile	38.0	14.1	4.0(4)**	0.3(2)	> 100

* Negative intercept was found, but rounded to zero.
** The slower rate in acetonitrile could be due to the acetic acid impurity which also gives oxidative addition to the metal centre (Cotton & Wilkinson, 1972:774).
# very large.

Although triphenylarsine complexes are expected to be less steric due to the longer Rh-As bond than Rh-P, the reaction was not enhanced. Instead, comparable kinetic data are obtained (Table 4.2). Therefore one can say either the starting complex was insignificantly manipulated in comparison to its phosphine analogue or due to the smaller bite angle of cupferrate it was already less sterically crowded to accommodate the small substrate such as iodomethane. Basson *et al*., (1990:1324) added excess PPh_3 to [Rh(cupf)(CO)(PPh_3)] to obtain the penta-coordinated complex, [Rh(cupf)(CO)(PPh_3)$_2$]. The accommodation of the bulky phosphine ligand to the coordination sphere of the metal can be ascribed to the cupferrate ligand's smaller bite angle creating more space in the equatorial plane of the trigonal bipyramidal geometry of the complex. Furthermore, the unexpectedly larger rate of oxidative addition of iodoethane to [Rh(cupf)(CO)($AsPh_3$)] relative to literature data, can only be interpreted by the less steric crowding of the complex. In other words, it can be said that electronic factors are likely to dominate steric effects in these complexes. Mcauliffe *et al*., (1997:69) found that the σ–donor power of group 15 ligands vary in the order PR_3 > AsR_3 > SbR_3 (R = constant). Moreover, Collman *et al*., (1987:71) found a similar order, with PPh_3 > $AsPh_3$ > $BiPh_3$. In order to confirm the relative influence of both factors and draw a

convincing conclusion, the results so far suggest that this study should be extended to include the kinetic studies of [Rh(cupf)(CO)(XPh_3)], where X = Sb, Bi. This means that since arsine is just below phosphorous in the periodic table, the properties of PPh_3 and $AsPh_3$ ligands (electronic and steric) are not expected to show a large difference. Important to note is that the reaction of CH_3I to the arsine complex showed insignificant intercepts (except in acetonitrile) giving large equilibrium constants (calculated from $K = k_1/k_{-1}$), which implies that the formation of Rh(III)-alkyl species is thermodynamically more favoured for arsine complexes than the corresponding phosphines.

Table 4.2 Comparison of oxidative addition rates of CH_3I to [Rh(cupf)(CO)(XPh_3)], X = As, P.

Solvent	**10^3 k_1($M^{-1}s^{-1}$)**	
	[Rh(cupf)(CO)($AsPh_3$)]	**[Rh(cupf)(CO)(PPh_3)]***
Ethyl acetate	0.22(1)	0.229(5)
Acetone	0.97(4)	1.22(2)
Methanol	3.8(2)	2.5(2)
Acetonirile	4.0(4)	4.2(2)

* Basson *et al*., 1987:31.

To conclude, arsine complexes are less steric and weaker σ-donors whereas the corresponding phosphines are relatively more bulky and possesses better σ-donating properties. Hence the more favourable steric property of arsine complexes is overshadowed by the weaker σ-donation power of the triphenylarsine ligand. In other words, the slow rate of arsine complexes can thus be due to a large contribution of electronic effects and that of corresponding phosphines can be due to greater steric demand. That is, one ligand disfavours the other, giving comparable rates. Finally, though the second-order rate constants are found comparable, it is interesting to note that the reaction is thermodynamically favoured towards the arsine complex.

4.5.1.1 The effect of temperature

The effect of temperature was studied in order to establish the temperature dependence of the rate of the oxidative addition reaction 4.3 and thus to determine the activation parameters, $\Delta S^{\#}$ and $\Delta H^{\#}$, using the Eyring equation (Eq. 4.2). The main aim for performing such kinetics was to obtain evidence/support for a mechanistic assignment.

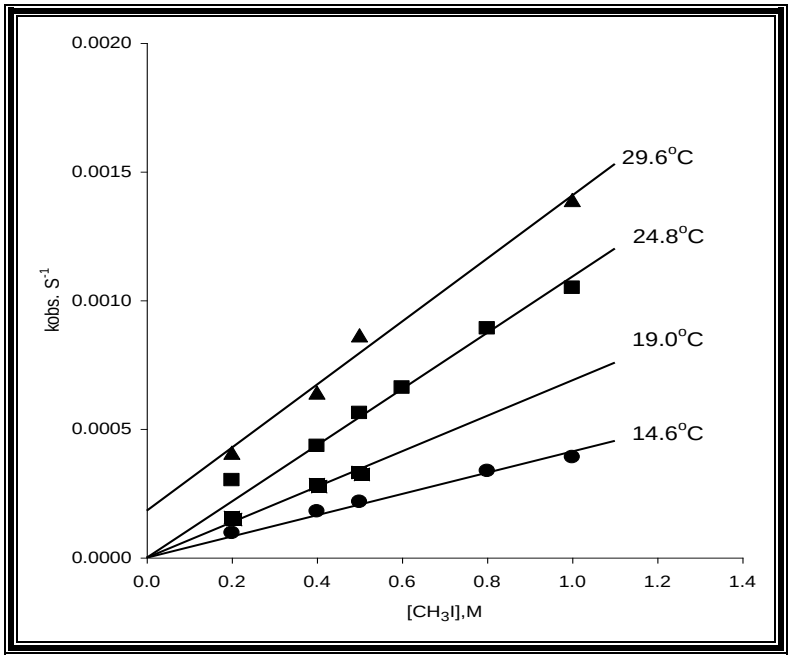

Figure 4.5 Plots of k_{obs} *vs* $[CH_3I]$ showing temperature and $[CH_3I]$ dependency of the reaction in acetone. (Supplementary data Table ST.2).

The second-order rate constant, k_2, were calculated from temperature data. From the plot of $\ln(k_2/T)$ *vs* 1/T the slope was 6720(36) and intercept 9(2). Hence from the Eyring equation (Eq.4.2),

$\Delta H^{\#} = 55.9(3)$ kJ mol^{-1} and $\Delta S^{\#} = -122.1$ J K^{-1} mol^{-1}

The value of $\Delta H^{\#}$ and the relatively large negative $\Delta S^{\#}$ value would possibly be an indication for an associative mechanism (Leipoldt *et al.*, 1991:2207 and

Uguagliati *et al*., 1970:724). The $\Delta G^{\#}$ for the arsine and phosphine complex is calculated as -19.48 and -17.64 kJ/mol respectively. Though the arsine complex has relatively larger $\Delta G^{\#}$ both are thermodynamically favourable. The relatively large $\Delta S^{\#}$ negative value of the phosphine complex (-180 compared to -122 J $K^{-1}mol^{-1}$) could indicate the formation of a more associated activated state. However, a comparison of $\Delta H^{\#}$ = 55.9(3) $kJmol^{-1}$ with the term $-T\Delta S^{\#}$ = -36,4 kJ mol^{-1} at 298 K shows that the present reaction is more entropy than enthalpy driven and thus that reorganization in the activated state is of more importance than bond breaking or making.

4.5.1.2 The effect of the bidentate ligand on rates of oxidative addition and CO-insertion

In this section kinetic investigations of the reaction between CH_3I and [Rh(L-L')(CO)($AsPh_3$)] complexes (L-L' = cupf and cupf.CH_3) are presented. These reactions were investigated by IR spectroscopy in the region 1650-2100 cm^{-1} in acetonitrile and 1900-2100 cm^{-1} in acetone. A typical concentration of the metal complex was 0.0027 M and for iodomethane 0.1975 M. Rh(III)-acyl formation could not be traced in acetone as a reaction medium because acetone has strong CO-peaks around 1720 cm^{-1}. As pointed out earlier, the variation of [CH_3I] in the study of the acyl formation was not necessary since it was proved that the graph of k_{obs} *vs* [CH_3I] was linear with insignificant intercepts.

Manipulation of electron density on the complex was achieved by introduction of a methyl group on the phenyl ring of cupferrate (2-methylcupferrate). The fact that this substituent is not directly bound to the five-membered ring of the cupferrate ligand, makes it relatively far from the metal centre and hence would insignificantly shield the metal centre from incoming molecules. Therefore steric influence of both complexes can approximately be compared and the rate of activation/deactivation towards oxidative addition should thus be expected due to electronic factors.

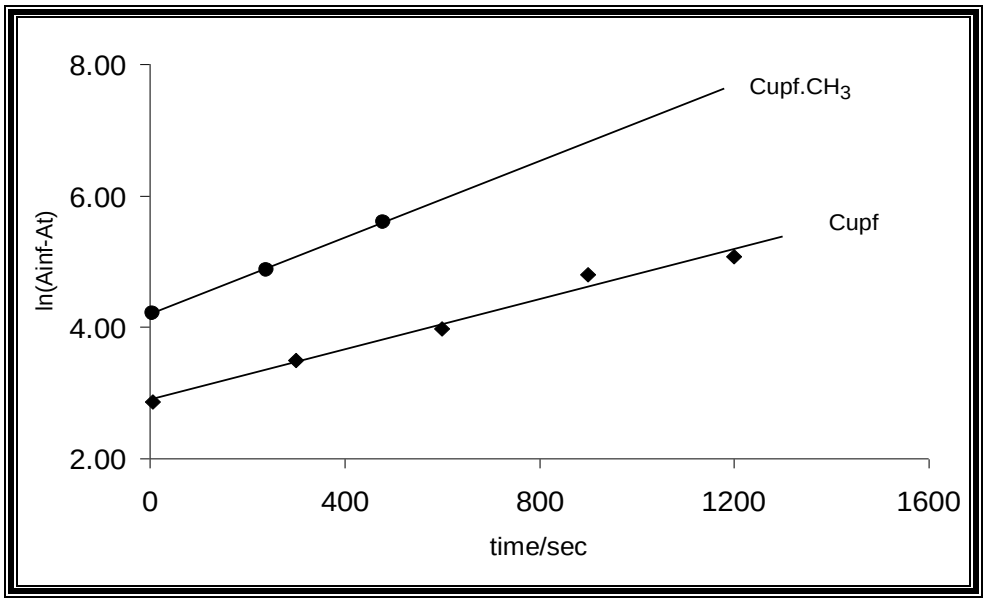

Figure 4.6a Kinetic runs using absorbance changes of the Rh(III)-CO alkyl peaks of [Rh(L-L')(CH_3)(CO)($AsPh_3$] (L-L' = cupferrate and 2-methylcupferrate) complexes in acetonitrile at T= 25 ^oC, [complex] = 0.0027M, [CH_3I] = 0.1975M. (Supplementary data Table ST.3).

It is clear from Table 4.3 and Figure 4.6a that the oxidative addition rate involving cupf.CH_3 is faster. For example in acetone a factor of 3 enhancement was observed from the unsubstituted cupferrate to the substituted 2-methylcupferrate. This enhancement is in agreement with the expected effect of the electron releasing CH_3 substituent. In short, electron releasing substituents enhance the Lewis basicity of Rh(I) complexes by making the metal centre electron rich. The nucleophilic attack by the metal centre at the sp^3 carbon of CH_3I is thus enhanced.

However, upon comparison of the rate of the subsequent reaction, i.e. the migratory carbonyl insertion reaction, it is clear that deactivation was induced by the methyl substituent. The k_2 value in Table 4.3 decreased by half. This result agrees with the literature, where strong electron donating ligands such as PEt_3 (Ranki *et al*., 1997:1835) which substantially accelerated oxidative addition reaction have inhibited CO-insertions. A likely explanation is the fact that a stable methyl product was isolated (with PEt_3 ligands) which probably indicates stronger Rh-Me bond. Besides, high electron density

on the metal also leads to stronger M → CO(π*) back bonding which both are thought to inhibit CO insertion.

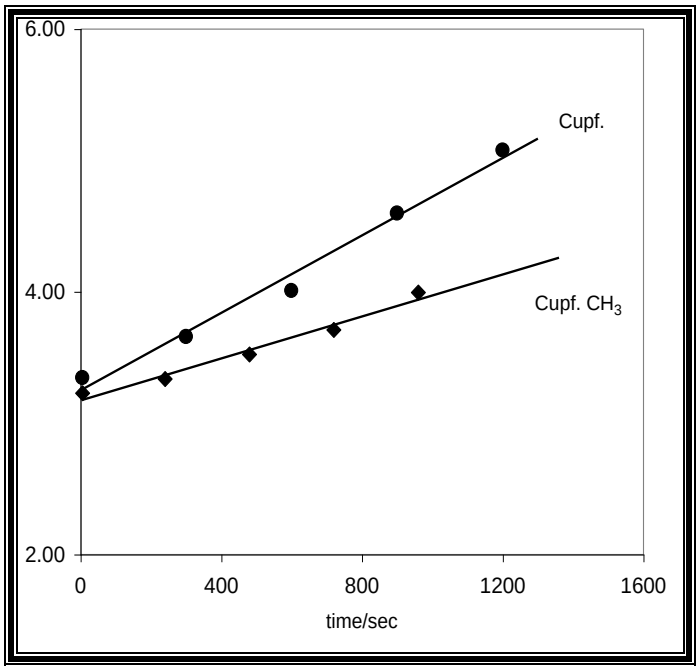

Figure 4.6b Kinetic runs using absorbance changes of the Rh(III)-acyl peaks of [Rh(L-L')(CH_3CO)($AsPh_3$)] complexes, (L-L'= cupferrate and 2-methylcupferrate), in acetonitrile at 25 ^oC, [complex] = 0.0027 M, [CH_3I] = 0.1975 M. (Supplementary data Table ST.4).

Table 4.3 First-order rates for oxidative addition and CO-insertion reactions for the reaction between CH_3I and [Rh(L-L')(CO)($Asph_3$)]. [complex] = 0.0027 M and [CH_3I] = 0.1975 M.

Solvent	**10^3k_1 (s^{-1})***		**10^3 k_2 (s^{-1})**	
	L-L' = cupf	**L-L' = cupf.CH_3**	**BID = cupf**	**BID=cupf.CH_3**
Acetone	0.28(5)	0.9(1)	-----	----
Acetonitrile	1.9(1)	2.92(9)	1.4(1)	0.79(7)

* k_1 and k_2 rate of Rh(III)-alkyl and Rh(III)-acyl formation respectively.

4.5.2 Electronic and steric effects in Rh(I) arsine complexes

Next, the reaction between CH_3I and [Rh(L-L')(CO)(X)], L-L' = cupf and cupf.CH_3 and X = $AsPh_3$, $AsMePh_2$ was investigated in chloroform. The reactions were studied with regard to electronic and steric factors. The complex was tuned by interchanging $AsPh_3$ for $AsMePh_2$. As mentioned above, manipulation of electron density on the metal centre was accomplished by the introduction of a methyl substituent on the phenyl ring of cupferrate
(2-methylcupferrate). Both manipulations, particularly the former, are expected to enhance the complex's reactivity towards oxidative addition. Some qualitative data with respect to the reactivity of the complexes manipulated are presented and a detailed discussion will follow the table and figures.

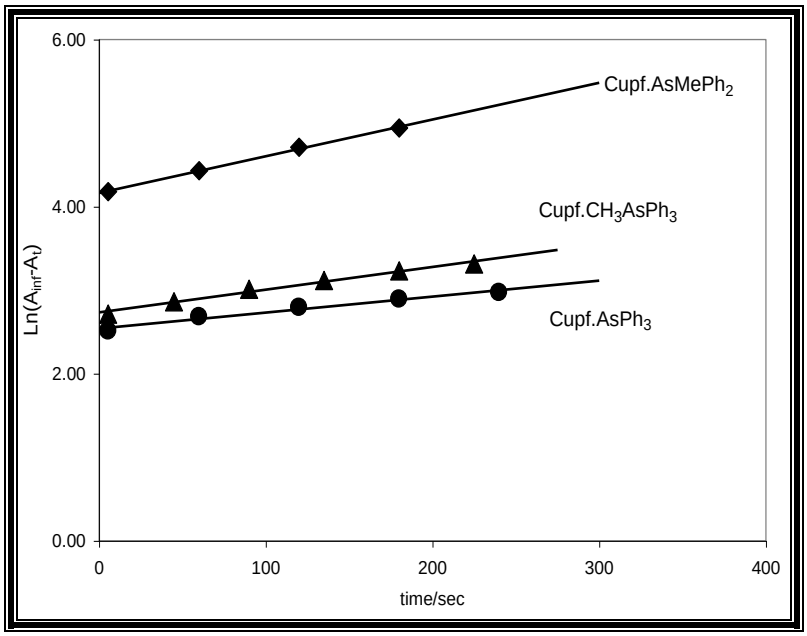

Figure 4.7a Kinetic runs using IR spectroscopy for the formation of Rh(III)-alkyl complexes with various bidentate and arsine ligands. Solvent: chloroform and T = 25 °C. [complex] = 0.002 M, [CH_3I] = 0.1904 M. (Supplementary data Table ST.5).

The plots of ln(|A_∞-At|) *vs* time for the formation of the Rh(III)-alkyl (obtained from IR-spectroscopy) were linear for *ca*. 65% conversion of the parent complex. The first-order rate constants for oxidative addition (k_1, from Table 4.4), showed an increase

from complex 1 to 2 and to 3, which is in agreement with the fact that a higher electron density on the Rh(I) centre results in an increase in CH_3I oxidative addition rates.

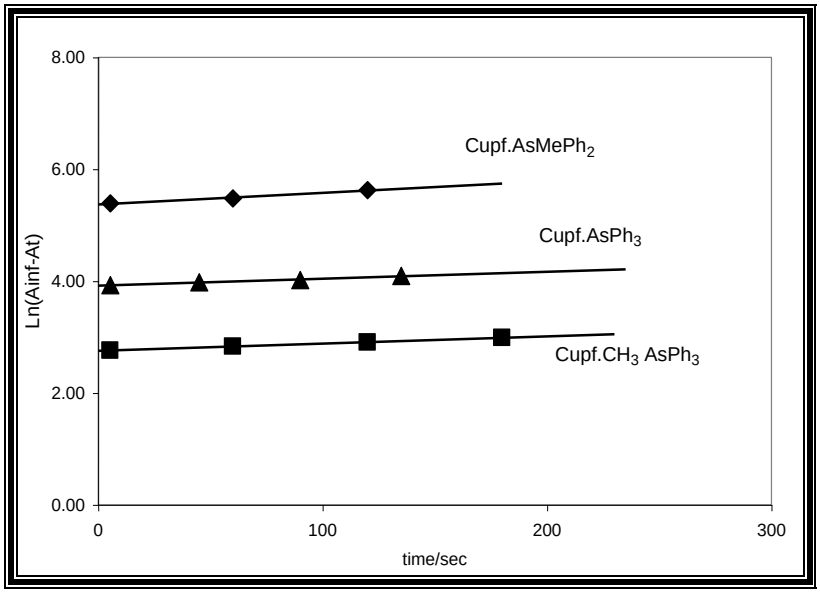

Figure 4.7b Kinetic runs using IR spectroscopy for the formation of Rh(III)-acyl complexes with various bidentate and arsine ligands. Solvent: chloroform and T = 25 °C. [complex] = 0.002 M, [CH_3I] = 0.1904 M. (Supplementary data Table ST.6).

Table 4.4 First-order rate constants for the reaction between CH_3I and Rh-complexes at 25 °C in chloroform.

Complex	**υ(CO), cm^{-1}**	**10^3 k_1 (s^{-1})***	**10^3 k_2 (s^{-1})***
[Rh(cupf)(CO)($AsPh_3$)], **1**	1978.8	1.9(1)	1.2(1)
[Rh(cupf.CH_3)($AsPh_3$)], **2**	1976.5	2.7(1)	1.29(1)
[Rh(cupf)(CO)($AsMePh_2$)], **3**	1965.5	4.3(1)	2.0(2)

* k_1 and k_2 observed rate constants for alkyl and acyl formation respectively.

The replacement of $AsPh_3$ with $AsMePh_2$ is expected to favour the oxidative addition reaction, since the complex is changed sterically as well as electronically. The fact that the CH_3 group is less steric and more electron donating than the phenyl group can be found in literature.

Tolman (1970:2953) noticed that replacement of one substituent on a phosphorus ligand by another causes to change the carbonyl wavenumber of a complex. Using nickel complexes of the form $[Ni(CO)_3(PX_1X_2X_3)]$ and tri-*t*-butylphosphine, the most basic ligand, he succeeded in compiling substituent values for organic groups X_1, X_2 and X_3 in such a way that it could serve as a measurement of the Lewis basicity of these substituents (Table 4.5). The larger the χ_i value, a measurement of the substituent contribution, the less electron donating this group becomes (Eq. 4.5).

$$\upsilon(CO)(A1) = 2056.1 + \sum_{i=1}^{3} \chi_i \, (cm^{-1}) \qquad \textbf{(4.5)}$$

Table 4.5 Substituent contribution to υ(CO) of [Ni(CO)3($PX_1X_2X_3$)] complexes for some selected substituents (Tolman, 1970:2953).

Substituent	**χ_i, cm^{-1}**
Ethyl	1.8
Methyl	2.6
Phenyl	4.3
hydride(H^-)	8.3
CF_3	19.6

This confirms that the CH_3 group is expected to release a larger amount of electron density to the Rh-atom than the phenyl group. Thus the replacement of a phenyl substituent by a methyl group in the $AsPh_3$ ligand, or the introduction of a methyl substituent in the bidentate ligand, would be expected to decrease the χ_i value by nearly 1.7 cm^{-1} (since 4.3 - 2.6 = 1.7), at least in Ni-complexes. The same article noted that this principle could be applied to other complexes as well. It is clear from Table 4.4 that the above expectation is revealed in case of complex 2, however the pronounced decrease of υ(CO) from 1978.8 to 1965.5 cm^{-1} for the [Rh(cupf)(CO)($AsPh_3$)] and [Rh(cupf)(CO)($AsMePh_2$)] complexes respectively, could be interpreted due to packing effects. Structural analysis of [Rh(acac)(CO)(PPh_2Fc)] (Fc = ferrocenyl) revealed that

the complex crystallised as two independent Rh-moieties in the solid state with υ(CO) values of 1974 and 1958 cm^{-1} (Roodt *et al*., 1998:2447). In any case, the lower CO stretching frequency obtained indicates a decrease of electronegativity of the ligand (or increase of electron donation ability) and hence the electron density of the metal centre increases. As result of this, the rate of oxidative addition is enhanced when the metal acts as nucleophile.

Furthermore, Tolman (1970:2956) calculated the cone angle for the phosphine analogue of the $AsMePh_2$ ligand ($PMePh_2$) to be 136º, which is smaller than triphenylphosphine's 145º. The corresponding arsine ligands are expected to show similar steric (cone angle) changes.

These two arguments are fairly convincing evidence that the CH_3 group is less steric and more electron donating than the phenyl group. Various studies indicate that both electronic and steric effects are operative during reactions. However, reliable and good evidence comes from kinetically investigated reactions. Kinetic studies done by Deeming and Shaw (1969:1802) reported that the rates of the reaction of methyl iodide with *trans*-$[IrCl(CO)L_2]$ increased in the order L = PPh_3 < $PMePh_2$ < PMe_2Ph. Furthermore, Kubota *et al*., (1973:195) found that the rate of oxidative addition of iodomethane to the iridium vaska complex increased five-fold when one of the phenyl groups was replaced with a methyl group. A large 14-fold increase was observed when the second phenyl was replaced with the same substituent. Deeming and Shaw (1969:1802) observed that the rate of oxidative addition of benzoic acid to the same complex increased about 360 times when methyl groups replaced all the phenyl groups. These results are in agreement with the current rate data obtained, since the rate of the reaction is faster for the Rh-complex containing the more basic and less steric arsine. That is, the diphenylmethylarsine complex containing the less steric and more electron donating arsine ligand reacted *ca*. 2 times faster than the triphenylarsine complex.

Similarly, as expected and was observed, the rate of the reaction with a CH_3 group on the phenyl ring of cupferrate was enhanced due to the electron donating power of the substituent. Kinetic results done in this laboratory show that electron-releasing substituents on bidentate ligands can also increase the rate of oxidative additions as was mentioned in Chapter 2. Furthermore, the results show that the methyl on the phenyl ring of cupferron does not cause steric hindrance, most probably due to its location, which is relatively far from the metal centre.

4.5.3 A mechanism for the reaction

The mechanism of oxidative addition of iodomethane to [Rh(cupf)(CO)($AsPh_3$)] was studied with the help of UV/VIS and IR spectrophotometry. Infrared analysis of the reaction progress in terms of decay of the Rh(I)-CO peak and the formation of both of Rh(III)-alkyl or acyl complexes provided a powerful method in elucidating the main reaction pathway. However, the proposed mechanism is supported by kinetic results obtained from UV/VIS spectrophotometry.

In the solvents chloroform, acetonitrile and 1,2-dichloroethane, IR-multi-scans between 2100-1650 cm^{-1} showed intensity decreases of Rh(I)-CO peaks and growth of two new CO peaks around 2062-2066 cm^{-1} and 1710-1720 cm^{-1}. The latter two peaks seem as if they are formed simultaneously but careful consideration of the spectra showed that the former changes to the latter as soon as it forms. As the reaction progresses yet another peak around 2052-2058 cm^{-1} developed (Figure 4.8.1 and 4.8.2).

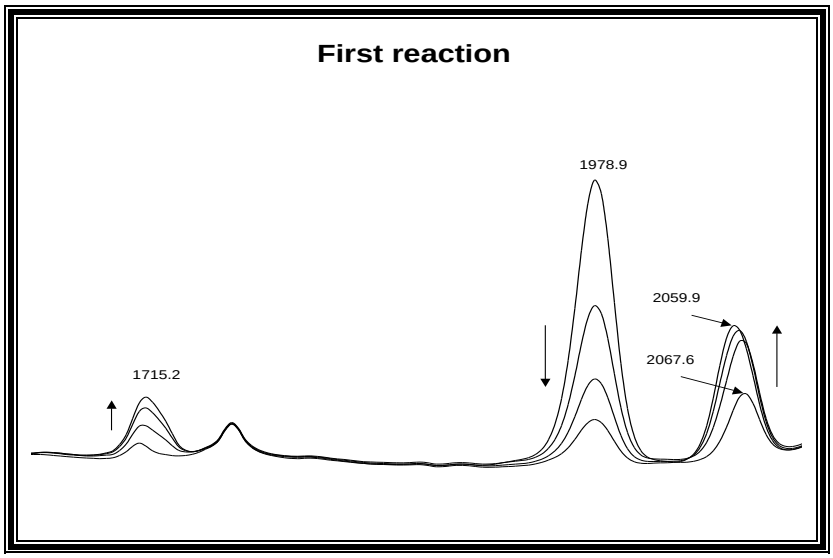

Figure 4.8.1 Infrared spectra of the reaction between [Rh(cupf)(CO)($AsPh_3$)] and CH_3I in chloroform showing only the first four spectra (out of ten) at 3 minute intervals. The disappearance of the Rh(I) starting complex is accompanied by the formation of Rh(III)-alkyl and acyl species. The fourth peak starts to slide to lower υ(CO) values due to the formation of another Rh(III)-alkyl species.

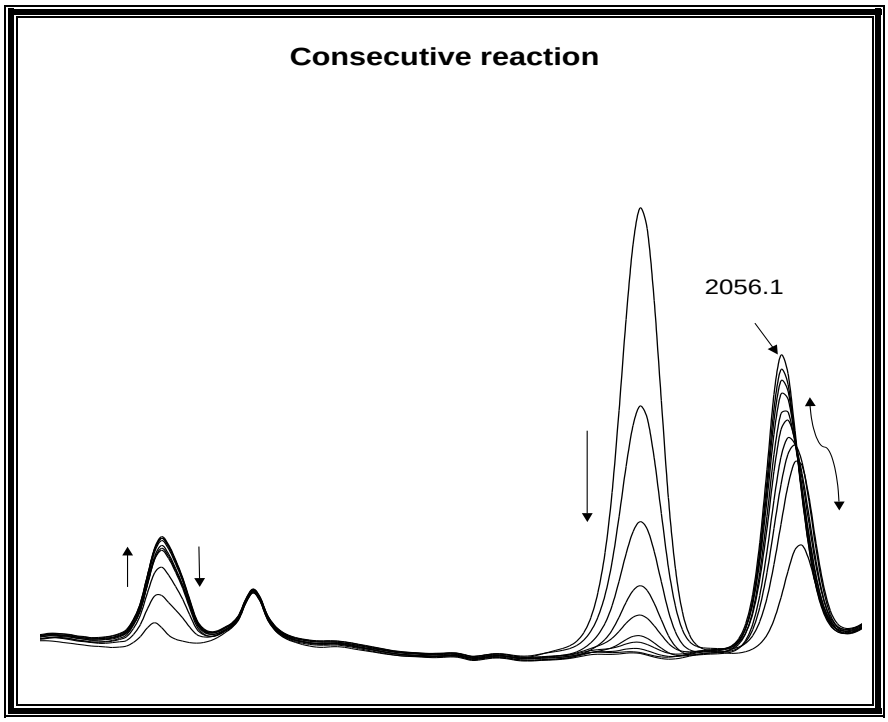

Figure 4.8.2 Infrared spectra of the same reaction showing all ten spectra. Rh(III)-acyl rearranges to a new Rh(III)-CO alkyl at υ(CO) = 2056.1cm^{-1} which has a lower υ(CO) than the Rh(III)–CO alkyl in Figure 4.8.1.

Table 4.6 υ(CO) values for the reactants, intermediates and products of rhodium complexes.

Solvent	Dielectric constant, ε	Rh(I)	Rh(III)-alkyl, OA1	Rh(III)-acyl	Rh(III)-alkyl, OA2
Acetonitrile	36.2	1975.01	2063.99	1710-1685*	2055.53
Chloroform	4.70	1978.88	2066.86	1717	2056.10
1,2-Dichloroethane	10.4	1974.22	2062.93	1717	2052.11

*In acetonitrile the υ(CO) of the acyl peak was broad. Studies by Cheng *et al*., (1977:3003) indicates an anionic acyl complex $[RhI(COR)(PPh_3)(mnt)]^-$ characterised by a broad acyl stretch of υ(CO) = 1695-1685 cm^{-1}. In further discussions these complexes will be referred to as OA1 for the Rh(III)-alkyl with higher υ(CO) and OA2 for the lower υ(CO).

For discussion purposes and to easily notice the rate differences, the above two IR spectra in Figures 4.8.1 and 4.8.2 can be shown on the x-y plane as in Figure 4.9.

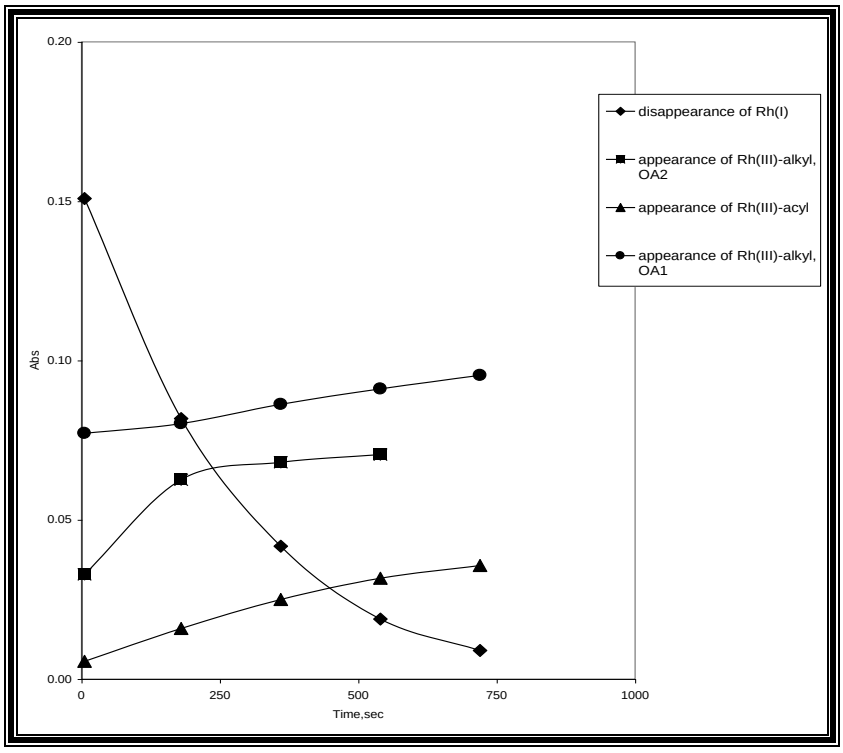

Figure 4.9 Graphical representation of Figures 4.8.1 and 4.8.2 showing the formation of OA1, Rh(III)-acyl, OA2 and the disappearance of the starting material Rh(I), from IR spectroscopy in the range 2100 to 1650 cm^{-1}. Data points taken with 3 minute intervals. (Supplementary data Table ST.7).

From the Figures 4.8 and 4.9 one can suggest, though not quantitatively, that the decay or disappearance of the reactant, [Rh(cupf)(CO)($AsPh_3$)], proceeds to completion. This can be interpreted that if an equilibrium for the oxidative addition step prevails, it should have a large equilibrium constant.

In order to present the mechanistic scheme of the reaction, the following arguments were utilized:

1. The decrease in the Rh(I)-CO peak is accompanied by significant increase in the Rh(III)-CO species at around 2062-2066 cm^{-1} in all three solvents. Kinetic data suggest that the observed intermediate should be a polar Rh(III)-species, probably [Rh(cupf)(CO)(CH_3)($AsPh_3$)]$^+I^-$, where I^- is held in close proximity of the reaction. This suggestion is based on the isolation of the more insoluble white tetraphenylborate salts, for example [Rh(C_5H_5)(CO)(CH_3)($P(CH_3)_2(Ph)$]$^+BPh_4^-$ with υ(CO) = 2068 cm^{-1} (Davis & Graham, 1970:2658). Furthermore, the same article reported that Ir-complexes of cyclopentadiene, [Ir(C_5H_5)(CO)(Ph_3)], produces stable ionic species when iodomethane adds oxidatively to it. However, the authors could not isolate the corresponding Co and Rh complexes, i.e. these ionic species are only intermediate species which collapse in a rapid second step involving coordination of iodide ion. As stated in Section 4.4, the reaction in acetone gave two Rh(III)-alkyl isomers with υ(CO) = 2052 cm^{-1} and 2032 cm^{-1}.

2. The slow growth of the Rh(III)–CO peak at about 1710 cm^{-1} is characteristic for a Rh(III)-acyl complex. The evidence is based on literature studies which led to the isolation and x-ray crystallographic characterisation of [Rh(L-L')($COCH_3$)(PX_3)$_2$] complexes, where L-L' = macsm, stsc (Steyn *et al*., 1993:11). In the present study, this peak developed at a slower rate compared to that of the OA1. One can observe that (from IR-multi-scans) it is relatively stable, but it can also slowly rearrange/isomerise to the second Rh(III)-alkyl complex (OA2) with the lower CO stretching frequency of 2032-2056 cm^{-1}. Thus, there are two Rh(III)-alkyl complexes formed during the reaction.

The first appears at higher stretching frequency υ(CO) ≈ 2062 cm^{-1}, and in a consecutive isomerisation reaction a second complex with υ(CO) ≈ 2052 cm^{-1} is formed.

3. At longer reaction times the final and slower disappearance of Rh(III)-acyl is accompanied by the formation of a third Rh(III)-CO peak *ca*.10 cm^{-1} lower than the OA1, i.e. 2032-2058 cm^{-1}. This CO-peak should correspond to the final oxidative addition product, i.e. Rh(III)-alkyl species, [RhI(cupf)(CO)(CH_3)($AsPh_3$)]. Basson *et al*., (1987:31) observed 2050-2060 cm^{-1} for the oxidative addition product of its phosphine analogue in acetone medium. It was also observed that if a solution, prepared by dissolving the solid oxidative addition product OA1, was scanned repeatedly in the IR region, a slow conversion occurred (with three isosbestic points) to OA2 i.e. OA1 and OA2 are linked through an isomerisation equilibrium (Figure 4.12). The lowering of υ(CO) from OA1 to OA2 alkyl should be due to the constant entrance of iodide, I^-, into the coordination sphere of the Rh-centre.

4. When OA2 started to appear at the cost of disappearance of the Rh(III)-acyl peak, the starting material (Rh(I)-CO peak) was still decreasing to near zero absorbance value. This can be an indication for irreversibility of the oxidative addition. Basson *et al*., (1984:167), however, observed that when the reaction between Rh(III)-acyl and Rh(III)-alkyl tended to equilibrate, the Rh(I)-CO peak started to appear at an appropriate wavenumber. The above observation can further be confirmed by the spectra obtained from IR-multi-time-scans of the isolated Rh(III)-alkyl intermediate in solution, where the spectra did not show a Rh(I)-CO peak, instead a Rh(III)-CO acyl peak has grown at the expected wavenumber (Figure 4.12).

5. The fact that the reaction begins through a nucleophilic attack by Rh-metal on the α-carbon of the alkyl iodide can be evidenced as follows:

i) Higher electron density favoured the reaction, for example [Rh(cupf)(CO)($AsMePh_2$)] reacted faster than [Rh(cupf)(CO)($AsPh_3$)] with CH_3I.

ii) Iodoethane, having a comparable bond dissociation energy (Weast, 1973) reacted slower than iodomethane (Figure 4.11). This can only be accounted for by nucleophilic attack of the rhodium atom on the α-carbon of the alkyl halide, which is hampered by the larger steric demand of the ethyl in comparison to the methyl group.

iii) Almost all kinetic studies performed on similar reactions suggest that the reaction commences by nucleophilic attack on the carbon of CH_3I. Furthermore, it was already mentioned in Chapters 1 and 2 that complexes containing transition metals, for example rhodium, act as a Lewis base on polar molecules.

The rate data and other arguments above, together with evidence for a polar intermediate as well as other related kinetic studies strongly imply that this oxidative addition reaction follows a nucleophilic attack by the rhodium atom on the carbon of methyl iodide. All these results are in favour of an ionic S_N2 two-step mechanistic route. The transition state for such systems may possibly be the linear one shown below and cannot be three-centred since the latter leads to a less polar transition state.

$$[Rh^{\delta-}\text{------ } CH_3{}^{\delta+}\text{------- } I^{\delta-}]$$

Figure 4.10 Linear transition state.

As presented previously, the rate of the reaction was enhanced in polar solvents such as acetonitrile and methanol which could probably be another indication that the reaction proceeds by way of a linear transition state at least in those solvents. If the literature is examined, various spectroscopic and high-pressure dependence studies of oxidative addition of iodomethane to such complexes showed that the most likely transition state is the linear one (Venter *et al*., 1991:2207).

Hence in the system studied, the oxidative addition step of the reaction by way of a linear transition state can be presented as follows:

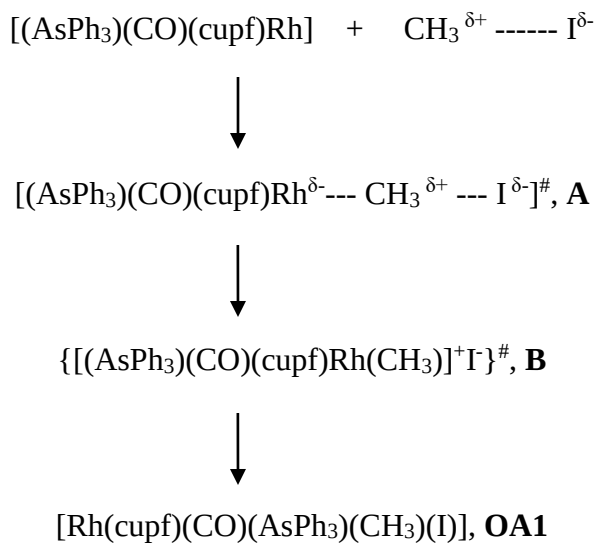

Scheme 4.3 Proposed mechanism for the first step of the oxidative addition reaction.

If a solvent can stabilise B it may become the product of the reaction as was shown in a few literature cases.

Collectively, all the above arguments, kinetic data and type of IR-multi-scans obtained suggest that the reaction proceeds through an initial ionic/polar transition state followed by two consecutive steps, the first involving acetyl formation followed by Rh(III)-acyl-to-alkyl rearrangement to give OA2 as the final product. Thus, based on all these evidence, the following reaction mechanism is anticipated for the reaction between CH_3I and the [Rh(cupf)(CO)($AsPh_3$)] type of complexes**.**

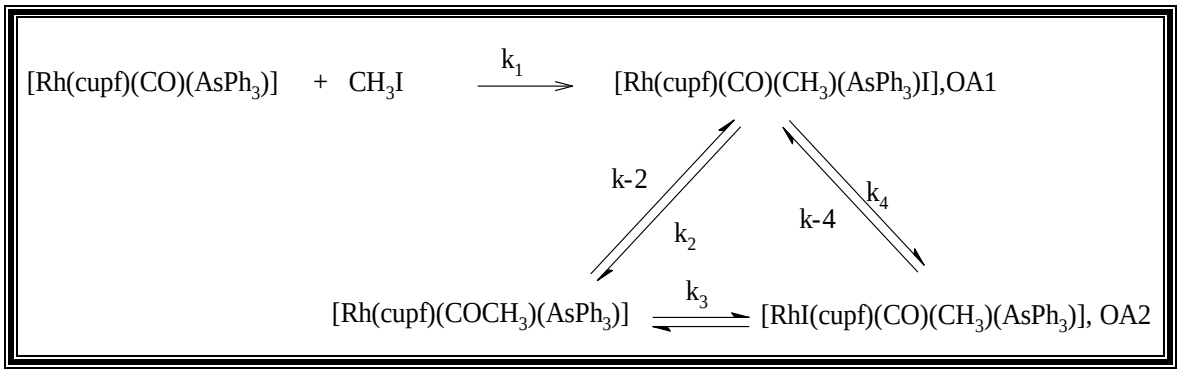

Scheme 4.4 Proposed mechanism for the reaction studied.

4.5.4 The effect of various substrates on the rate of oxidative addition

Under this topic the effect of different organic halide substrates on the rate of oxidative addition is presented below. The study was extended beyond CH_3I to include the oxidative addition of CH_3Br and C_2H_5I to [Rh(cupf)(CO)($AsPh_3$)]. The reactions were studied kinetically using UV/VIS spectroscopy under pseudo-first-order conditions. The rate data are organized and summarised in Table 4.7 and Figure 4.11 to facilitate comparison and discussion.

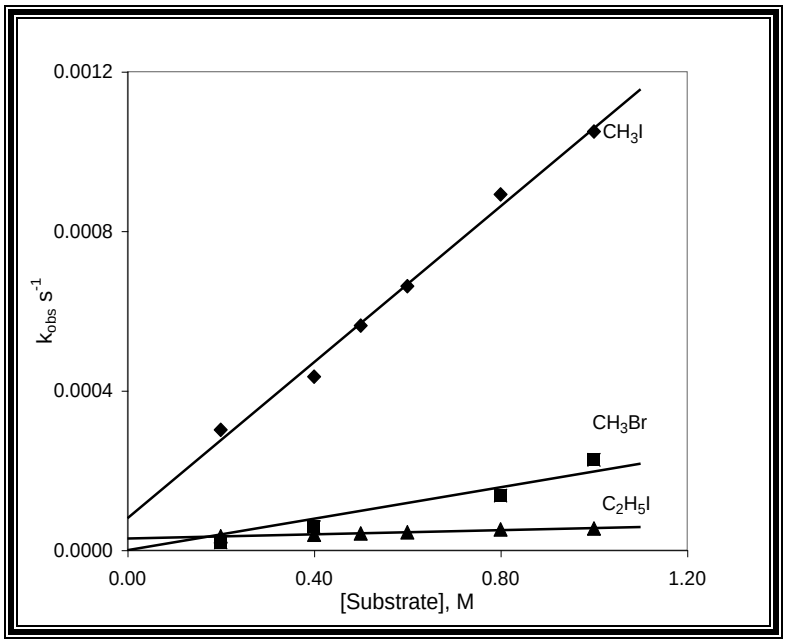

Figure 4.11 Plots of the observed rate constants *vs* substrate concentrations for the reactions of [Rh(cupf)(CO)($AsPh_3$)] with the substrates shown, at 24.8 °C in acetone. [complex] = 1.7×10^{-4} M, (Supplementary data Table ST.8).

It is clear from Figure 4.11 and Table 4.7 that CH_3I exhibited enhanced reactivity compared to the other two substrates. In terms of the second-order rate constants obtained, a decrease by a factor of *ca*. 4 and 40 were observed on changing from iodomethane to bromomethane and from iodomethane to iodoethane respectively. Such results were expected and were observed in the oxidative addition of the same substrates to [M(C_2H_5)(CO)L], (M = Co, Rh, Ir). In the reaction ethyl iodide reacted 400-1200 times slower than methyl iodide (Davis & Graham, 1970:2658). Basson *et. al*., (1984:167) also found that [Rh(acac)(CO)(PPh_3)] reacted 120 times faster with CH_3I compared to ethyl iodide. In comparison to literature results, the reaction with C_2H_5I in the current study is found to be faster. The reason must be due to steric effects. Chock and Halpern (1966:3511) found the reaction between CH_3Br and [IrCl(CO)(PPh_3)] was too slow to be measured by conventional means, but the second-order rate constant with the corresponding iodide was 2.8×10^{-2} M^{-1} s^{-1} in DMF. The rate retardation for CH_3Br is expected to be much larger if it could be performed in acetone rather than in acetonitrile.

Table 4.7 Rate constants for oxidative addition of [Rh(cupf)(CO)($AsPh_3$)] in acetone at 24.8 °C.

Substrate	k_1, ($M^{-1}s^{-1}$)
CH_3I	0.00097(4)
$CH_3Br^{\#}$	0.00024(3)
C_2H_5I	0.000026(1)

- In acetonitrile.

For the sake of comparison it was sensible to perform the kinetics of the reaction with CH_3Br in acetone, but unfortunately the high volatile nature of the substrate did not allow the low rate to be measured. Acetonitrile, being more polar than acetone, helped to minimise evaporation of the substrate by making the reaction faster.

Next, possible analysis of the data and mechanism of C_2H_5I addition is considered. As it was already pointed out earlier, these reactions are considered as bimolecular displacements at carbon where the metal centre acts as a nucleophile and attacks the α-carbon of the alkyl halide. As we know, in ionic reaction chemistry cations favour anions and therefore in the above reactions nucleophiles should favour a substrate with a more electrophilic carbon. The carbon-iodide (C–I) bond energy in iodomethane and ethane is 56.0 and 53.0 kcal/mol (Weast, 1973) respectively, and since these values are almost equal, a possible conclusion to be drawn is that the retardation observed by ethyl iodide should be due to the relative bulkiness of the substrate which hinders the nucleophilic attack by the metal.

A probable mechanism for nucleophilic attack by the metal on the carbon atom of ethyl iodide could be

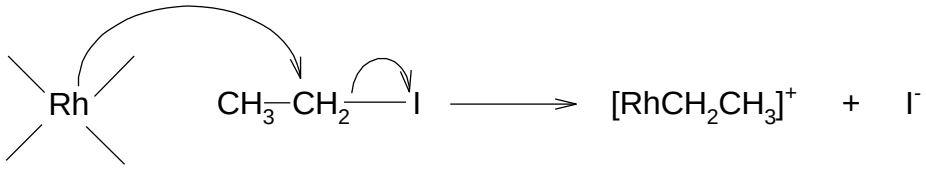

(4.6)

OR

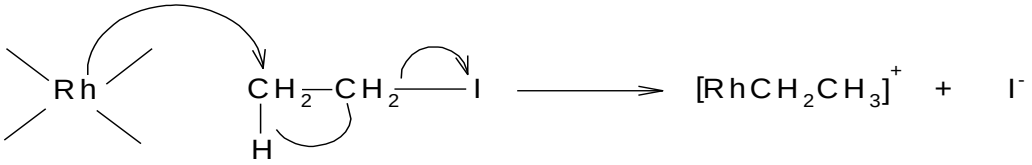

(4.7)

The most probable and expected mechanism should be Eq. 4.6. since

i) nucleophiles attack the most electrophilic atom/s, in this case CH_2 is more electrophilic than its adjacent CH_3.

ii) nucleophilic complexes favour less steric substrates, for example kinetic data of this study shows that CH_3I reacts faster than CH_3CH_2I. Since the CH_2 group seems to be more sterically crowded due to the bulky CH_3 group, it is expected that a nucleophilic attack should be retarded.

The possibility of β-elimination, which commonly occurs in organtransition-metal compounds, is worth mentioning. Although bonding featuring β-elimination has a concerted nature and is favoured by conditions such as coordinative unsaturation of the metal centre and presence of a β-carbon hydrogen in the $[RhCH_2CH_3]^+$ intermediate, it is very unlikely that β-elimination will accompany the first step of the reaction and partially account for the low rate observed. That is to say, β-

elimination is expected to be blocked by a fast nucleophilic attack of I^- filling a vacant site on the coordinatively unsaturated metal centre.

Unlike C_2H_5I, the retardation caused by CH_3Br should be due to electronic factors, because the bond dissociation energy (BDE) of $CH_3{-}Br$ is higher than that of $CH_3{-}I$ by 14 kcal/mol. This high energy keeps the bromine atom very tightly bonded to the carbon atom of the methyl group. It is also true that the electrophilic power of carbon attached to halide decreases with an increase in bond energy.

With regard to the mode of addition, the product of CH_3Br addition is expected to be similar to that of CH_3I. Pearson and Muir (1970:5519) found similar stereochemistry for the products of both CH_3I and CH_3Br addition to $[Ir(CO)(Cl)(PMePh_2)_2]$ with *trans* addition observed in both cases. Therefore, it is safe to assume that oxidative addition of CH_3Br to $[Rh(cupf)(CO)(AsPh_3)]$ proceeds similarly as addition of CH_3I. Additional evidence is that Br^- is smaller than I^- (1.96 *vs* 2.20 Å) (Ball & Norbory, 1974:34) and can be accommodated more easily within the coordination sphere of the metal. However, this will happen only if, as expected, the steric demand of ligands plays a dominant role during coordination to the metal centre. In the case of C_2H_5I, the product could be different due to steric requirement of the ethyl group in the coordination sphere of the metal. However, the small bite angle of cupferrate, combined with the longer bond length of Rh–As, could favour accommodation of both fragments in a similar mode of addition as the above substrates.

4.5.5 Solvent dependence of migratory CO-insertion reactions

Kinetic runs of the oxidative addition product, [RhI(cupf)(CO)(CH_3)($AsPh_3$)],OA1, in a number of solvents were investigated with IR-spectroscopy in the region between 1650-2100 cm^{-1} in order to study solvent effects during alkyl migration or CO-insertion. The solvents chosen were selected for insignificant IR absorption in the specified IR region but also for solvent parameter variations in terms of dielectric constant.

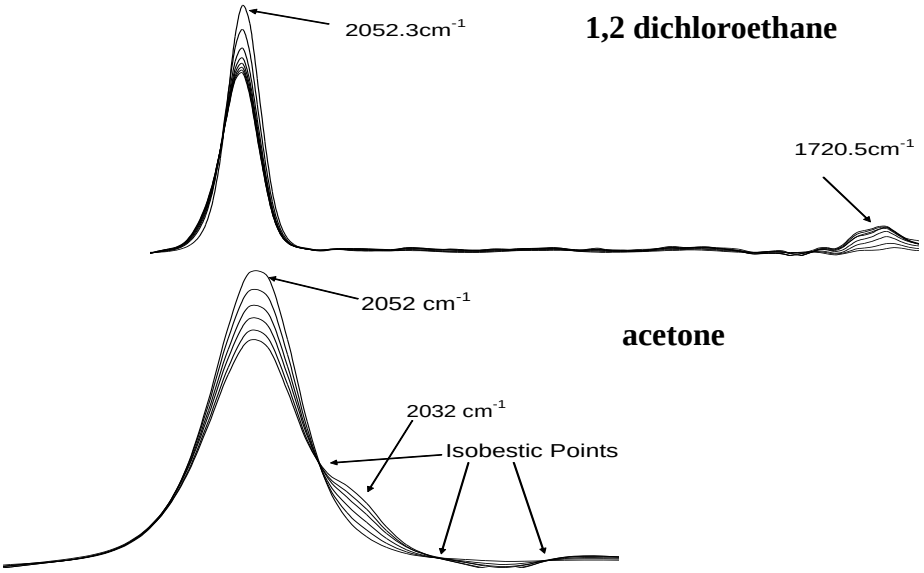

Figure 4.12 IR-multi-scanned spectra for solutions prepared by dissolving solid Rh(III)-alkyl complex, OA1, in 1,2-dichloroethane (10 minute intervals) and acetone(7 minute intervals) in the range of 2100-1650 cm^{-1} and 2100-1900 cm^{-1} respectively. Three isosbestic points are observed in acetone.
Rh(III)-alkyl, υ(CO) = 2052 cm^{-1} $\rightarrow$ Rh(III)-alkyl, υ(CO) = 2032 cm^{-1}

In all solvents employed, except acetone, the Rh(III)-alkyl (OA1) peak depleted formed a very small peak at *ca*.1712 cm^{-1} (corresponding to the Rh(III)-acyl species, Figure 4.12). The rates of acyl formation were determined from the slow appearance of this peak and the data are organized in Table 4.8 and illustrated in Figure 4.13.

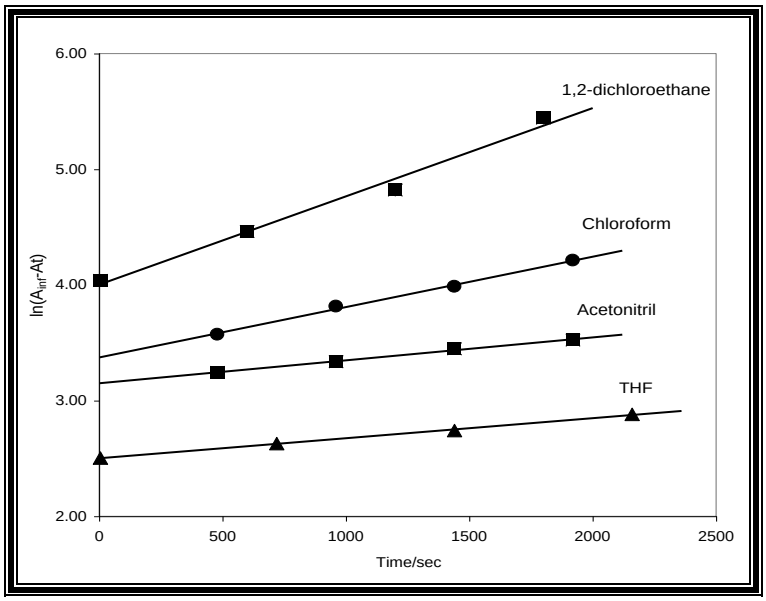

Figure 4.13 Solvent dependence for the formation of the Rh(III)-acyl from the corresponding alkyl solution. $[RhI(cupf)(CO)(CH_3)(AsPh_3)]$ = 0.00186 M. (Supplementary data Table ST.9).

Table 4.8 contains first-order rate constants obtained from the slope of plots in Figure 4.13 for the different solvents used. A comparison of the rate constants shows that halogenated solvents aided the migration slightly. Furthermore, though it is difficult to make a definite judgement, polarity of the solvent has no or very small influence. It can be seen from the table that the variation in k_{obs} from acetonitrile to THF does not parallel the variation in ε. Moreover, examination of data in the literature shows similar results, i.e. large changes in polarity cause relatively small effects in rate. A good example is methanol (ε = 32.6), which enhanced the rate of methyl migratory CO-insertion in the case of $[IrMe(CO)_2I_3]^-$ (Haynes *et al*., 1996:2187) and $[Mn(CH_3)(CO)_5]$ (Mawby *et al*., 1964:3994) more than nitromethane having ε = 38.6. This way literature studies indicate that the coordinating ability of a solvent may also be important.

The role of a solvent may also be judged from the mechanism of methyl migratory (carbonyl insertion) reactions. The critical step during migration, which is thought to be the rupture of the M–C bond (metal-carbon), is the facilitation of partial bond formation

by the methyl group to an adjacent carbonyl. Complete migration will not occur until a solvent molecule enters the coordination sphere. Therefore, if this proposed mechanism is assumed to be correct, then coordination ability of solvents will have a greater role to play. Since charge formations are not expected during migration, polarity, which is measured by dielectric constant and defined as the ability of a solvent to separate charges, will probably have no role to play.

Table 4.8 Solvent effects for the formation of Rh(III)-acyl from the corresponding alkyl solutions.

Solvent	**Solvent parameter (ε)**	**υ(CO) of Rh(III)-species (cm^{-1})**		**k_{obs}(s^{-1})***
		alkyl (OA1)	**acyl**	
THF	7.6	2048.3	1696.7	0.000173(5)
Acetonitrile	38.0	2052.7	1712.1	0.000198(9)
Chloroform	4.80	2055.3	1711.5	0.00043(1)
1,2-Dichloroethane	10.36	2052.1	1710-1730**	0.00076(6)

* Strictly, $k_{obs} = k_4 + k_{-4}$ (Scheme 4.4) and ** Broad peak.

When the reaction is monitored by IR-time-scans in acetone from 2100 to 1900 cm^{-1}, it shows isomerisation of the starting complex, [RhI(cupf)(CO)(CH_3)($AsPh_3$)] (OA1), with υ(CO) = 2052 cm^{-1}, to another Rh(III)-species (OA2) at 2032 cm^{-1}, with isosbestic points at *ca.* 2040, 2013 and 1994 cm^{-1} (Figure 4.12). IR microanalysis of the solution could not detect acyl formation due to solvent interference (acetone shows strong CO-peaks that mask other peaks in the vicinity of acyl peaks). Crystallisation did not yield the acyl species, but instead a Rh(III)-alkyl at 2040.2 cm^{-1} was characterised. This is midway between υ(CO) values of OA1 and OA2 and probably a mixture of both.

Although triphenylarsine complexes are less steric due to the longer Rh–As bond than Rh–P, the reaction was not enhanced. Instead, comparable kinetic data are obtained (Table 4.2). Therefore, either the starting complex was insignificantly manipulated in

comparison to its phosphine analogue or due to the small bite angle of cupferrate it was already sterically not too crowded and able to accommodate the small substrate, iodomethane with relative ease. Basson *et al*., (1990:1324) added excess PPh_3 to [Rh(cupf)(CO)(PPh_3)] and obtained penta-coordinated [Rh(cupf)(CO)(PPh_3)$_2$]. Furthermore, the unexpected faster rate of oxidative addition of iodoethane to [Rh(cupf)(CO)($AsPh_3$)] relative to literature data (refer Section 4.8), can only be interpreted by the less steric crowding of the complex. In other words, it can be said that electronic factors seem to dominate steric effects in these complexes. Mcauliffe *et al*., (1997:69) found that the σ–donor power of group 15 ligands vary in the order PR_3 > AsR_3 > SbR_3 (R = constant). Moreover**,** important to note is that the reaction of CH_3I to the arsine complex showed insignificant intercepts (except in acetonitrile) giving large equilibrium constants (calculated from $K = k_1/k_{-1}$), which implies that the formation of the Rh(III)-alkyl species is thermodynamically more favoured for arsine complexes than the corresponding phosphines. All spectra obtained indicate that Scheme 4.4 is the expected reaction mechanism for the reaction between CH_3I and [Rh(cupf)(CO)($AsPh_3$)].

References

Ball, M.C. and Norbory, A.H., *Physical Data For Inorganic Chemists*, Longman Limited, 1974, London, 34.

Basson, S.S., Leipoldt, J.G. and Nel, J.T., *Inorg. Chim. Acta*, (1984), **84**, 167.

Basson, S.S., Leipoldt, J.G., Roodt, A. and Venter, J.A., *Inorg. Chim. Acta*, (1987), **128**, 31.

Basson, S.S., Leipoldt, J.G. and Venter, J.A., *Acta. Cryst*., (1990), **C46**, 1324-1326.

Cheng, C.H, Spivack, B.D, Eisenberg, R., *J. Am. Chem. Soc*., (1977), **99**, 3003.

Chock, P.B. and J. Halpern, J., *J. Am. Chem. Soc*., (1966), **88**, 3511-14.

Collman, J.P., Hegedus, L.S., Norton, J.R. and R.G. Finke, *Principles and Application Of Organotransition Metal Chemistry*, University Science Books, Mill vally. CA., 1987, 71.

Deeming, A.J. and Shaw, B.L., *J. Chem. Soc*., (1969), 1802.

Hart-Davis, J. and Graham, W.A.G., *Inorg. Chem*., (1970), **9**, 2658.

Kubota, M., Kiefer, G.W., Ishikawa, R.M. and Bencala, K.E., *Inorg. Chim. Acta*, (1973), **7**, 195.

Leipoldt, J.G., Basson, S.S., Botha, L.J., *Inorg. Chim. Acta*, (1990), **168**, 215.

Maitlis, P.M., Haynes, A., Sunley, G. J. and Howard, M.J., *J. Chem. Soc., Dalton. Trans*. 1996, 2187-2196.

Mawby, R.J., Basolo, F. and R.G. Pearson, *J. Am. Chem. Soc*., (1964), **86**, 3994.

McAuliffe, C.A., Levasa, W., *Phosphine, Arsine And Stibine Complexes Of The Transition Elements*, Elsevier Scientist Publisher Co., the Netherlands, 1979, 69.

Micromath Scientist for Windows, 1990-1995 Microsoft Corporation.

Otto, S., Roodt, A., Erasmus, J.J.C., Swarts, J.C., *Polyhedron*, (1998), **17**, 2447.

Pearson, R. G. and Muir, W.R., *J. Am. Chem. Soc*., (1970), **92**, 5519.

Ranki, J., Poole, A.D., Benyei, A.C., Cole-Hamilton, D.J., *Chem. Commun*., (1997), 1835.

Roodt, A. and Steyn, G.J.J., *Inorg.Chem*., (2000), **2**, 1-23.

Steyn, G.J.J., Roodt, A. and Leipoldt, J.G., *Rhodium Express*, (1993), **0**, 11-15.

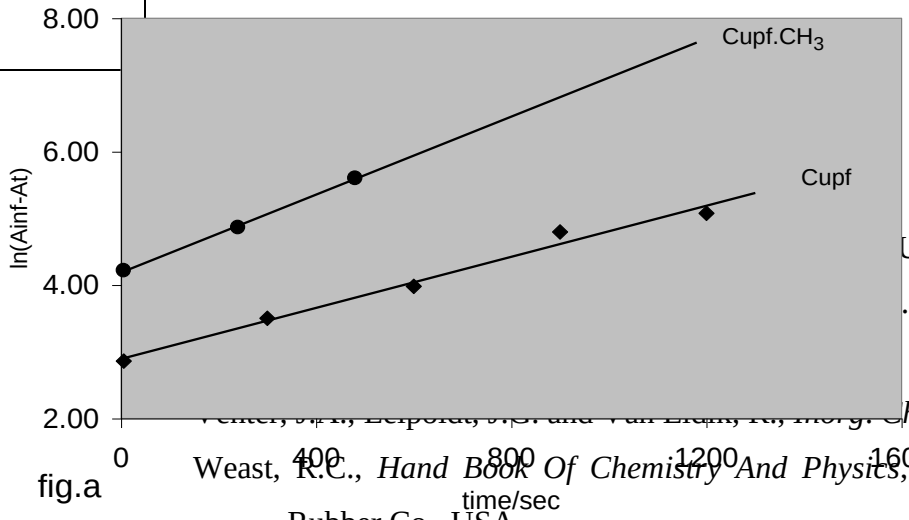

fig.a

U., *Inorg. Chem.* (1970), **9**, 724.

. Roodt and G.J. Van Zyl, *Trans*

hem., (1991), **30**, 2207-2209.

Weast, R.C., *Hand Book Of Chemistry And Physics*, 54th-edition, 1973-74, Chemical Rubber Co., USA.

CHAPTER 5

EVALUATION OF THE STUDY

5.1 PRESENT FINDINGS

Complexes containing the triphenylarsine ligand, [Rh(cupf)(CO)($AsPh_3$)], and its arsine and cupferrate substituted complexes such as [Rh(cupf.CH_3)(CO)($AsPh_3$)] and [Rh(cupf)(CO)($AsMePh_2$)] were synthesised and characterised by ^1H NMR and IR spectroscopy. X-ray crystallographic characterisation of the widely used starting complex, [Rh(cupf)(CO)($AsPh_3$)], was not essential, not only because of the aim of the study which was to investigate and compare the kinetic data obtained (with its phosphine analogue), but also because Basson *et al*., (1987:31) have already characterised its phosphine analogue and isomorphism is commonly observed phenomena in phosphine and arsine analogues of complexes. Furthermore, the less steric crowding of the metal centre which would have kinetic significance, was expected due to the longer Rh–As bond and the smaller cone angle of the arsine ligand.

Kinetic data obtained for iodomethane oxidative addition to the [Rh(cupf)(CO)($AsPh_3$)] complex indicated second-order rate constants comparable to those for its corresponding phosphine analogue. The nucleophilicity of the Rh metal centre in [Rh(cupf)(CO)($AsPh_3$)] was increased by introducing a methyl substituted cupferron, 2-methyl cupf, and $AsMePh_2$. The relative increase in rate in the case of

$AsMePh_2$ should be attributed to a smaller cone angle and more electron donating power of the ligand. Generally, it can be said that in this study the complex was successfully manipulated, both electronically as well as sterically. It was thus possible to determine the relative reactivity of the complexes giving valuable information about the effects induced by the various substituents or ligands.

The kinetic investigation was not limited to iodomethane rate data but was also focused on collecting data for bromomethane and iodoethane. Correlation between kinetic data and physical constants such as bond dissociation energy was made and reasonable relationships between these parameters were found. Activation parameters were determined for the reaction between iodomethane and [Rh(cupf)(CO)($AsPh_3$)] in acetone using data obtained at four different temperatures. The parameters confirm the associative mode of addition and also that the reaction progress towards the activated state is more entropy than enthalpy driven.

5.2 RECOMMENDED FUTURE RESEARCH

In terms of second-order rate constants obtained, the rate of oxidative addition of iodomethane to [Rh(cupf)(CO)($AsPh_3$)] was comparable with its phosphine analogue. These data may imply steric factors are more important than electronic factors. However, it is not safe to make a definite judgement since kinetic investigations should be extended to include $SbPh_3$ and $BiPh_3$ ligands in order to determine or recognize the relative importance of steric and electronic effects in such complexes.

Furthermore, solvent variation played an important role in the reactivity of these complexes. Specifically, the reaction in methanol as reaction medium was thermodynamically favoured towards the oxidative addition product. Methanol was also found to significantly accelerate the migratory CO-insertion step in case of the iridium-catalysed Cativa carbonylation process. Although the current prospect is based on coordination ability of the solvent, future research needs to be planned to investigate the role of methanol (and if higher alcohols behave similarly) in the oxidative and CO-insertion reactions.

Another area which needs further follow-up is the formation of two simultaneous species observed in acetone. It was shown by IR micro analysis of the reaction between iodomethane and [Rh(cupf)(CO)($AsPh_3$)] in acetone that a strong Rh(I)-CO peak around 1975 cm^{-1} disappears with the simultaneous formation of two medium intensity Rh(III)-CO peaks at *ca*. 2052 cm^{-1} and 2033 cm^{-1}. The peak at υ(CO) = 2033 cm^{-1} is small and unexpected compared to the 2050-2060 cm^{-1} range for the oxidative addition product in acetone medium. Although this study has presented some suggestions, future investigations should be done to characterise these complexes fully with respect to stereospecific preferences.

CHAPTER 6

SUMMARY

Results obtained for the reaction between [Rh(cupf)(CO)($AsPh_3$)] and CH_3I in a range of solvents indicated that the second-order rate constants are comparable with its phosphine analogue. A likely explanation given was that steric factors are probably overshadowed by electronic ones. This suggestion is supported by literature findings specifying the σ-donor order of group 15 ligands as PR_3 > AsR_3 > SbR_3. Rhodium complexes with phosphine ligands should thus have more electron density than those with corresponding arsine ligands. The less steric crowding at the Rh centre of the starting complex was proved by rate enhancement (relative to other similar rhodium complexes) of oxidative addition of the bulky substrate, iodoethane, to the complex. The oxidative addition kinetics showed insignificant intercepts for the plots of k_{obs} *vs* [CH_3I] which implied a reaction thermodynamically favoured towards the Rh(III)-alkyl complex product.

Electron density and steric constraints of the rhodium(I) species were manipulated in the study by using different arsine ligands. [Rh(cupf.CH_3)(CO)($AsPh_3$)] and [Rh(cupf)(CO)($AsMePh_2$)] were thus prepared and analysed. Both complexes enhanced the rate of oxidative addition, which is in agreement with the higher electron density at the metal due to the more efficient electron donating property of the methyl group compared to the phenyl group. The increased reactivity of

[Rh(cupf)(CO)(AsMePh$_2$)] could also be ascribed to the smaller cone angle of AsMePh$_2$ compared to AsPh$_3$. The rate of oxidative addition of iodoethane was lower, which indicated that the first step of the reaction was a nucleophilic attack by the metal centre (rhodium) on the α-carbon of the haloalkanes.

The first-order rate constant for CO-insertion was determined from IR-multi-scans in acetonitrile and chloroform. Although UV/VIS spectra of the reaction showed biphasic kinetics in acetonitrile and methanol, the second step after the initial oxidative addition reaction was not only CO-insertion but, as revealed from IR-multi-scanned spectra, also isomerisation from a Rh(III)-acyl to alkyl species in the same step. In other words, the UV/VIS spectra did not show clearly for which species the specific rate was measured in the second part of the biphasic plots. However, IR-multi-scanned spectra of the reaction at fixed [CH$_3$I] for the oxidative addition step (Rh(I)–CO peak disappearance) was possible since it was proved that the graph of k_{obs} *vs* [CH$_3$I] was linear with insignificant intercepts. The IR-multi-scanned spectra together with the UV/VIS rate data indicated that the fast equilibrium for the formation of the alkyl complex was followed by a second slower CO-insertion reaction. This was consistent with the proposed mechanism of the title reaction as shown below.

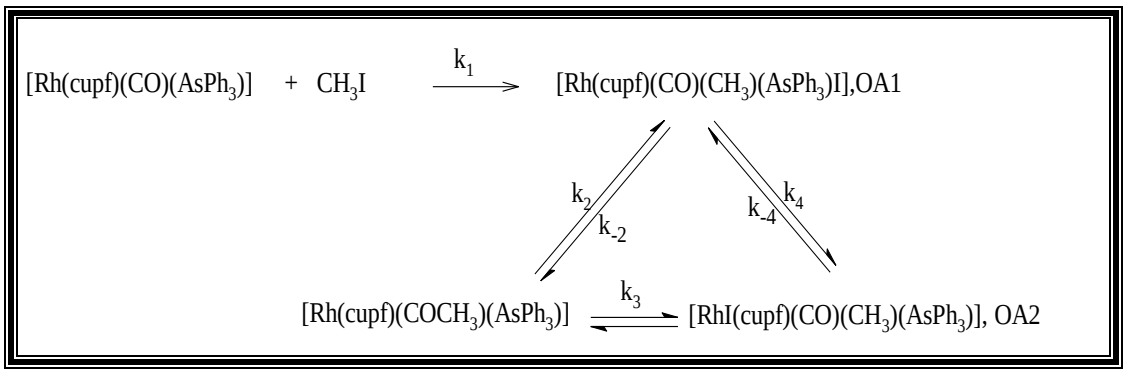

Scheme: Proposed mechanism of the reaction [Rh(cupf)(CO)(AsPh$_3$)] and CH$_3$I.

The observed rate enhancement due to the increase in electron density of the starting complex together with the activation parameters found (relatively large negative $\Delta S^{\#}$) and the type of IR-multi-scans spectra obtained are all indicative of an associative mechanism. Furthermore, the activation of the second-order rate constants from non-polar to highly polar solvents could be taken as an indication of a polar transition state. Although activation parameters and IR multi-scanned spectra were performed in different solvents, i.e. in acetone and chloroform, it would not be expected to affect the proposed mechanism. On the basis of a combined solvent, temperature and pressure dependence study conducted, activation parameters for the reaction between CH_3I and [Rh(cupf)(CO)(PPh_3)] in acetone and chloroform were very close to those obtained for the title reaction in this investigation.

In this study, the effect of organic halide substrates on the rate of the reaction by changing the substrate from CH_3I to CH_3Br and C_2H_5I was also investigated. In comparison to literature data, the rate of the reaction with C_2H_5I was faster, i.e. only a 40-fold deactivation was found. Both CH_3Br and C_2H_5I retarded the reaction. Possible explanations could be due to electronic factors (bond energy, BE, of CH_3–Br = 70 *vs* CH_3–I = 56 kcal/mol). Since BE of CH_3CH_2–I is 53 kcal/mol, decreased reactivity observed could be interpreted in terms of the large size of the ethyl group. With regard to the mode of addition, oxidative addition of CH_3I to [Rh(cupf)(CO)($AsPh_3$)] is expected to proceed by addition of iodide (I^-) and CH_3 adjacently (*cis* to one another) like in its phosphine analogue.

Another aspect of this study was kinetic runs of the oxidative addition product, [IRh(cupf)(CO)(CH_3)($AsPh_3$)], performed in a range of solvents. Most kinetic studies only employ Rh(I) or Ir(I) complexes as a starting material, but in this study the Rh(III)-alkyl product was also utilized as a starting complex. In all solvents employed, the product was depleted and gave rise to a small peak at *ca*. 1712 cm^{-1} corresponding to a Rh(III)-acyl species. The rate of acyl formation was thus determined by the slow appearance of this peak.

SUPPLEMENTARY SECTION

APPENDIX A: RATE EQUATIONS

7.1 FIRST-ORDER, PSEUDO-FIRST-ORDER REACTIONS

Since the reaction studied showed a first-order dependence on iodomethane concentration, basic theory concerning such reactions is presented below. In first-order reactions, rate depends only on the first power of reactant concentration.

Consider the conversion of A to Z,

$$A \longrightarrow Z \qquad \textbf{(6.1)}$$

The reaction proceeds to completion according to the following rate law,

$$-\frac{d[A]}{dt} = \frac{d[Z]}{dt} = k[A] \qquad \textbf{(6.2)}$$

Assuming that at $t_o = 0$, $[A] = [A]_o$ and at $t_1 = t$, $[A] = [A]_t$, then its integrated form is,

$$\int_{[A]_0}^{[A]t} \frac{d[A]}{dt} = -k \int_{o}^{t} dt \qquad \textbf{(6.3)}$$

The result of the integration is

$$\ln \frac{[A]_t}{[A]_o} = -kt \qquad \textbf{(6.4)}$$

Eq.6.4 can be rewritten as,

$$\ln[A]_t = \ln[A]_o - kt \qquad \textbf{(6.5)}$$

It is possible to follow concentration changes spectroscopically by applying the Beer-Lambert law,

$$A = \varepsilon \ell [A] \qquad \textbf{(6.6)}$$

where ε = molar absorption coefficient, ℓ = light path length and [A] = molar concentration of species A.

Substitution in Eq. 6.5 gives

$$\ln(A_\infty - A_t) = \ln(A_\infty - A_o) - kt \qquad \textbf{(6.7)}$$

where $[A_t]$ α $(A_\infty - A_t)$ and $[A_o]$ α $(A_\infty - A_t)$.

A_∞, A_t and A_o are absorbance at infinite time, time t and at the start of the reaction, respectively.

If absorbance increases exponentially with time, then according to Eq. 6.7 a plot of $\ln(|A_\infty - A_t|)$ against time is a straight line with slope of –k, which represents the rate constant of the reaction.

At 50% conversion the half-life ($t_{1/2}$) of the reaction is given by

$$\ln\left(\frac{\frac{[A]_O}{2}}{[A]_O}\right) = -k\, t_{1/2} \qquad \textbf{(6.8)}$$

Applying mathematical operations, Eq. 6.8 reduces to

$$t_{1/2} = \frac{\ln 2}{k} \qquad \textbf{(6.9)}$$

where $t_{1/2}$ = time required for a reactant concentration to decay to one-half of its initial value. It is also independent of $[A]_o$.

The rate of a second-order reaction given below is proportional to two concentrations given by Eq. 6.10,

$$A + B \longrightarrow C$$

$$R = k[A][B] \qquad \textbf{(6.10)}$$

If $[B]_o > 10[A]_o$, i.e. at least 10 times in excess, then [B] decreases during the reaction run to $0.90[A]_o$. The analysed data provides k', the pseudo-first-order rate constant. To obtain k, one divides k' by $[B]_{Av}$ i.e.,

$$k = \frac{k'}{[B]_{Av}} \qquad \textbf{(6.11)}$$

In practice, a range of $[B]_o$ in excess of a constant $[A]_o$ gives corresponding k' values for which a plot of k' *vs* corresponding $[B]_o$ values will yield a straight line with zero

intercept. The slope of this graph is equal to k. In kinetics this is known as the method of flooding, or the method of isolation (of one of the reagents).

7.2 TWO CONSECUTIVE REACTIONS WITH A REVERSIBLE STEP

The general scheme

$$A + B \underset{k_{-1}}{\overset{k_1, K}{\rightleftharpoons}} C \xrightarrow{k_2} D \qquad \textbf{(6.12)}$$

was found to be operative for many kinetic studies involving oxidative addition reactions of iodomethane and rhodium(I) complexes. The formation of C is usually followed so that equilibrium between A and B and the product C is maintained throughout the total reaction for the formation of D. Under such conditions the pseudo-first-order rate constant's equation can be derived as follows:

$$K_1 = \frac{k_1}{k_{-1}} = \frac{[C]}{[A][B]} \qquad \textbf{(6.13)}$$

The reaction can be monitored by the disappearance of A and C or equivalent gain in D, i.e.

$$\frac{d[D]}{dt} = k_{obs}([A] + [C]) = k_2([C])$$

Substitute [C] from Eq. 6.13 gives

$$k_{obs} = \frac{k_2 K_1 [A][B]}{[A]+[C]}$$

Further substitution of [A] from Eq. 6.13 gives

$$k = \frac{[A][B]k_2 K_1}{[C][\frac{1}{K_1[B]}+1]}$$

and with $\frac{[A]}{[C]} = \frac{1}{K_1[B]}$ from Eq. 6.13, it follows that

$$k_{obs} = \frac{k_2 K_1 [B]}{1+K_1[B]} \qquad \textbf{(6.14)}$$

or $$\frac{1}{k_{obs}} = \left[\frac{1}{k_2 K_1}\right]\frac{1}{[B]} + \frac{1}{k_2} \qquad \textbf{(6.15)}$$

Eq 6.14 is also known as the rate equation for saturation kinetics due to its curvature and eventually levelling off in parts of k_{obs} against varying $[B]_o$, where $[B]_o > 10[A]_o$. If the first reaction is a fast equilibration step, the full curvature of Eq 6.14 is found and in practise this equation can be linearised (Eq. 6.15) by plotting $1/k_{obs}$ *vs* $1/[B]$ to result in an intercept ($1/k_2$) and slope ($1/k_2K_1$) from which K_1 can be calculated.

Two extreme cases may be operative and result in simpler forms of Eq. 6.14, viz

i) K_1 is small or [B] is small so that $K_1[B] << 1$, leading to $k_{obs} = k_2K_1[B]$. Plots of k_{obs} *vs* varying concentrations of [B] gives a straight line with zero intercept and slope = k_2K_1.

ii) If the reverse is true, i.e. $K_1[B] >> 1$, then $k_{obs} = k_2$. This coincides with the levelling off part (or plateau or maximum) of curved plots of k_{obs} *vs* varying [B].

iii) In a few cases of oxidative addition reactions involving Rh(I) complexes and iodomethane it was observed that especially with solvent variation, biphasic rate behaviour occurred i.e. absorbance-time plots show two distinctive sequential reactions. This may be a special case of Eq. 6.12 where A and B react to form C at a much faster rate compared to the disappearance of C to form D, i.e. there is a fast concentration build-up of C before the slower concentration increase or decrease of C to D can be measured. In such cases, the kinetics simplify to that of two separate processes on different time scales so that Eq.6.16 and 6.17 can be studied separately.

$$A + B \underset{k_{-1}}{\overset{k_1, K}{\rightleftharpoons}} C \qquad \textbf{(6.16)}$$

and

$$C \xrightarrow{k_2} D \qquad \textbf{(6.17)}$$

In the case of Eq 6.16 with $[B]_o > 10[A]_o$ the kinetics reduces to a pseudo-first-order reversible reaction for which it can be shown that

$$k_{obs} = k_1[B] + k_{-1} \qquad (\textbf{6.18})$$

This allows determination of both rate constants and therefore the equilibrium constant K_1. If Eq. 6.17 becomes an equilibrium, such as was found for the Rh(III)-alkyl to acyl conversion, the $k_{obs} = k_2 + k_{-2}$ for the disappearance of C is true.

APPENDIX B: SUPPLEMENTARY KINETIC DATA

Table ST#.1 Observed rate constant (k_{obs}) values for the oxidative addition of CH_3I to [Rh(cupf)(CO)($AsPh_3$)] in different solvents. (Supplementary data for Figure 4.4).

[CH_3I],M	k_{obs}(s^{-1})*				
	Acetonitrile	**Methanol**	**Acetone**	**Ethylacetate**	**Toluene**
0.2	0.00117(5)	0.000736(2)	0.000302(1)	0.00008(5)	0.0000022(2)
0.4	0.00183(3)	0.00144(1)	0.000435(6)	0.0001363(6)	0.00000600(2)
0.5	0.00250(4)	0.00197(2)	0.000563(2)	0.0001511(7)	0.0000123(4)
0.6	0.00273(1)	0.00201(6)	0.000662(2)	0.000178(1)	0.0000156(7)
0.8	-----	0.00310(7)	0.000892(3)	0.0002165(9)	0.00002255(3)
1.0	----	----	0.00105(1)	---	----

* Standard deviations in Parentheses.
# ST = Supplementary table.

Table ST.2 Observed rate constant (k_{obs}) values for the oxidative addition of CH_3I to [Rh(cupf)(CO)($AsPh_3$)] at various temperatures in acetone. (Supplementary data for Figure 4.5).

	First-order-rate constants (k_{obs} s^{-1})			
[CH_3I], M	**T=14.6 °C**	**T=19 °C**	**T=24.8 °C**	**T=29.6 °C**
0.2	0.0000973(3)	0.0001569(6)	0.000302(1)	0.000408(1)
0.4	0.0001813(1)	0.0002842(2)	0.000435(6)	0.000642(3)
0.5	0.0002187(3)	0.0003316(5)	0.000563(2)	0.000864(7)
0.6	----	----	0.000662(2)	----
0.8	0.000338(1)	----	0.000892(3)	----
1.0	0.000392(1)	----	0.00105(1)	0.00139(4)

Table ST.3 Kinetic data for Rh(III)-alkyl formation for the complexes shown in acetone. (Supplementary data for Figure 4.6a).

[Rh(cupf)(CO)($AsPh_3$)]		**[Rh(cupf.CH_3)(CO)($AsPh_3$)]**	
Time/sec	$\ln(\lvert A_\infty - A_t \rvert)$	Time/sec	$\ln(\lvert A_\infty - A_t \rvert)$
5.4	2.714635	5.4	2.609681
720	2.817795	300	3.014385
1440	2.982836	600	3.285603
2160	3.341213	900	3.454978

Table ST.4 Kinetic data for Rh(III)-alkyl and acyl formation for the complexes shown in acetonitrile.(Supplementary data for Figure 4.6b, T/s = time in seconds).

[Rh(cupf)(CO)($AsPh_3$)]			**[Rh(cupf.CH_3)(CO)($AsPh_3$)]**		
	Rh(III)-alkyl formation	**Rh(III)-acyl formation**		**Rh(III)-alkyl formation**	**Rh(III)-acyl formation**
T/s	$\ln(\lvert A_\infty - A_t \rvert)$	$\ln(\lvert A_\infty - A_t \rvert)$	T/s	$\ln(\lvert A_\infty - A_t \rvert)$	$\ln(\lvert A_\infty - A_t \rvert)$
5.4	2.861254	3.344088	5.4	4.21698	3.2280
300	3.501139	3.657575	240	4.86394	3.3355
600	3.982124	4.006499	480	5.60321	3.5223
900	4.7973	4.597301	720	----	3.7091
1200	5.075174	5.076775	960	----	3.9945

Table ST.5 Kinetic data for Rh(III)-alkyl formation for the complexes shown in chloroform. (Supplementary data for Figure 4.7a**,** T/s = time in seconds).

T/s	**[Rh(cupf)(CO)($AsMePh_2$)]**	**[Rh(cupf)(CO)($AsPh_3$)]**	**T/s**	**[Rh(cupf.CH_3)(CO)($AsPh_3$)]**
	$\ln(\lvert A_\infty - A_t \rvert)$	$\ln(\lvert A_\infty - A_t \rvert)$		$\ln(\lvert A_\infty - A_t \rvert)$
5.4	4.178498	2.511518	5.4	2.714803
60	4.428783	2.684138	45	2.861621
120	4.710642	2.794703	90	3.011841
180	4.940923	2.892905	135	3.117132
240	----	2.973443	180	3.232088

Table ST.6 Kinetic data for Rh(III)-acyl formation for the complexes shown. (Supplementary data for Figure 4.7b, T/s = time in seconds).

T/s	[Rh(cupf)(CO)(AsMePh$_2$)]	[Rh(cupf)(CO)(AsPh$_3$)]	T/s	[Rh(cupf.CH$_3$)(CO)(AsPh$_3$)]
	ln(|A_∞-A_t|)	ln(|A_∞-A_t|)		ln(|A_∞-A_t|)
5.4	5.388198	2.7599	5.4	3.927746
60	5.476679	2.830052	45	3.978056
120	5.626072	2.905508	90	4.017884
180	----	2.98711	135	4.093544

Table ST.7 IR-absorbance and time data for the formation of Rh(III)-acyl, alkyl and disappearance of Rh(I)-CO, for the reaction between CH_3I and [Rh(cupf)(CO)($AsPh_3$)] in chloroform.(Supplementary data for Figure 4.9).

Time/s	Disappearance of Rh(I)	Appearance of Rh(III)-alkyl, OA1	Appearance of Rh(III)-acyl	Appearance of Rh(III)-alkyl, OA1
5.4	0.15085	0.032851	0.0055469	0.077144
180	0.081761	0.062581	0.015862	0.080177
360	0.041666	0.068042	0.024963	0.086245
540	0.018843	0.070469	0.031643	0.091099
720	0.0089739	-----	0.035644	0.095346

Table ST.8 k_{obs} for the reaction between [Rh(cupf)(CO)($AsPh_3$)] with substrates shown at 24.8 °C in acetone. (Suppelementary data for Figure 4.11).

[substrate], M	k_{obs} (s^{-1})		
	CH_3I	CH_3Br #	C_2H_5I
0.2	0.000302(1)	0.0000196(1)	0.0000348(2)
0.4	0.000435(6)	0.0000578(3)	0.0000390(2)
0.5	0.000563(2)	------	0.0000420(4)
0.6	0.000662(2)	------	0.0000447(4)
0.8	0.000892(3)	0.0001368(7)	0.0000520(7)
1.0	0.00105(1)	0.0002265(7)	0.0000546(4)

* In acetonitrile.

Table ST.9 Kinetic data for the CO-insertion reaction starting with a solution of Rh(III)-alkyl in the solvents mentioned at 25 °C. (Supplementary data for Figure 4.13).

1,2-Dichloroethane		**Chloroform**	
Time/sec	$\ln(\lvert A_\infty - A_t \rvert)$	Time/sec	$\ln(\lvert A_\infty - A_t \rvert)$
5.4	4.038834	480	3.571345
720	4.461936	960	3.814896
1440	4.819974	1440	3.986369
2160	5.442188	1920	4.211103
Acetonitrile		**THF**	
Time/sec	$\ln(\lvert A_\infty - A_t \rvert)$	Time/sec	$\ln(\lvert A_\infty - A_t \rvert)$
480	3.243169	5.4	2.503955
960	3.336337	600	2.62862
1440	3.447346	1200	2.740904
1920	3.523365	1800	2.881654